

**DESIGN OF A CENTRIFUGAL COMPRESSOR INTEGRATED WITH A  
HERMETIC MOTOR FOR AUTOMOTIVE AIRCONDITIONERS**

by

Hayong Yun

B.S. Mechanical Design and Production Engineering

at the

Seoul National University  
(1991)

Submitted to the Department of  
Mechanical Engineering in Partial Fulfillment of  
the Requirements for the  
Degree of

**MASTER OF SCIENCE**  
in Mechanical Engineering  
at the

**Massachusetts Institute of Technology**

February 1993

© 1993 Massachusetts Institute of Technology  
All rights reserved

**Signature redacted**

Signature of Author \_\_\_\_\_

Department of Mechanical Engineering  
February, 1993

**Signature redacted**

Certified by \_\_\_\_\_

Professor Joseph L. Smith, Jr  
Department of Mechanical Engineering  
Thesis Supervisor

**Signature redacted**

Accepted by \_\_\_\_\_

Professor Ain A. Sonin  
Department of Mechanical Engineering  
Chairman, Graduate Committee

MASSACHUSETTS INSTITUTE  
OF TECHNOLOGY

# DESIGN OF A CENTRIFUGAL COMPRESSOR INTEGRATED WITH A HERMETIC MOTOR FOR AUTOMOTIVE AIRCONDITIONERS

by

HAYONG YUN

Submitted to the Department of Mechanical Engineering  
on February 2, 1993 in partial fulfillment of the  
requirements for the Degree of Master of Science in  
Mechanical Engineering

## ABSTRACT

A centrifugal compressor integrated with a hermetic motor has been designed. In order to design the integrated hermetic compressor-motor, methods optimizing the compressor and the motor designs, have also been developed. This work includes the stress analysis, critical speed analysis, and one dimensional aerodynamic design of the compressor-hermetic motor unit. The selection of an appropriate thermodynamic cycle with a working fluid has also been made. With these tools, a selected thermodynamic cycle, and a working fluid, a suggested example of the compressor-hermetic motor unit has been designed. The result of the design shows that the optimal motor design and the optimal compressor design are not necessarily compatible. A compromise between motor design and compressor design is, therefore, necessary. The integrated compressor-hermetic motor unit has taken these compromises into account and is expected to yield better performance than a compressor and motor that have been designed separately.

Thesis Supervisor: Dr. Joseph L. Smith, Jr

Title: Professor of Mechanical Engineering

## ACKNOWLEDGEMENT

I would like to thank my advisor, Professor Joseph L. Smith, Jr, for his insightful guidance through the course of my research. His support, advice, and encouragement were extremely helpful. Working with him has been a great pleasure and a privilege.

Many M.I.T. faculty members and staff have contributed significantly to my research activities. I would like to thank Professor Jeffrey H. Lang, Dr. Stephen D. Umans, and my colleague Kamakshi Shrinivasan at Laboratory for Electromagnetic and Electronic Systems for their invaluable cooperation in my research project. I owe a great deal of gratitude to Professor Markus I. Flik for his advice and interest on my research. I would also like to thank Professor Douglas A. Carmichael for his advice on turbomachinery and Professor Klaus-Jurgen Bathe for his advice on Finite Element Analysis.

I would like to thank the sponser of my research project Mr. M. Clement Vaturi. His generous funding enabled financially to proceed the research.

I am deeply indepted to Dr. Robert C. Dean, Jr for guiding me to the right resource for designing the centrifugal compressor. I am deeply grateful for the professional help that I received from Dr. David Japikse and his company Concept, ETI.

My colleagues in the Cryogenics Laboratory have been a geat help to me, not only in my research but also in my adjusting to life at M.I.T.. Dr. Byung-In Choi, Dr. Sankwon Jeong, and Sankar Sunder frequently provided me with new ideas for my research. I would especially like to thank Charles Dean for so patiently editing my thesis and improving my English in the process. Bill, Ed, Alex, Ken , Jeff, Mac, Mike, Eric Norman, Chris, Zhoumin, Maurice, thanks to each of you for being good friends and good colleagues, I have learned much from you. Also thanks to Lisa, Tom, and Amy for their invaluable assistance with administrative work.

Most of all, I would like to express my deepest gratitude to my parents Youn-Ok Lee and Zixang Yun. Their support, love, and advice have always been a great help. I owe them not only my life but also what I am.

## TABLE OF CONTENTS

Abstract.....	2
Acknowledgement.....	3
Table of Contents.....	5
Nomenclature.....	7
List of Figures.....	9
Chapter 1. Introduction.....	10
1.1. Background.....	10
1.2. Brief Introduction to the Airconditioning Systems.....	11
Chapter 2. Development of the Design Methods.....	14
2.1. Stress Analysis.....	14
2.1.1. Iterative Solution for Hoop Design.....	14
2.1.2. Finite Element Model for the Hoop Stress Analysis.....	17
2.2. Critical Speed Analysis.....	22
2.3. Design of the Centrifugal Compressor.....	24
Chapter 3. Selection of the Refrigerant.....	31
3.1. Background.....	31
3.2. Refrigerant Selection Procedure Description.....	32
3.3. Result of the Study.....	34
Chapter 4. Design of a Hermetic Compressor-Motor Unit.....	36
4.1. Overview.....	36
4.2. Establishing the Parameters in the Thermodynamic Cycle.....	36
4.3. Selection of the Rotational Speed.....	40
4.4. Geometric Configuration.....	42
Chapter 5. Future Work.....	46
Chapter 6. Conclusion.....	48

Appendix A. Detailed Derivation of the Stress Analysis.....	49
A.1. Motive for Stress Analysis.....	49
A.2. Pressure Fitting of the Hoop.....	49
A.3. Deformation after Rotation.....	50
A.4. Criterion for the Magnet and Rotor Contact.....	51
A.5. Criterion for the Strain Limit of the Hoop.....	52
A.6. Summary of the Equations and Unknowns.....	52
A.7. Solutions to the Given Equations.....	53
A.8. Summary of the Design Procedure.....	56
A.9. Micellaneous Derivations.....	59
A.9.1. Derivation of Equation (2).....	59
A.9.2. Derivation of Equation (3).....	60
A.9.3. Derivation of Equation (7).....	61
Appendix B. Finite Element Computer Input File.....	63
Appendix C. Critical Speed Estimation Program.....	66
Appendix D. Centrifugal Compressor Design Program.....	68
Appendix E. Compressor Design Data Using "COMPAL".....	97
References.....	103

## NOMENCLATURE

### Symbols

$E$	=	Young's Modulus
$\nu$	=	Poisson's Ratio
$R, r$	=	Radius
$y, u, \delta$	=	Deformation
$\rho$	=	Density
$\omega$	=	Rotational Speed
$\sigma$	=	Stress
$\tau$	=	Shear Stress
$\epsilon$	=	Strain
$F$	=	Force
$x$	=	Axial Position
$W_o$	=	Weight
$K, C_1, C_2$	=	Constant
$N, i$	=	Integer
$m$	=	Mass flow rate
$T$	=	Temperature
$P$	=	Pressure
$h$	=	Enthalpy
$\rho$	=	Density
$R$	=	Gas constant (Compressor)
$\gamma$	=	Specific heat ratio
$C_p$	=	Specific heat at constant pressure
$Q$	=	Volume flow rate
$N$	=	Rotational speed
$N_s$	=	Specific speed
$u$	=	Blade velocity
$v$	=	Absolute fluid velocity
$w$	=	Relative fluid velocity
$r$	=	Radius
$b$	=	width
$t$	=	Impeller thickness

$\xi$	=	Slip factor
A	=	Area
M	=	Mach number
$\alpha$	=	Absolute velocity angle
$\beta$	=	Relative velocity angle
$\eta_i$	=	Impeller efficiency
$\eta_c$	=	Compressor efficiency
$\theta$	=	Angle
$\sigma$	=	Solidity

### Subscripts

M	=	Magnet
R	=	Rotor
H	=	Hoop
o	=	Outer radius
i	=	Inner radius
$\theta, T$	=	Tangential (Stress)
r	=	Radial
Y	=	Yielding (Stress)
0	=	Stagnation property
1	=	Impeller inlet
2	=	Impeller exit
3	=	Vaneless diffuser exit
4	=	Vaned diffuser exit
5	=	Volute
s	=	Isentropic process
m	=	meridional (velocity)
t	=	tangential (velocity)
s	=	Shroud (velocity)
h	=	Hub (velocity)



## List of Figures

1.1.	Schematic Diagram of the Airconditioning Cycle.....	12
2.1.	Deformation of the Hoop and the Rotor.....	14
2.2.	Geometry of the Hoop and the Rotor.....	15
2.3.	Schematic Diagram of the Finite Element Model.....	18
2.4.	Finite Element Model Before Deformation.....	20
2.5.	Finite Element Model After Deformation.....	21
2.6.	Free Body Diagram of the Rotor.....	22
2.7.	Schematic Diagram of the Centrifugal Compressor.....	25
2.8.	Velocity Triangle of the Impeller Exit.....	26
2.9.	Velocity Triangle at Vaneless Diffuser Exit.....	27
2.10.	Velocity Triangle at Vaned Diffuser Exit.....	28
3.1.	Ozone Layer Depletion and Global Warming Potential of Various Refrigerants.....	31
3.2.	Single Stage Vapor-Compression Refrigeration Cycle.....	33
3.3.	Impeller Size for Various Refrigerants.....	35
4.1.	Two Stage Vapor-Compression Refrigeration Cycle.....	38
4.2.	Pressure Ratio versus Specific Speed Diagram.....	39
4.3.	Specific Speed versus Compressor Efficiency Diagram.....	40
4.4.	Rotational Speed versus Motor Efficiency Diagram.....	41
4.5.	Schematic Diagram of the Integrated Hermetic Compressor-Motor Unit.....	44
A.1.	Deformation of the Hoop and the Rotor.....	49
A.2.	Graphical Representation of the Hoop Contact Criterion.....	54
A.3.	Graphical Representation of the Hoop Strain Limit.....	55
A.4.	Geometry of the Hoop and the Rotor.....	57
A.5.	Stresses in Polar Coordinates.....	59
A.6.	Thin Hoop under Internal Pressure.....	61

## Chapter 1. INTRODUCTION

### 1.1. Background.

The design project to develop a new type of an automotive airconditioner began at M.I.T.'s Cryogenic Engineering Laboratory and Laboratory for Electromagnetic and Electronic Systems (LEES) in 1991. This new type of automotive airconditioner is expected to improve several features of conventional automotive airconditioners.

Unlike conventional automotive airconditioners, the new automotive airconditioner uses a rotating type compressor rather than a reciprocating type compressor. This is advantageous in reducing the compressor size because the rotating compressors have larger mass flow rates for their given size. The rotating compressors additionally have lower levels of noise and require fewer components hence simplifying their manufacture and reducing production costs.

Another important potential improvement over conventional automotive airconditioners is the integration of the compressor and the motor structure. This is expected to improve current problems with sealing and speed control. The driving source (Motor) is the same unit as the compressor, thus we can build the bearings and shaft inside the compressor-motor unit housing and make the unit hermetic. By integrating the compressor and the motor, we can control of the speed of the compressor. This is different from many conventional automotive airconditioners which get their driving source from the automotive engine shaft via pulley-belt and magnetic clutch. The conventional automotive airconditioners can have only ON-mode and OFF-mode. The integrated compressor, however, can operate at variable speeds according to different operating conditions. This can yield improved performance over conventional airconditioners because by adjusting the speed for different conditions, the airconditioner can operate at local peak efficiency point.

The last advantageous feature of the new automotive airconditioners is the refrigerant. The conventional Chlorofluorocarbon (CFC) based refrigerants have high ozone layer depletion potential and global warming potential, and are considered to be environmentally harmful. To solve this problem, the new automotive airconditioners are designed to use a new type of Hydrochlorofluorocarbon (HCFC) based refrigerant. These new refrigerants have relatively low ozone layer depletion potential and global warming potential compared to the CFC based refrigerants. The new automotive airconditioners are, therefore, expected to contribute to reducing the environmental pollution problem.

For the above reasons, the development of new automotive airconditioners is considered necessary. This work will mainly discuss the design of the integrated compressor motor unit by illustrating the development of the necessary design tools used in the integrated compressor-motor unit and then describing the actual design of the integrated compressor-motor unit. Data from computer simulation for compressor efficiency have been used to compare the performance of designs under various operating conditions. The computer simulation have been done by a computer software "COMPAL" made by Concepts, Education and Technology for Industry (Concept, ETI).

## **1.2. Brief Introduction to the Airconditioning Systems.**

Although many introductory thermodynamic textbooks describe the basic refrigeration cycles [Reference 21], for better understanding of the following chapters, the mechanisms of the airconditioning systems used in this design will be briefly discussed.

The new automotive airconditioner employs a vapor-compression refrigeration cycle. This is also called an inverse rankine cycle because it operates the same way as the rankine cycle, but in the opposite direction. There are several variations of this cycle. For example, the compression stroke can be done by several stages or between each compression stage there can be an inter-cooling stage. However, these variations are not

much significant in understanding the basic vapor-compression refrigeration cycle. The basic vapor-compression refrigeration cycle consists of four processes: evaporation, compression, condensation, and throttling. In the evaporation process, a heat transfer

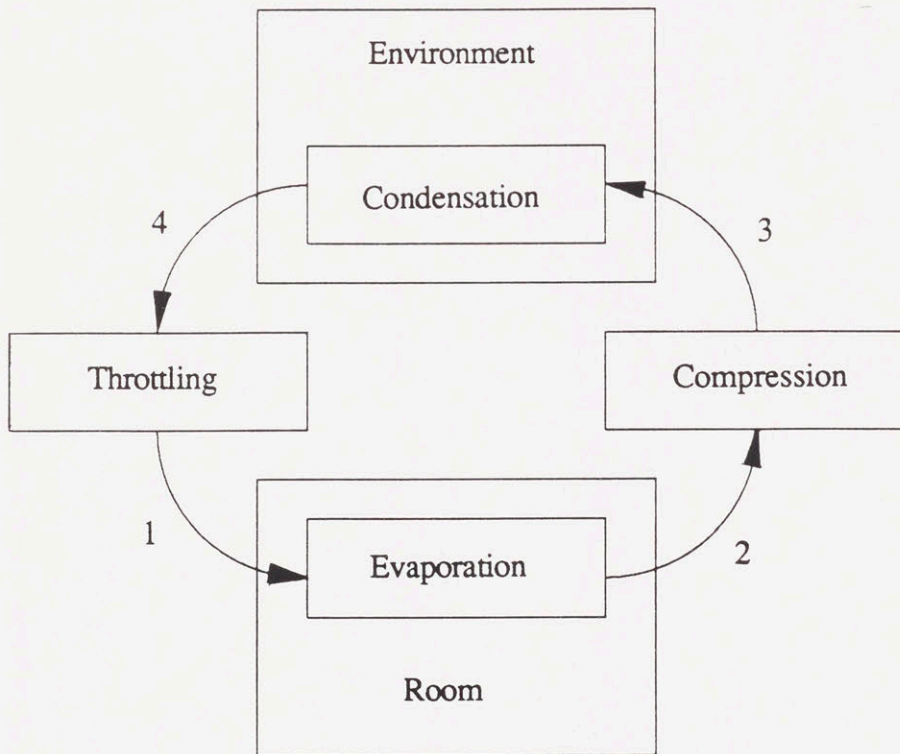


Figure 1-1 Schematic Diagram of the Airconditioning Cycle

occurs from the room to the cold refrigerant. As a result, the room is cooled by heating the refrigerant. After the evaporation process, the temperature of the refrigerant has to be raised to a higher temperature than the environment. This can be achieved by compressing the refrigerant. Once the temperature of the refrigerant is raised higher than the environment, the condenser transfers heat from the refrigerant to the environment. This is

the actual process of dumping the heat of the room to the environment. The last step is throttling the refrigerant to reach the initial state and completing the cycle. This is the basic mechanism of the vapor-compression refrigeration cycle. Several changes have been made in this cycle to improve the performance. These changes will be discussed in later chapters.

## Chapter 2. DEVELOPMENT OF THE DESIGN METHODS

### 2.1. Stress Analysis

#### 2.1.1. Iterative Solution for Hoop Design

The integrated hermetic compressor-motor unit is expected to rotate at high speed. The high rotational speed causes large centrifugal force on the rotor of the motor of the integrated hermetic compressor-motor unit. This raises the question for the proper mechanical support of the magnet and rotor of the integrated hermetic compressor-motor unit. A prestressed tension hoop is introduced to attach the magnet on the rotor of the integrated hermetic compressor-motor unit. This section will discuss the procedure for determining the hoop thickness and the amount the hoop is prestressed.

Initially, when the rotor of the integrated hermetic compressor-motor unit is not

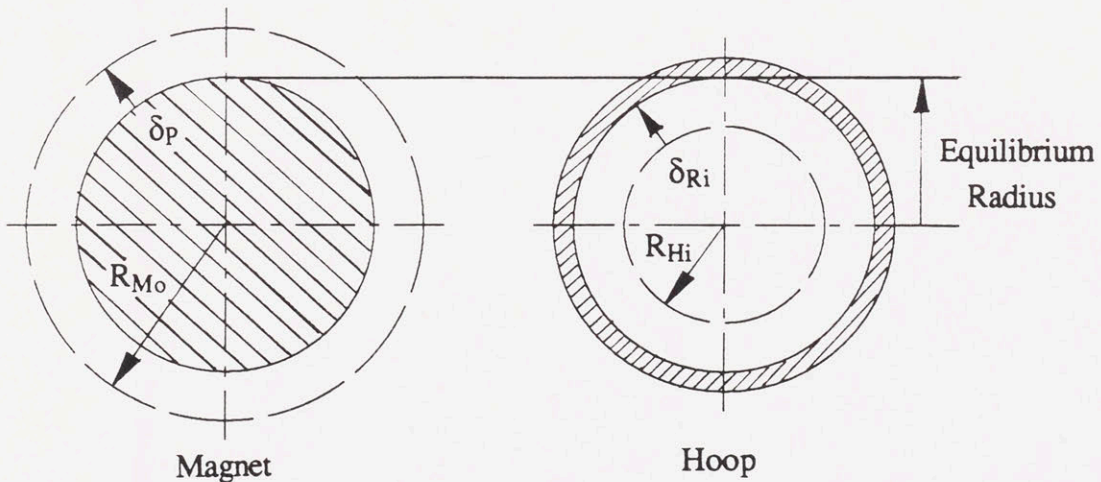


Figure 2-1 Deformation of the Hoop and the Rotor

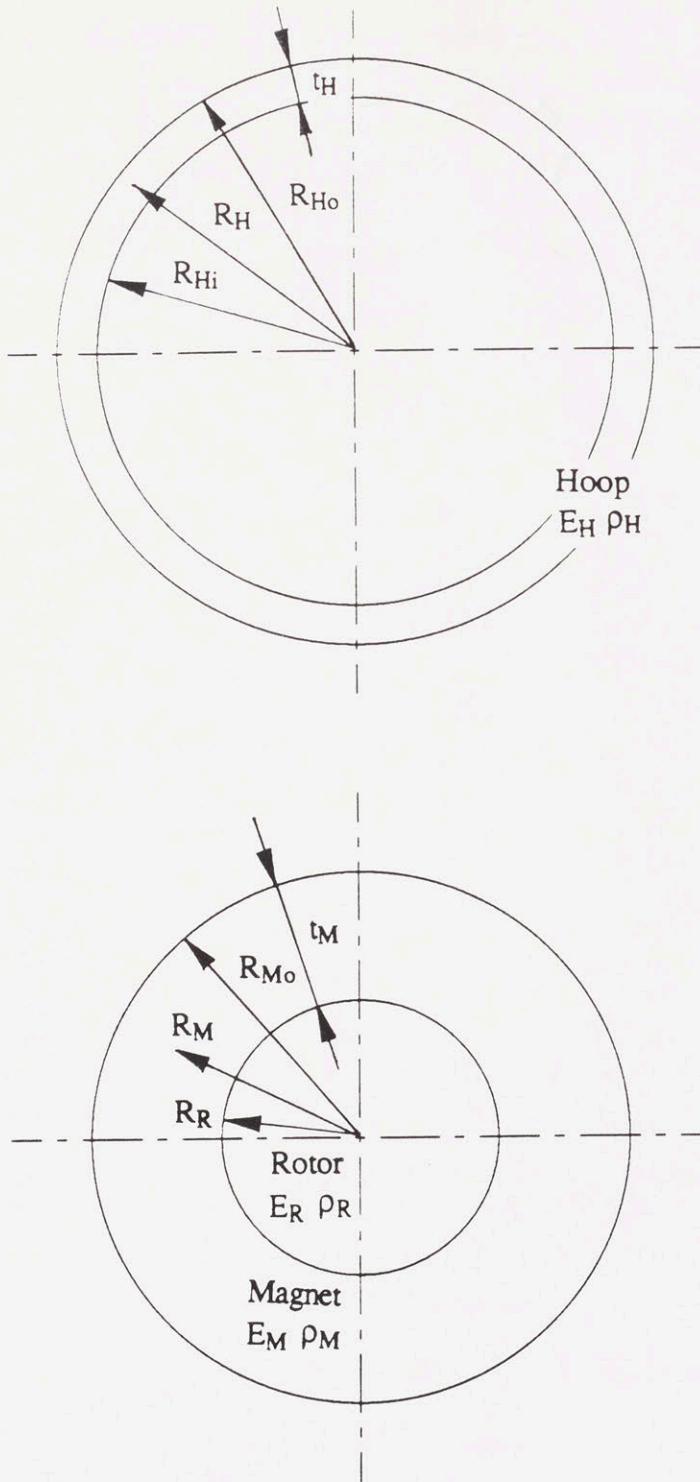


Figure 2-2 Geometry of the Hoop and the Rotor

rotating, the hoop is pressure fitted. By geometry, the hoop inner radius must equal the magnet's outside radius. The amount of deformation of the hoop due to the pressure fitting can be found by modelling this situation as a thin hoop under internal pressure [Reference 13]. The amount of deformation of the magnet and the rotor can be found from modelling this situation as an elastic rotor deformation under external pressure [Reference 16]. The resulting equation is

$$R_{M_o} - P \left\{ \frac{R_R}{E_R} (1 - \nu_R) + \frac{R_{M_o} - R_R}{E_M} (1 - \nu_M) \right\} = R_{Hi} + \frac{P R_{Hi}^2}{t_H E_H} \left( 1 + \frac{t_H}{2 R_{Hi}} \right) \quad (1)$$

Where  $P$  is the prestress,  $R_R$  is the rotor middle radius,  $R_{M_o}$  is the magnet outside radius,  $R_{Hi}$  is the hoop inside radius,  $E_R$  is the hoop's Young's modulus,  $E_M$  is the magnet's Young's modulus,  $E_H$  is the hoop's Young's modulus,  $\nu_M$  is the magnet's Poisson's ratio,  $\nu_R$  is the rotor's Poisson's ratio, and  $t_H$  is the thickness of the hoop. When the rotor of the integrated hermetic compressor-motor unit is rotating, the hoop experiences additional internal pressure due to the centrifugal force of the magnet and the rotor of the integrated hermetic compressor-motor unit. The resulting radial expansion of the hoop due to the rotation becomes

$$\delta_{Expansion} = \frac{(P + \rho_M t_M R_M \omega^2) R_{Hi}^2}{t_H E_H} \left( 1 + \frac{t_H}{2 R_{Hi}} \right) + (1 - \nu_R) \frac{\rho_R \omega^2 R_R^3}{4 E_R} \quad (2)$$

Where  $\delta_{Expansion}$  is the radial expansion of the hoop,  $\rho_M$  is the density of the magnet, and  $\omega$  is the rotational speed. For the magnet to be attached to the rotor geometrically, the expansion of the hoop after the rotation should be smaller than the deformation of the rotor due to the centrifugal force. This relation can be expressed as

$$\frac{1 - 2\nu_R + \nu_R^2}{1 - \nu_R} \left( \frac{\rho_R \omega^2 R_R^3}{4 E_R} \right) + \frac{(\rho_M t_M R_M \omega^2) R_{Hi}^2}{t_H E_H} \left( 1 + \frac{t_H}{2 R_{Hi}} \right) \leq K_1 P \left\{ \frac{R_R}{E_R} (1 - \nu_R) + \frac{R_{M_o} - R_R}{E_M} (1 - \nu_M) \right\} \quad (3)$$



where  $K_1$  is a safety factor ( $K_1 < 1$ ). For the safe operation of the integrated hermetic compressor-motor unit, the hoop has to satisfy one more relation. The tangential strain due to the centrifugal force should remain within the strain limit of the hoop material. This can be expressed as

$$\frac{1}{R_{Hi} + \frac{t_H}{2}} \left\{ \frac{1 - 2\nu_R + \nu_R^2}{1 - \nu_R} \left( \frac{\rho_R \omega^2 R_R^3}{4 E_R} \right) + \frac{(P + \rho_M t_M R_M \omega^2) R_{Hi}^2}{t_H E_H} \left( 1 + \frac{t_H}{2 R_{Hi}} \right) \right\} \leq K_2 \frac{\sigma_Y}{E_H} \quad (4)$$

where  $\sigma_Y$  is the elastic stress limit of the hoop,  $\rho_R$  is the density of the rotor, and  $K_2$  is a safety factor ( $K_2 < 1$ ). The equation derived above are nonlinear in three variables, the hoop inner radius  $R_{Hi}$ , the hoop thickness  $t_h$ , and the amount of prestress  $P$ . Solving these equations directly would be painful if not impossible. Instead of solving these sets of equations directly, an iterative solution that will satisfy equation (1) and two inequalities (3) and (4) has been chosen. The basic idea of this iterative solution is to try two values of  $R_{Hi}$  and  $t_h$ . With these two values, the prestress  $P$  can be found by equation (1). This iteration will be continued until  $R_{Hi}$ ,  $t_h$ , and  $P$  satisfy two inequality equations, (3) and (4).

### 2.1.2. Finite Element Model for the Hoop Stress Analysis

The iterative design procedure shown in the previous sections is expected to be sufficient for this stage of the design. For the future design, however, an advanced finite element model might be necessary. A prototype finite element model for the motor has, therefore, been developed. To simplify the problem we modelled the motor as a three component structure consisting of a rotor and magnet, dummy material to fill the gap between the magnets, and a hoop element. Furthermore, I have assumed that the rotor and the magnet are long enough so that the stress in the axial direction can be neglected. This

situation can be modelled as a flat disk with plane strain condition. Through symmetry, we need to consider only one quarter of the whole disk. This finite element model has been implemented in ADINA and the source file is listed in Appendix 2. Most of the ADINA input file uses the basic concept of ADINA, such as input nodes or lines. Readers who are familiar with ADINA can understand this input file without difficulty. I would like to

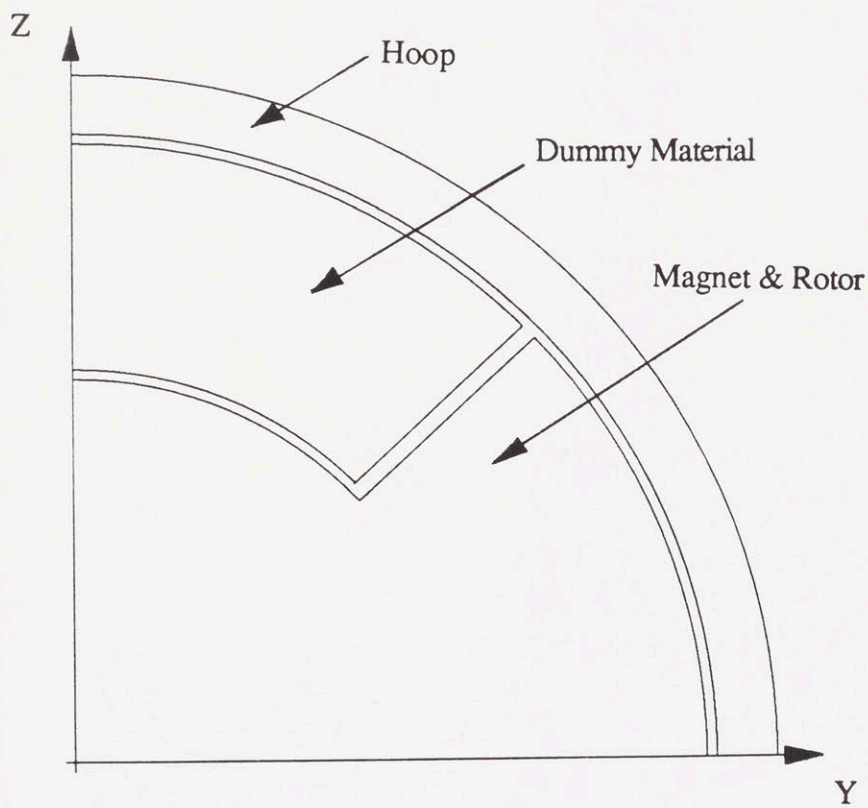


Figure 2-3 Schematic Diagram of the Finite Element Model

mention two points which may cause confusion. The first point is about node 10 in Figure 2-3a. Since each element group must be properly supported [Reference 20] (i.e. no rigid body motions are allowed), a spring which has a very small spring constant is attached between node 10 and the ground node 21 to remove the rigid body mode in the z-direction for the dummy material. The second point is about the contact surfaces between the magnet, the dummy material, and the hoop [Reference 20]. A generic node of 2 dimensional contact surface cannot belong to more than one contact surface. Node 16 in Figure 2-3a cannot be used for two contact surfaces and we introduce another node 23 at the same physical position. As a result, the shape after deformation shows that the dummy material edge has gone into the hoop space which is physically unreasonable but unavoidable due to the modelling limitations. As far as the topology of the motor (i.e. the relative positions of the magnet and rotor, the dummy material, and the hoop), it is the same as the finite model shown in this section, the change of the specific size or the material data in ADINA input file is a trivial problem. Because of this, only one prototype ADINA input file is listed in Appendix 2.

ORIGINAL XVMIN 0.  
 0.003795 XVMAX 0.04300  
 YVMIN 0.  
 YVMAX 0.04300

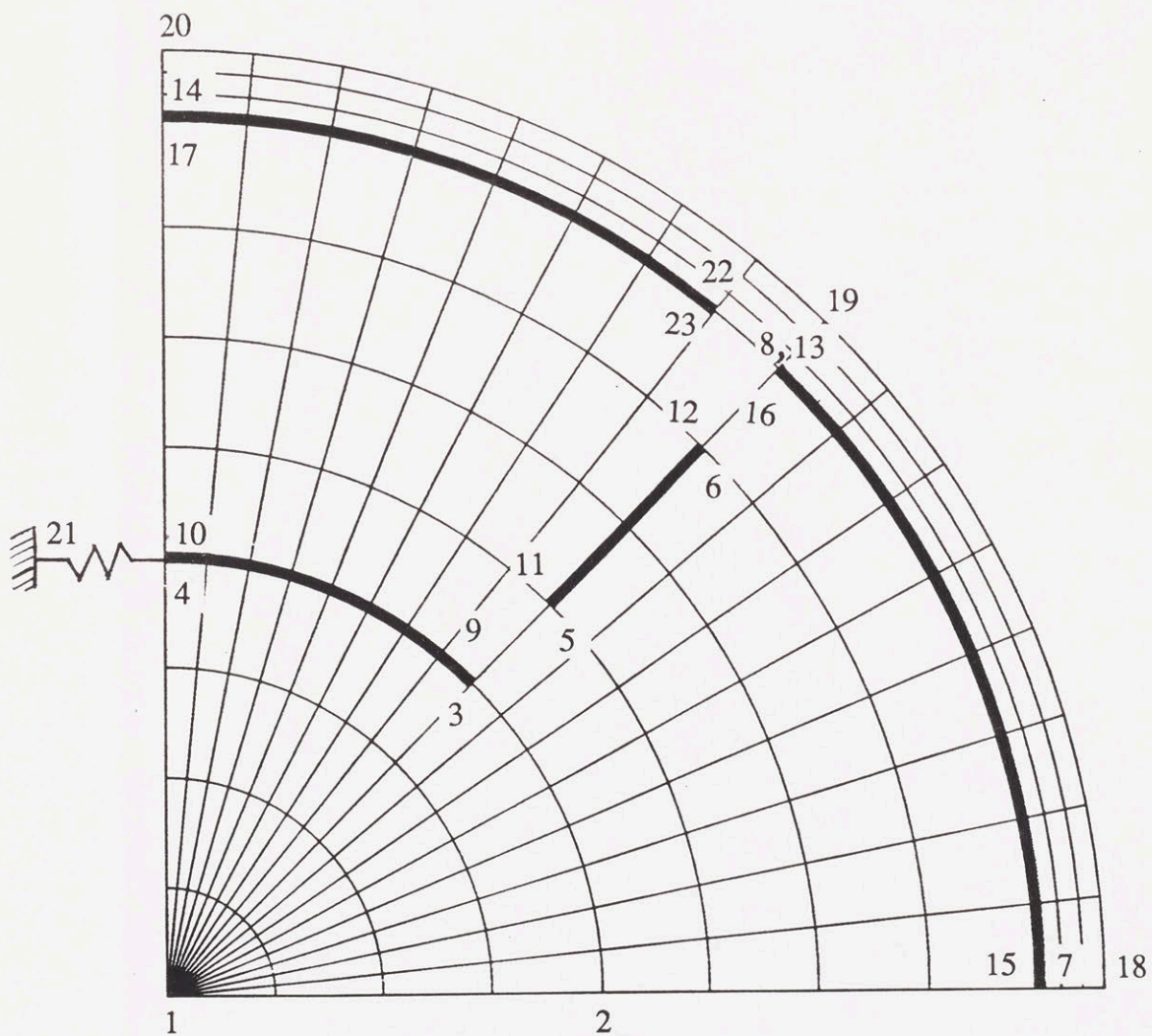


Figure 2-4 Finite Element Model Before Deformation

ADINA-PLOT VERSION 4.0.2, 21 APRIL 1992  
PR1 - PLANE STRAIN CYLINDER

ADINA	ORIGINAL	DEFORMED	XVMIN	-0.0004488
LOAD_STEP	└─┘	└─┘	XVMAX	0.04383
TIME 1.000	0.003448	0.0008856	YVMIN	-2.660e-05
			YVMAX	0.04645

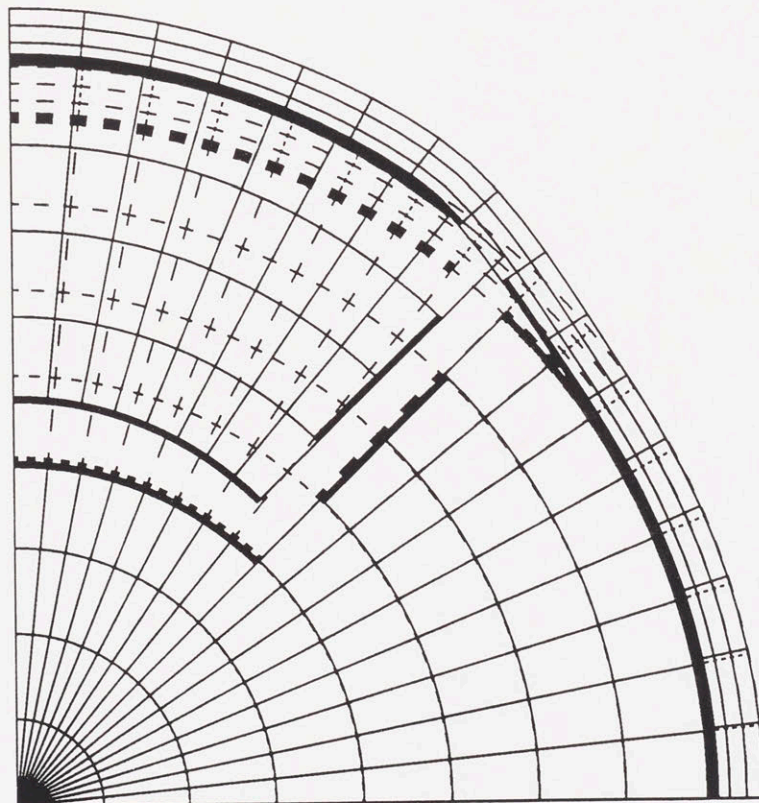


Figure 2-5 Finite Element Model After Deformation

## 2.2. Critical Speed Analysis

When a rotor is rotating at its resonant frequency, a small disturbance can be amplified large enough to destroy the rotor structure. It is therefore desirable to avoid operating at resonant frequency, which is called the critical speed. The critical speed can be found by equating the kinetic energy due to the rotation with the potential energy due to the load on the rotor [Reference 4]. In order to find the potential energy and kinetic energy, the deflection due to the distributed mass of the rotor itself must be found first. This deflection can be found by modelling the rotor as an elastic bar with distributed mass and calculating

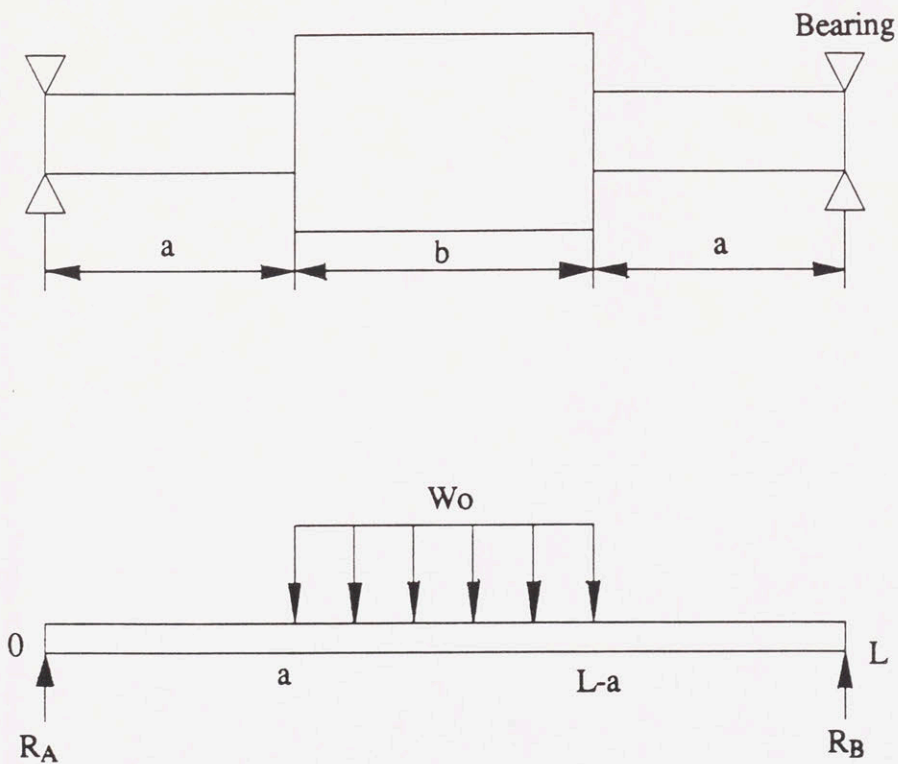


Figure 2-6 Free Body Diagram of the Rotor

the bending moment of the bar. From the stress-strain relation, the deflection can be found as

$$y = \frac{1}{EI} \left\{ \frac{b \times W_o}{12} x^3 - \frac{W_o}{24} (x-a)^4 + C_1 x \right\} \quad (5)$$

$$C_1 = -\frac{R_A(2a+b)^2}{6} + \frac{W_o(a+b)^4}{24(2a+b)} + \frac{W_o a^4}{24(2a+b)}$$

Where  $W_o$  is the weight per unit mass of the rotor,  $y_i$  is the deflection of the rotor, and  $R_A$  and  $R_B$  are the reactions of the bearings. Using this deflection, we can find the kinetic energy and potential energy of the rotor. The potential energy becomes

$$E_P = \sum_{i=0}^N \frac{y_i W_i}{2} \quad (6)$$

The kinetic energy becomes

$$E_K = \frac{\omega^2}{2g} \sum_{i=0}^N y_i^2 W_i \quad (7)$$

If there are no energy loss in the bar, the maximum potential energy  $E_P$  must equal the kinetic energy  $E_K$ .

$$\sum_{i=0}^N \frac{y_i W_i}{2} = \frac{\omega^2}{2g} \sum_{i=0}^N y_i^2 W_i \quad (8)$$

The critical speed using these kinetic and the potential energies for the distributed mass of the bar becomes

$$\omega = \sqrt{g \frac{\sum_{i=0}^{N-1} W_i y_i}{\sum_{i=0}^{N-1} W_i y_i^2}} \quad (9)$$

### 2.3. Design of the Centrifugal Compressor

This section describes the design procedure for the centrifugal compressor. This design procedure is based on a term project of a mechanical engineering course at M.I.T. (2.601J "Design of Thermal Power Systems"). Several modifications have been made to the term project to match my design purpose. The fundamental design procedure, however, is not new and the purpose of this section is to clarify the notations and design methods that I have used in my modified design procedure. Before we start to discuss the design procedure of the centrifugal compressor, it is appropriate to describe the geometry and function of the centrifugal compressor. The basic components of the centrifugal compressor in this design are the impeller, the vaneless diffuser, the vaned diffuser, and the volute. The impeller is the rotating part of the centrifugal compressor and transfers shaft work into the working fluid. The vaneless diffuser is converting the kinetic energy into pressure without causing a shock wave. The vaned diffuser is also converting the kinetic energy of the working fluid into pressure but the vaned diffuser increases the pressure more rapidly by the blades in its channel, which may cause a shock wave. The volute collects the working fluid from the exit of the vaned diffuser and transfers the working fluid into the condenser. The design procedure starts from relating the enthalpy difference of the compressor inlet and outlet with the stagnation temperatures from the inlet and the outlet of the compressor. This can be achieved by using the first law of thermodynamics in the bulk flow case.



$$h_{02} - h_{01} = C_p (T_{02} - T_{01}) = \xi u_2^2 \quad (10)$$

where  $\xi$  is the slip factor,  $h_{01}$  is the enthalpy at inlet,  $h_{02}$  is the enthalpy at outlet,  $u_2$  is the blade tip speed. The slip factor is a proportionality factor to compensate for the swirl in the opposite direction of the impeller rotation, caused by the conservation of angular momentum. The next step is to find the dimensions of the impeller. The important basic

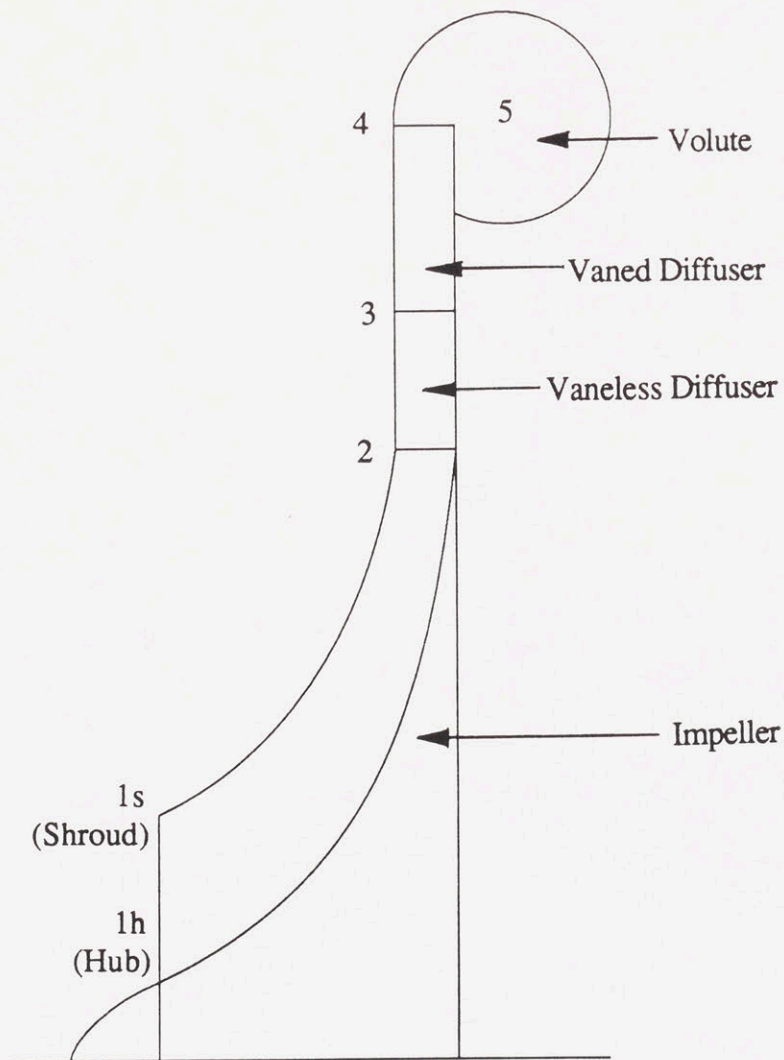


Figure 2-7 Schematic Diagram of the Centrifugal Compressor

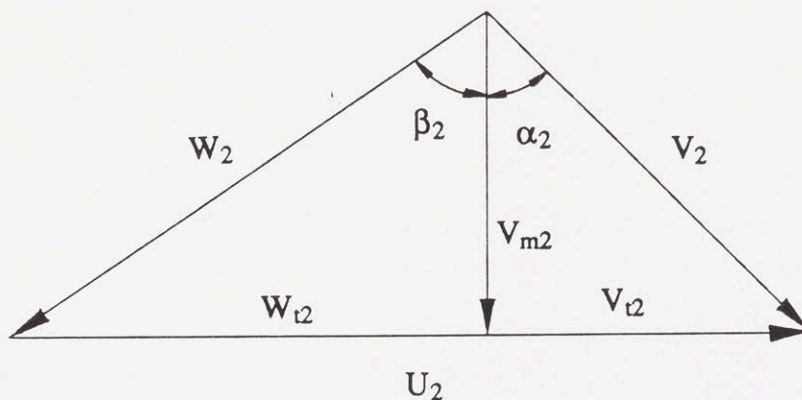
dimensions are the hub radius  $r_{1h}$ , the shroud radius  $r_{1s}$ , the impeller radius  $r_2$ , and the impeller exit flow passage depth  $b$ . The impeller exit radius can be found from the basic relation between the rotational speed and tangential velocity in circular motion, which is

$$r_2 = \frac{60u_2}{2\pi N} \quad (11)$$

The hub radius is assumed to be a certain fraction of the impeller radius. [Reference 67]. For large impellers the usual fraction is 0.2 and for smaller impellers the fraction will be larger than 0.2 depending on the size. The minimum hub radius should be large enough to withstand the torque transmitted by the shaft.

$$r_{1h} = C \times r_2 \quad \text{and} \quad C = 0.2 \text{ to } 0.45 \quad (12)$$

The shroud radius is selected so as to minimize the inlet relative mach number. The reason



- $V_2$  = Absolute Velocity at the Impeller Exit
- $V_{m2}$  = Absolute Meridional Velocity at the Impeller Exit
- $V_{t2}$  = Absolute Tangential Velocity at the Impeller Exit
- $W_2$  = Relative Velocity at the Impeller Exit
- $W_{t2}$  = Relative Tangential Velocity at the Impeller Exit
- $U_2$  = Blade Tip Speed at the Impeller Exit
- $\alpha_2$  = Absolute Velocity Angle
- $\beta_2$  = Relative Velocity Angle

Figure 2-8 Velocity Triangle of the Impeller Exit

for minimizing the inlet relative mach number is to avoid a shock wave inside the impeller which may cause a large loss of energy. Once the hub radius, the shroud radius, and the impeller radius are determined, the velocity triangle of the impeller exit can be found from simple trigonometry as shown in Figure 2-7. The impeller exit flow passage depth can be found from the mass conservation of the impeller exit

$$b = \frac{m}{2\pi r_2 \rho_2 v_2 \cos \alpha_2} \quad (13)$$

Where  $b$  is the impeller exit flow passage depth,  $m$  is the mass flow rate,  $\rho_2$  is the density,  $v_2$  is the absolute velocity,  $r_2$  is the radius,  $\alpha_2$  is the absolute velocity angle. After the basic dimensions of the impeller are found, the diffuser dimensions and its velocity triangles have to be determined.

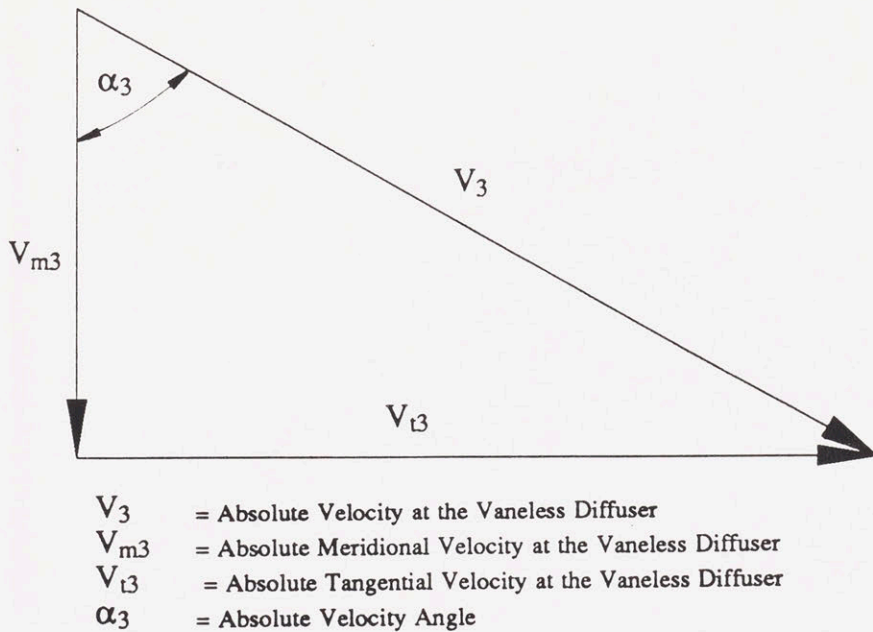


Figure 2-9 Velocity Triangle at Vaneless Diffuser Exit

The vaneless diffuser has to reduce the velocity of the fluid exiting the impeller until the mach number drops sufficiently to prevent a shock wave. A suggested Mach number at the exit is 0.8 or 0.9 times the mach number of the impeller exit if that product is less than 0.8 [Reference 67]. From this mach number, the velocity triangle at the vaneless diffuser exit can be completed. By using conservation of angular momentum, the radius of the vaneless diffuser can be found as

$$r_3 = r_2 \frac{v_2 \sin \alpha_2}{v_3 \sin \alpha_3} \quad (14)$$

The radius of the vaned diffuser can be found from the mass conservation and the sine rule

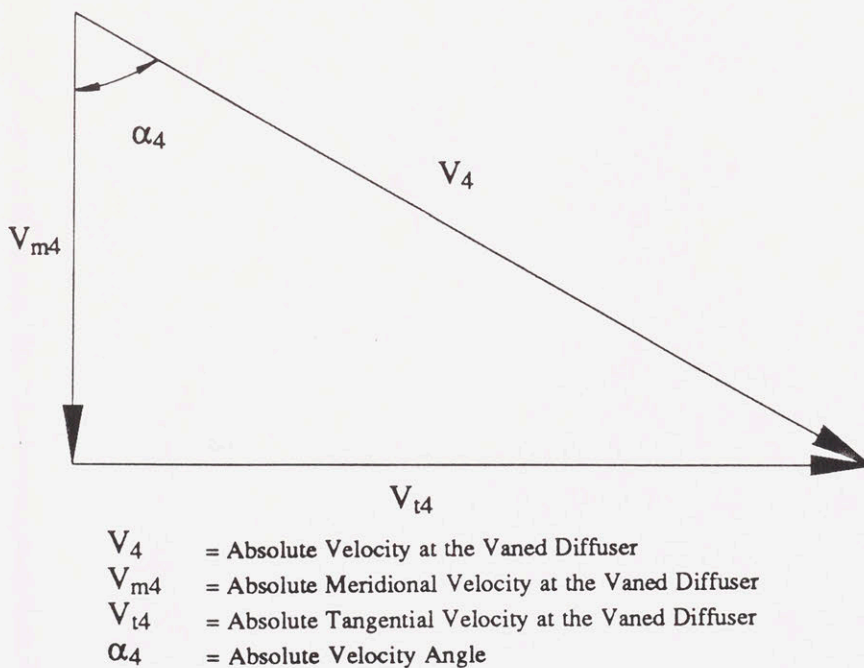


Figure 2-10 Velocity Triangle at Vaned Diffuser Exit

for the vaned diffuser section.

$$r_4 = r_3 \frac{v_3 \sin \alpha_3}{v_4 \sin \alpha_4} \quad (15)$$

and

$$\alpha_4 = \arctan\left(\frac{\rho_4 v_4}{\rho_3 v_3} \tan \alpha_3\right)$$

Again, the other components of the velocity triangle can be found through simple trigonometry.

The last component of the centrifugal compressor is the volute. The significant parameter in the volute are the exit area and the exit velocity of the volute. The exit velocity of the volute can be found from the conservation of angular momentum which gives us,

$$v_5 = v_{t4} \quad (16)$$

The exit area of the volute can be found from the mass conservation of the volute

$$(\text{Volute exit area}) = \pi r_{\text{Volute}}^2 = \frac{m}{\rho_5 v_5} \quad (17)$$

The single stage centrifugal compressor design is completed at this point. Each stage of the two stage centrifugal compressor can be designed in similar manner as we did for the single stage centrifugal compressor design. There are several differences, however between the single stage centrifugal compressor design and two stage centrifugal compressor design. The two stage centrifugal compressor has no volute in the first stage. Instead, between the first stage and the second stage there is a return channel which connects both stages. In addition, the velocity of the first stage exit is selected to equal to the second stage inlet. By matching these two velocities, the dimensions of the first stage vaned diffuser will be slightly changed.

So far I have described the basic design methods for designing the hoop of the rotor for the integrated hermetic compressor-motor unit, for finding the critical speed, and for the centrifugal compressor. These methods are implemented in a computer program found in

Appendix D and are used in designing the integrated hermetic compressor-motor unit shown in Chapter 4.

## Chapter 3. SELECTION OF THE REFRIGERANT

### 3.1 Background

One of the important tasks in designing air conditioning systems is the selection of the working fluid (i.e. refrigerant). For a given type of thermodynamic cycle, the refrigerant determines several important design parameters such as mass flow rate, pressure ratio, and inlet and outlet thermodynamic properties (temperature, pressure, enthalpy) for each component of the air conditioning system. This chapter will discuss the effect of the refrigerant on the centrifugal compressor's impeller. The effect of the refrigerant on other components such as the condenser, the evaporator, and the bearings will be discussed briefly in Chapter 5. The refrigerant has an important effect on the overall performance of the air conditioning system, and therefore, the characteristics of a desirable refrigerant have

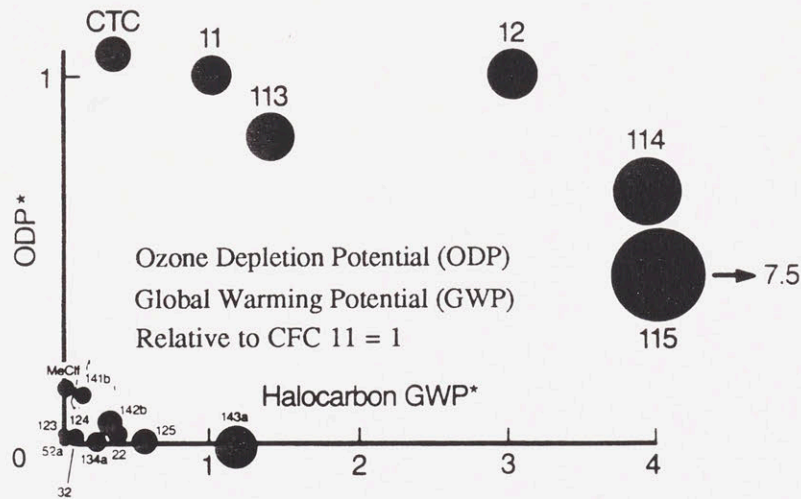


Figure 3-1 Ozone Layer Depletion and Global Warming Potential of Various Refrigerants : Data from Reference 36

been studied for many years. One such study was presented in the American Society of Heating, Refrigerating and Air-conditioning Engineers (ASHRAE) Journal [Reference 62] This study suggests that for centrifugal compressors, refrigerants should have acceptable cycle efficiencies, fairly large specific volumes, and reasonable "head" or "lift" characteristics. If they are nontoxic, nonflammable, and chemically stable, they are ever better [Reference 62]. In the last decade, much effort has been made in the characteristics of the chemical stability of the refrigerants, especially where they might be linked to the depletion of the earth's ozone layer and global warming. A recent study shows that the Chlorofluorocarbons (CFC) based refrigerants, such as Freon which has been widely used in air conditioning and refrigeration, have high ozone depletion and global warming potential [Reference 36].

As a result of the above concerns, the Montreal protocol was amended in 1990. This protocol is an international agreement among governments, scientists, industry, and environmental groups to regulate the use and production of CFCs. According to the Revised Montreal Protocol, the complete phaseout of CFC production will be made by the year of 2000 [Reference 36]. Due to the protocol, this chapters study of the impacts of refrigerants on the performance of air conditioning systems, will be concentrated on the Hydrofluorocarbons (HFC) and Hydrochlorofluorocarbons (HCFC) refrigerants. The CFC refrigerants will be studied only for comparison. These HFC and HCFC refrigerants have lower ozone layer depletion and global warming potentials and they are expected to substitute the CFC based refrigerants.

### **3.2. Refrigerant Selection Procedure Description**

To study the effects of the refrigerants on the impeller size, a single stage vapor-compression refrigeration cycle has been selected. Each refrigerant has been analyzed



according to the following thermodynamic cycle for a given condensation temperature and evaporation temperature.

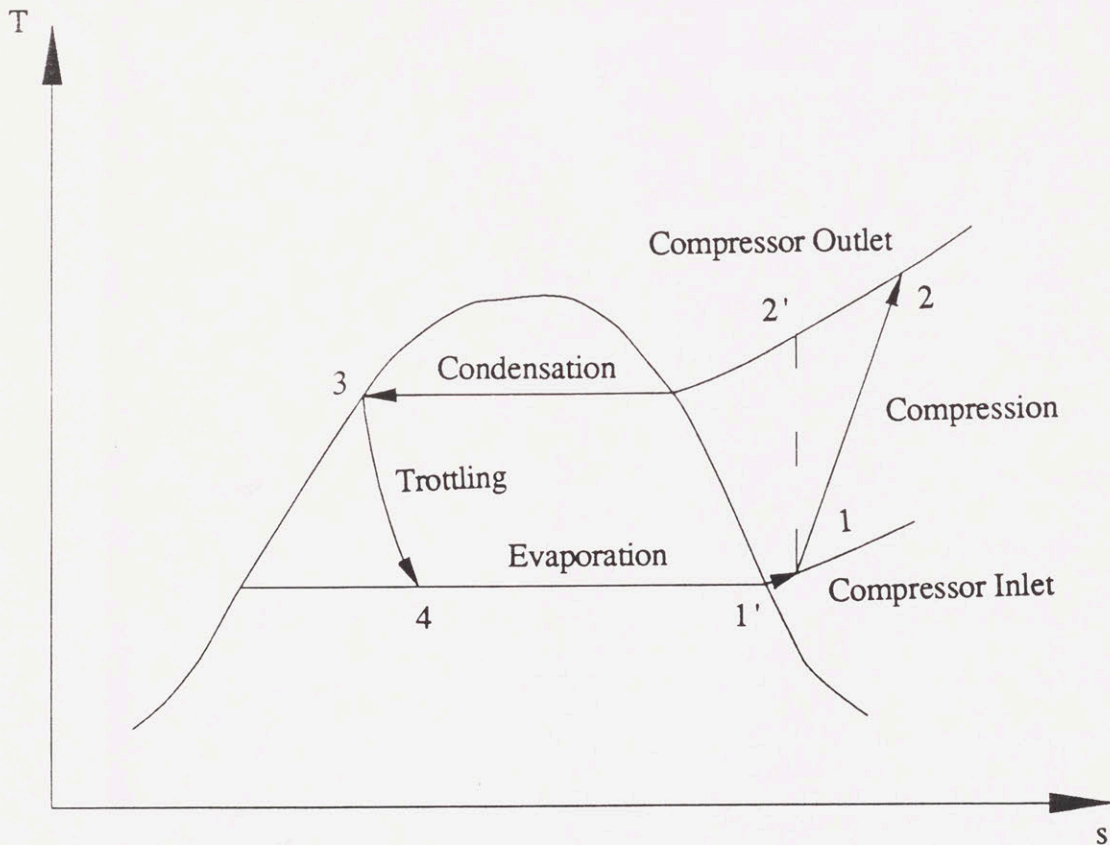


Figure 3-2 Single Stage Vapor-Compression Refrigeration Cycle

As a result, the inlet and outlet thermodynamic states can be evaluated. These inlet and outlet thermodynamic states will be used as input information for the centrifugal compressor design procedure described in Chapter 2. As a result, the basic geometrical configuration of a single stage centrifugal compressor will be evaluated. The result of the impeller size for each refrigerant can be compared to select the most desirable refrigerant for our design purpose.

### 3. Result of the Study

The study of the impact of various refrigerants on the centrifugal compressor's impeller size shows that the impeller blade tip height is very small compared to the impeller diameter. The size of the impeller blade tip height varies from 0.1mm to 1.0mm depending on the refrigerant. This is undesirable because the extremely small size is expected to increase the machining cost. The small aspect ratio of blade tip height to the impeller radius is undesirable because it is expected to have an adverse effect on compressor efficiency due to the large amount of friction loss. Due to these considerations steps have been taken to find a refrigerant that yields the largest impeller blade tip height and the largest aspect ratio.

Figure 3-3a shows the inlet density versus impeller exit blade tip height. This suggests that R113 and R123 yield fairly large exit blade tip heights compared to the other refrigerants. An interesting feature can be found from comparing Figure 3-3a through Figure 3-3c. The distribution of the datapoints for the three figures are almost the same and we can conclude that by selecting the refrigerant which has the largest specific speed, we will automatically selecting the refrigerant which has the most favorable aspect ratio and the largest blade tip height. As a conclusion, although R113 yields the largest blade tip size, we can see in Figure 3-1 that R113 has a high ozone layer depletion and global warming potentials. Consequently, R123, which yields the second largest blade tip size among the refrigerants investigated, is expected to be the most appropriate refrigerant for our design purpose.

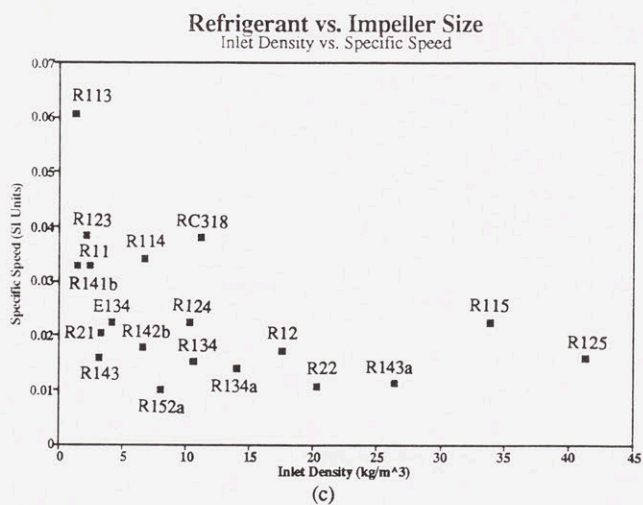
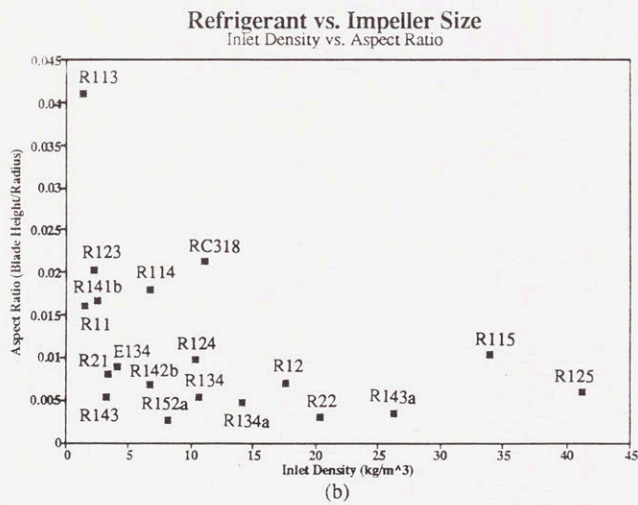
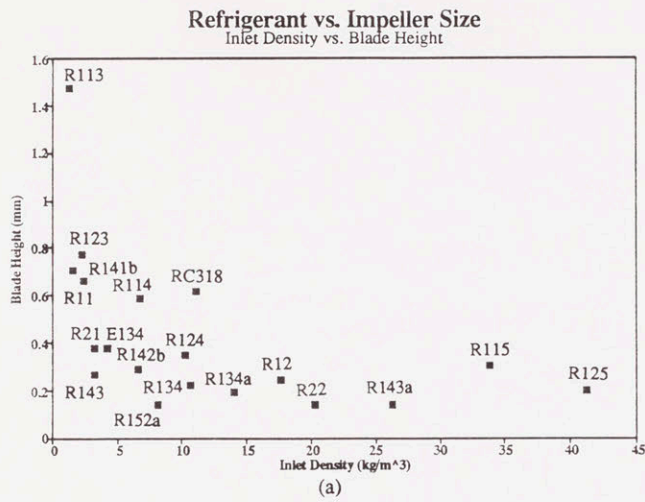


Figure 3-3 Impeller Size for Various Refrigerants

## **4. DESIGN OF A HERMETIC COMPRESSOR-MOTOR UNIT**

### **4.1. Overview.**

With the tools developed in Chapter 3, a design for the hermetic compressor-motor unit can be completed. Besides the design tools described previously, information on electrical motor and compressor efficiency have been added. The electrical design of the hermetic compressor-motor has been provided by LEES and the aerodynamic efficiency data of the hermetic compressor has been produced by using a computer program "COMPAL" made by Concepts, ETI. By comparing and compromising the electrical aspects and the mechanical aspects of the hermetic compressor-motor unit, an optimized design can be produced. In this chapter an optimized design of the hermetic compressor-motor is provided. The overall design procedure can be divided into three steps. The first step is to select appropriate values for the thermodynamic cycle. This step includes selecting the evaporation temperature, condensing temperature, overall pressure ratio, etc. The second step is to select an appropriate range of rotational speeds for the hermetic compressor-motor unit. The third step is to determine the basic dimensions of the motor and the compressor and devise an appropriate layout for the geometric configuration of the integrated hermetic compressor-motor unit. At the end of this chapter, an exemplary diagram of the integrated hermetic compressor-motor unit will be shown.

### **4.2. Establishing the Parameters in the Thermodynamic Cycle.**

Determining the appropriate thermodynamic cycle and the parameters of the thermodynamic cycle are the most important tasks in this hermetic compressor-motor design. Most of the input information of the compressor design comes from the

thermodynamic cycle. By selecting the thermodynamic cycle and the parameters of the thermodynamic cycle, an inherent limit is given no matter how well the detailed compressor design is conducted.

The first task is to determine the evaporation temperature and the condensation temperature of the vapor-compression refrigeration cycle. These numbers have been selected by referring to Reference 44. According to this report, for a hot summer day of 37 C, the design point condensation temperature is set to 48 C, and the design point evaporation temperature is set to 5 C. In my design, a conservative assumption has been made to reduce the future potential problems of heat exchanger design because a detailed cooling load and heat exchanger analysis has not yet been completed. The design point condensation temperature has been set as 49 C and the evaporation temperature has been set as 0 C.

Once the condensation temperature and the evaporation temperatures have been chosen, the overall pressure ratio can be evaluated. By using the refrigerant selected in Chapter 3, the inlet pressure of the compressor is 33 kPa and the outlet pressure is 205.8 kPa; the overall pressure ratio is approximately 6.2. This is rather a high pressure ratio for a single stage design. By a brief evaluation of the basic dimensions using the design methods provided in Chapter 3, the single stage design turns out to be inappropriate. The reason is because the impeller exit gap is too small compared to the impeller radius. This is expected to yield a poor performance due to the high friction loss. To solve this problem, a two stage design has been selected instead of a single stage design. In order to cool the motor windings and the refrigerant at the first stage compressor exit, an intercooling stage has been introduced. This intercooling stage is achieved by feeding back the refrigerant from the condenser exit and injecting this refrigerant into the return channel between the first stage and second stage compressor. The schematic temperature-entropy diagram is provided in Figure 4-1. Notice that the temperature increases after the first stage compression, due to the cooling of the motor winding.

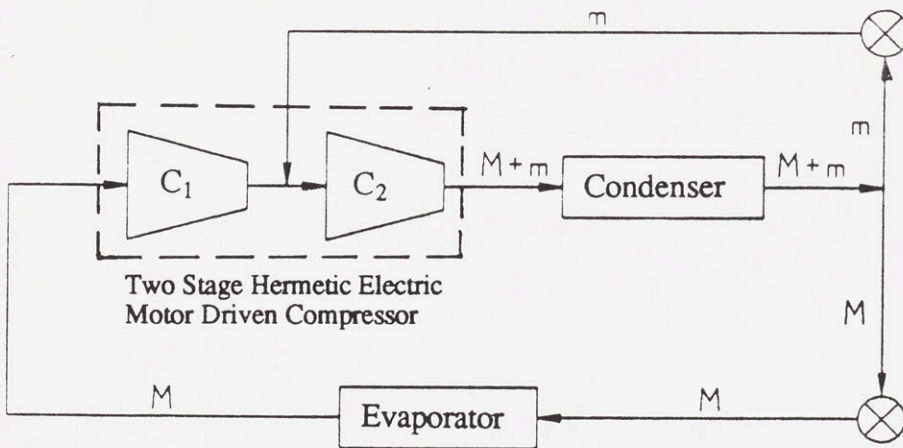
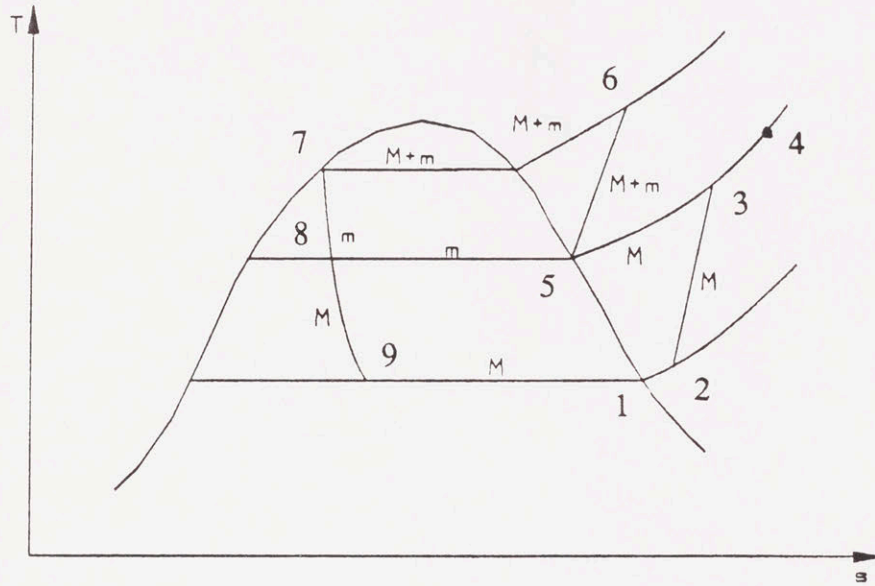


Figure 4-1 Two Stage Vapor-Compression Refrigeration Cycle

The next step is to determine the pressure ratio of each compression stage, which can be determined by comparing the specific speed of each stage of the compressor. The proper choice of a pressure ratio for each stage will be where the specific speed becomes the same in both compression stages because the specific speed indicates the relative size of the impeller. By having a similar value of specific speeds, we can achieve similarly shaped compressors for both stages.

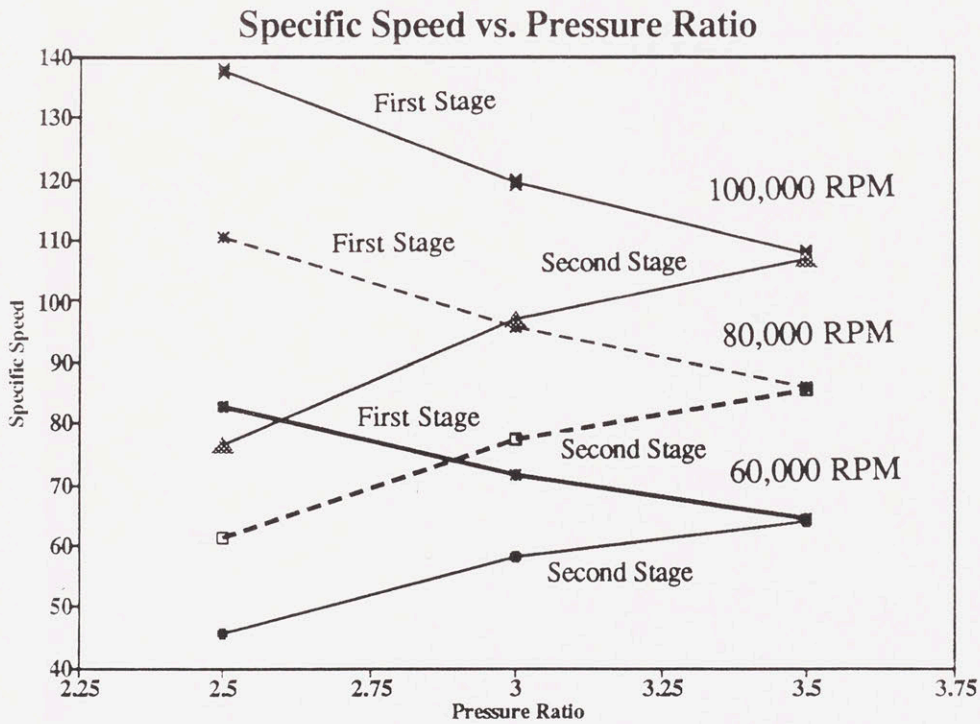


Figure 4-2 Pressure Ratio versus Specific Speed Diagram

As we can see in Figure 4-2, the specific speed of each stage approaches one value approximately at a pressure ratio of 3.5 for the each stage. The right choice of the pressure

ratio will be 3.5 for the first stage. The overall pressure ratio is given as 6.2, hence the pressure ratio for the second stage is 1.77.

### 4.3. Selection of the Rotational Speed.

Once the thermodynamic cycle is determined, the rotational speed has to be determined in order to have enough information for the compressor design input. The rotational speed is an important variable for both compressor and motor design, especially in terms of size and performance. The rotational speed of the integrated hermetic compressor-motor unit has to be determined by considering the size and efficiency of the compressor and the motor design. Figure 4-3 shows specific speed versus efficiency. The efficiency of

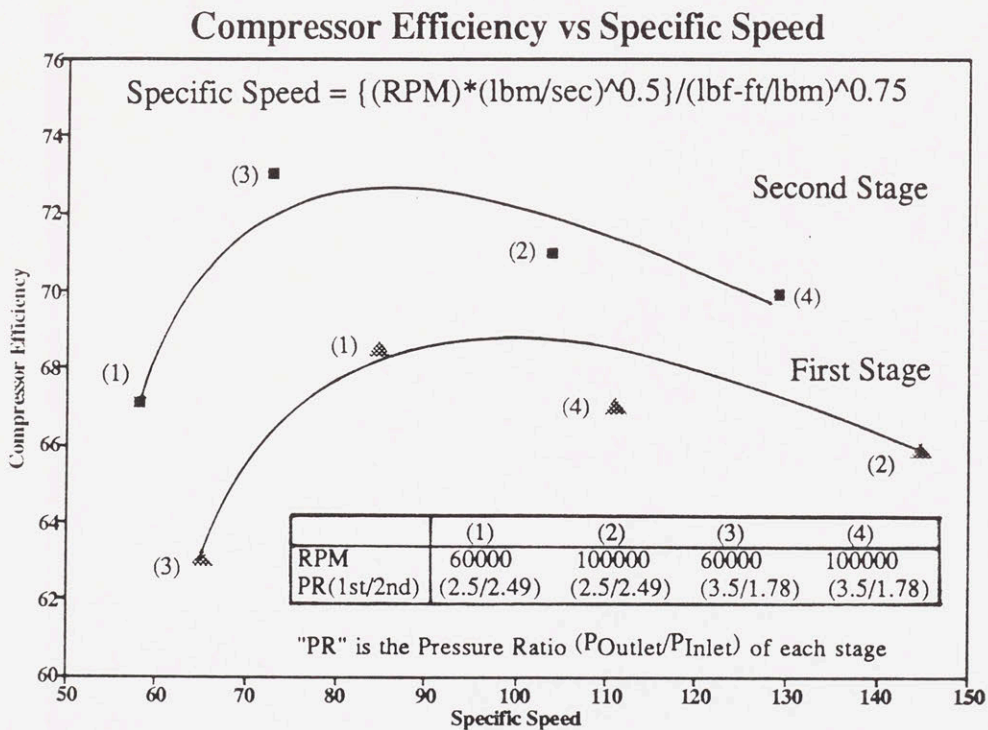


Figure 4-3 Specific Speed versus Compressor Efficiency Diagram



the first stage drops significantly at speeds below 60000 rpm. This indicates that in order to achieve good performance, the rotational speed has to be larger than 60000 rpm. From the figure we can also see that the efficiency drops at high rotational speeds, say 100000 rpm. The efficiency drop at high speed is expected due to the high relative mach number at the impeller inlet. For moderately high rotational speed, the relative inlet mach number remains below 1, and no shock wave loss is induced. For higher rotational speeds, the relative inlet mach number is over 1 and an additional loss due to the shock wave is expected. In the aerodynamic design point of view, the rotational speed of the integrated hermetic compressor-motor unit should remain in the range of 60000 rpm to 100000 rpm.

In the motor design point of view, a different rule applies. The data provided from LEES, has been plotted in Figure 4-4. This figure shows that the efficiency decreases as

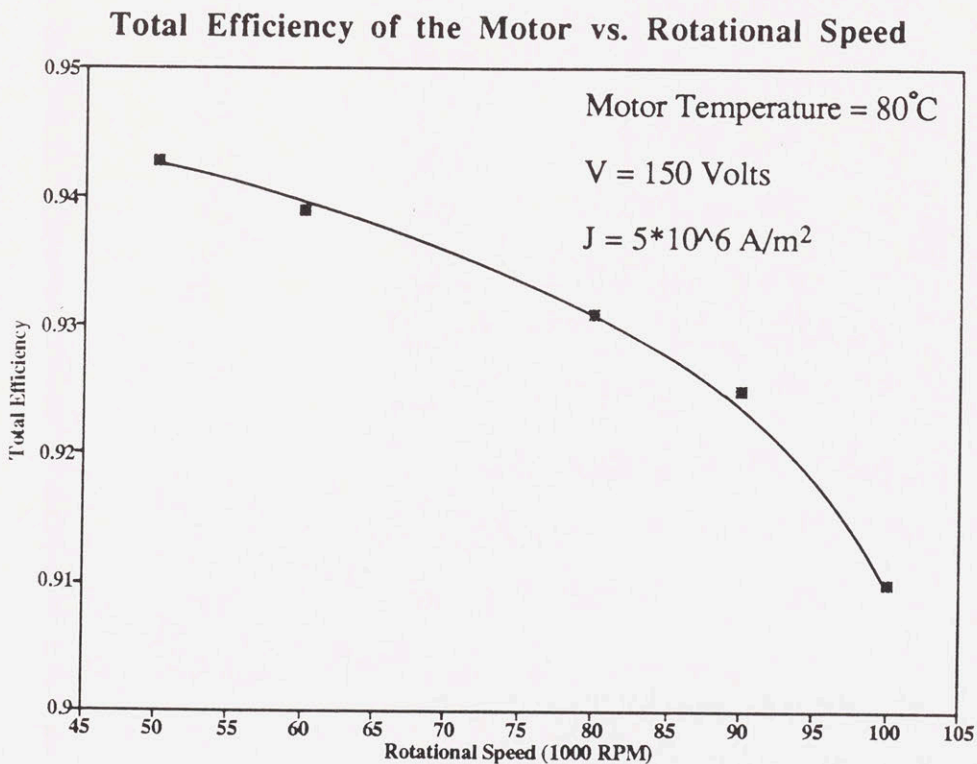


Figure 4-4 Rotational Speed versus Motor Efficiency Diagram

the rotational speed increases. The decrease in efficiency becomes larger at high rotational speeds. This suggests, in the motor design point of view, that the rotational speed must remain below 90000 rpm to achieve a good motor performance. In order to achieve a good performance in integrated hermetic compressor-motor design, the rotational speed must, therefore, remain in the range of 60000 to 90000 rpm.

One more interesting comment on this performance study is on Reynolds number. Although the second stage has a smaller aerodynamic passage due to its higher density, the efficiency is still higher than the first stage. This is due to the high Reynolds number in the second stage. The second stage has approximately 50% larger value of Reynolds number than the first stage, which yields a significantly lower friction coefficient in the second stage than the first stage.

#### **4.4. Geometric Configuration.**

From the given thermodynamic information at the inlet and outlet of each compressor stage and the rotational speed, the basic dimensions of the compressor can be determined. The basic dimensions of the motor are provided by LEES for a given rotational speed. With the basic dimensions of the compressor and the motor, a geometrical configuration has to be made. The first concern is the layout of each compressor stage. In order to reduce the length of the aerodynamic passage, each compressor is connected in series facing the first stage compressor outlet with the second stage inlet. This is considered to be better than facing each compressor stage back to back because a back to back configuration yields longer aerodynamic passages which yield more friction loss in the passage. The next concern is combining the compressor with the electrical motor. The resulting dimensions of the second stage compressor is much smaller than the size of the rotor of the electrical motor. This suggests the idea of inserting the second stage of the compressor into the rotor of the electrical motor. The above ideas have been incorporated

in Figure 4-5. There are several interesting features in this diagram. The first feature is the connection between the interstage channel and the second stage inlet. The interstage channel goes axially through the motor where the second stage inlet is located. The second feature is, as mentioned earlier, the rotor of the motor forms the second stage compressor shroud. The third feature is the inter stage return channel has an liquid injection for the motor winding cooling and the inter stage cooling. The last feature is that the rotor structure is a multi component combined by a tension bolt, and more stages can be stacked by minor changes in the design configuration.

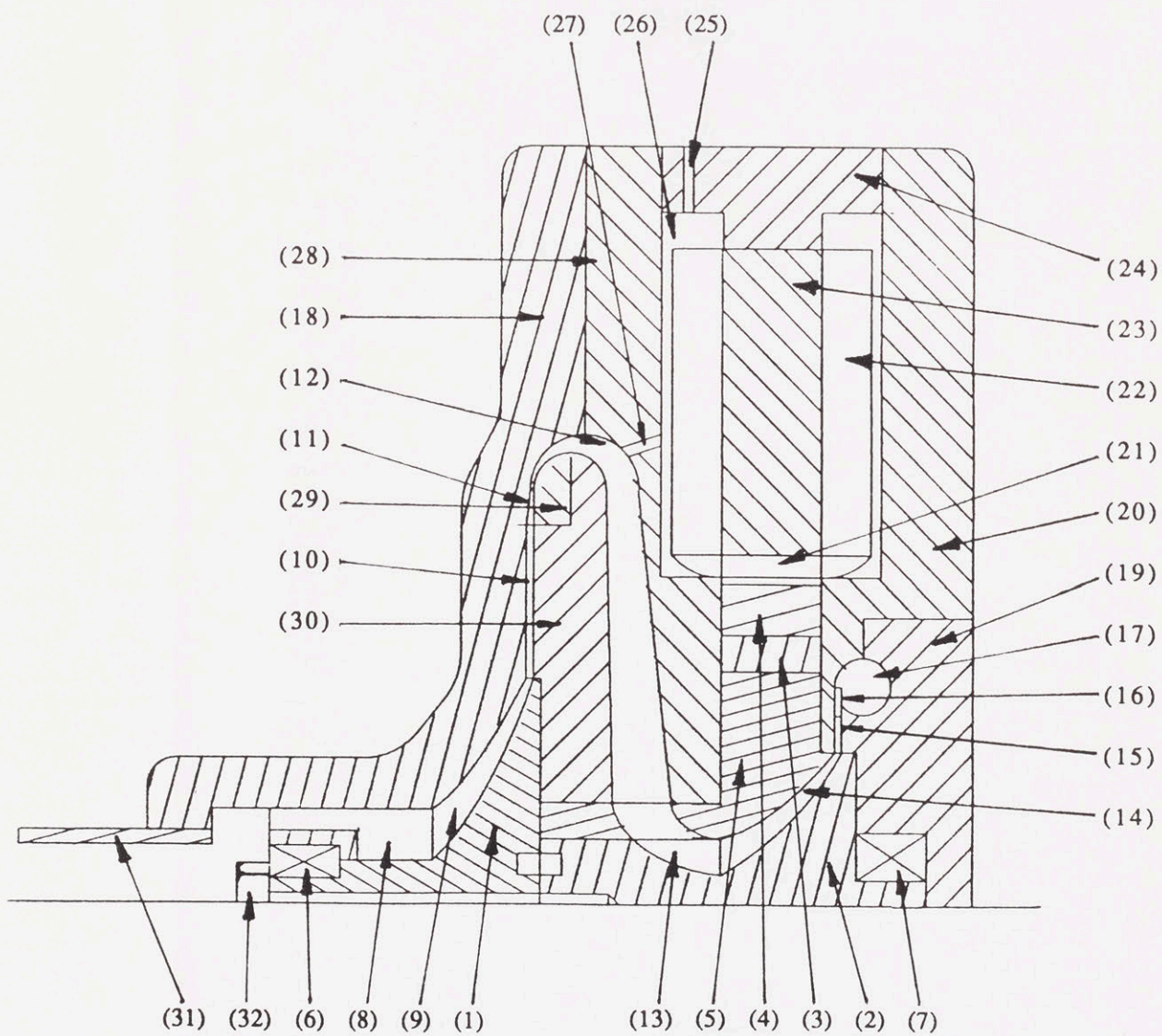


Figure 4-5 Schematic Diagram of the Integrated Hermetic Compressor-Motor Unit

- Single rotor
  - First stage impeller (1)
  - Second stage impeller (2)
  - Motor rotor
    - Permanent magnet (3)
    - Retaining hoop (4)
    - Back iron for return flux path and second stage shroud (5)
  - Bearings (6),(7)
- Suction inlet (8)
- First stage blade (9)
- First stage vaneless diffuser (10)
- First stage bladed diffuser (11)
- Interstage connecting passage (12)
- Second stage inlet path (13)
- Second stage blade (14)
- Second stage vaneless diffuser (15)
- Second stage bladed diffuser (16)
- Exit volute (17)
- Inlet side housing (18)
- Discharge side housing (19),(20)
- Motor stator
  - Windings (21)
  - End turns (22)
  - Laminated iron (23)
  - Stator housing (24)
- Liquid injection passage (25)
- Motor cooling passage (26)
- Injection port into interstage passage (27)
- Housing (28),(29),(30)
- Inlet pipe (31)
- Tension bolt (32)

Figure 4-5 (Continued) Description of the Integrated Hermetic Compressor-Motor Unit

## Chapter 5. FUTURE WORK

Despite the integrated hermetic compressor-motor unit having the interesting features mentioned in Chapter 4, the study of the other components of the airconditioning system, such as the evaporator, the condenser, and the bearings, has yet to be made to complete the airconditioner's design.

The evaporator and the condenser are expected to effect the condensation and the evaporation temperatures. When temperature differences between the environment and condenser or the room and the evaporator are increased, the size of the condenser or the evaporator can be decreased due to the increase in the heat transfer capacity for a given heat transfer area. The increase in in condensation temperature or the decrease in the evaporation temperature will induce larger shaft work in the compressor. This is due to the increase in the overall pressure ratio and will have an unfavorable effect on the compressor. The specific numerical relationship between the condenser's or the evaporator's size and the condensation or the evaporation temperatures requires further study.

The performance of the integrated hermetic compressor-motor unit is very sensitive to the clearance between the impeller and the housing, which is controlled by the bearing system. The bearings for the integrated hermetic compressor-motor unit are expected to have a significant effect on the efficiency of an airconditioning system. For example, the computer simulation data from Concepts, ETI (Appendix 5), shows that an increase in the clearance between the impeller and the housing, from 0.004" to 0.007 " causes a 6.3 % decrease in efficiency. Considering that 0.007" clearance is quite small in practice, the study of the bearing system will have to be carefully conducted in order to maintain a high efficiency.

Another important aspect of the airconditioning system design is the manufacturing of the impeller. The size of the impeller blade computed by Concept's "COMPAL" program

is 0.004" to 0.007", depending on the operating speed. Such small impellers are extremely expensive to manufacture due to the precision machining involved.

When the above work is completed, the integrated hermetic compressor-motor unit can be tested in an airconditioning system which includes the evaporator, condenser, and the bearings. The test data can be used to compare the performance of the new airconditioning system, with the conventional systems presently in use.

## Chapter 6. CONCLUSION

An integrated hermetic compressor-motor unit for a new concept in automotive airconditioners has been designed. This design shows that an optimization between the mechanical compressor design and the electrical motor design is possible. The refrigerant employed in this machine is an HCFC type material. The HCFC type refrigerants have lower ozone layer depletion and global warming potentials.

These new automotive airconditioners that use an integrated hermetic compressor-motor unit are expected to have smaller size, lower levels of noise, and reduce environmental pollution. A similar design approach in many other technological areas can likewise benefit the environment and improve the efficiency of mechanical systems.



## Appendix A. DETAILED DERIVATION OF THE STRESS ANALYSIS

### A.1. Motive for Stress Analysis

The motor of the integrated hermetic compressor-motor unit is rotating at high speeds. The mechanical support for the magnet has to be strong enough to prevent the magnet from slipping or being separated from the rotor due to the centrifugal force of the motor structure itself. To solve this problem, a pre-stressed hoop covers the magnet-rotor unit. This chapter will derive a design procedure for determining the hoop thickness and the amount the hoop is pre-stressed.

### A.2. Pressure Fitting of the Hoop

Initially the hoop and the magnet-rotor unit will be pressure fitted. Hence, by

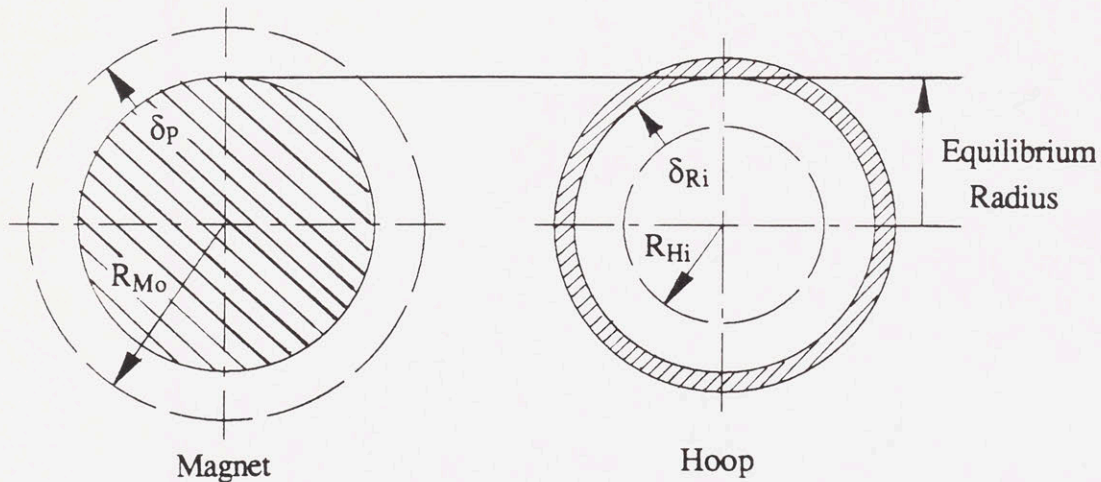


Figure A-1 Deformation of the Hoop and the Rotor

geometry the hoop inside radius must equal the magnet's outside radius.

$$(\text{Equilibrium Radius}) = R_{M0} - \delta_{Pi} = R_{Hi} + \delta_{Ri} \quad (1)$$

Also from Appendix A.9.1, we get the deformation of the magnet due to the external pressure P.

$$\delta_P = \frac{P}{E_R} (1-\nu_R) R_R + \frac{P}{E_M} (1-\nu_M) (R_{M0}-R_R) \quad (2)$$

And from Appendix A.9.2, we get the deformation of the hoop due to the internal pressure P.

$$\delta_{R1} = \frac{P R_{Hi}^2}{t_H E_H} \left(1 + \frac{t_H}{2 R_{Hi}}\right) \quad (3)$$

If we combine these equations, we get

$$R_{M0} - P \left\{ \frac{R_R}{E_R} (1-\nu_R) + \frac{R_{M0}-R_R}{E_M} (1-\nu_M) \right\} = R_{Hi} + \frac{P R_{Hi}^2}{t_H E_H} \left(1 + \frac{t_H}{2 R_{Hi}}\right) \quad (4)$$

### A.3. Deformation after Rotation

The hoop expands radially when the shaft rotates due to the centrifugal force of the magnet.

$$\delta_{H\omega} = \delta_{R2} - \delta_{R1} = \frac{\left(\frac{\text{Centrifugal Force}}{\text{Area}}\right) R_{Hi}^2}{t_H E_H} \left(1 + \frac{t_H}{2 R_{Hi}}\right) = \frac{(\rho_M t_M R_M \omega^2) R_{Hi}^2}{t_H E_H} \left(1 + \frac{t_H}{2 R_{Hi}}\right) \quad (5)$$

where  $\delta_{R1}$  is the deformation after preload

and  $\delta_{R2}$  is the deformation after rotation.

hence, the deformation after rotation is the deformation due to the preload plus the deformation due to the centrifugal force only.

$$\delta_{R2} = \frac{(P + \rho_M t_M R_M \omega^2) R_{Hi}^2}{t_H E_H} \left(1 + \frac{t_H}{2 R_{Hi}}\right) \quad (6)$$

And the hoop expansion due to the rotating inertia force of the rotor itself which is derived in Appendix A.9.3 , becomes

$$\delta_{R\omega} = \frac{1 - 2\nu_R + \nu_R^2}{1 - \nu_R} \left(\frac{\rho_R \omega^2 R_R^3}{4 E_R}\right) = (1 - \nu_R) \frac{\rho_R \omega^2 R_R^3}{4 E_R} \quad (7)$$

Therefore the total hoop expansion due to the rotation is

$$\delta_{Expansion} = \delta_{R\omega} + \delta_{H\omega} \quad (8)$$

#### A.4. Criterion for the Magnet and Rotor Contact

For the magnet to be attached to the rotor geometrically, the expansion of the hoop after rotation should be smaller than the deformation of the rotor due to the preload. i.e.

$$\delta_{Expansion} \leq K_1 \delta_P \quad (9)$$

where  $K_1$  is a safety factor ( $K_1 < 1$ ).

combining all these above equation yields,

$$\frac{1 - 2\nu_R + \nu_R^2}{1 - \nu_R} \left(\frac{\rho_R \omega^2 R_R^3}{4 E_R}\right) + \frac{(\rho_M t_M R_M \omega^2) R_{Hi}^2}{t_H E_H} \left(1 + \frac{t_H}{2 R_{Hi}}\right) \leq K_1 P \left\{ \frac{R_R}{E_R} (1 - \nu_R) + \frac{R_{Mo} - R_R}{E_M} (1 - \nu_M) \right\} \quad (10)$$

this is the criterion for the magnet to be in contact with the rotor.

### A.5. Criterion for the Strain Limit of the Hoop

For a safe operation of the motor, the hoop strain should remain within the strain limit of the hoop material. The tangential strain due to the deformation of the hoop is

$$\begin{aligned}\epsilon_{H\theta} &= \frac{2\pi(\delta_{R2} + \delta_{R\omega})}{2\pi R_H} \\ &= \frac{1}{R_{Hi} + \frac{t_H}{2}} \left\{ \frac{1 - 2\nu_R + \nu_R^2}{1 - \nu_R} \left( \frac{\rho_R \omega^2 R_R^3}{4 E_R} \right) + \frac{(P + \rho_M t_M R_M \omega^2) R_{Hi}^2}{t_H E_H} \left( 1 + \frac{t_H}{2 R_{Hi}} \right) \right\}\end{aligned}\quad (11)$$

and this tangential strain should be smaller than the elastic strain limit of the hoop material. This can be expressed as,

$$\epsilon_{H\theta} \leq K_2 \frac{\sigma_Y}{E_H} \quad (12)$$

where  $\sigma_Y$  is the elastic stress limit of the hoop material and  $K_2$  is a safety factor ( $K_2 < 1$ ).

### A.6. Summary of the Equations and Unknowns

So far we have derived the conditions and the corresponding equations of the hoop design.

These equations can be simplified to the following three equations.

$$R_{M0} - P \left\{ \frac{R_R}{E_R} (1 - \nu_R) + \frac{R_{M0} - R_R}{E_M} (1 - \nu_M) \right\} = R_{Hi} + \frac{P R_{Hi}^2}{t_H E_H} \left( 1 + \frac{t_H}{2 R_{Hi}} \right) \quad (13)$$

$$\frac{1-2\nu_R+\nu_R^2}{1-\nu_R}\left(\frac{\rho_R\omega^2R_R^3}{4E_R}\right)+\frac{(\rho_M t_M R_M \omega^2)R_{Hi}^2}{t_H E_H}\left(1+\frac{t_H}{2R_{Hi}}\right)\leq K_1 P\left\{\frac{R_R}{E_R}(1-\nu_R)+\frac{R_{Mo}-R_R}{E_M}(1-\nu_M)\right\} \quad (14)$$

$$\frac{1}{R_{Hi}+\frac{t_H}{2}}\left\{\frac{1-2\nu_R+\nu_R^2}{1-\nu_R}\left(\frac{\rho_R\omega^2R_R^3}{4E_R}\right)+\frac{(P+\rho_M t_M R_M \omega^2)R_{Hi}^2}{t_H E_H}\left(1+\frac{t_H}{2R_{Hi}}\right)\right\}\leq K_2 \frac{\sigma_Y}{E_H} \quad (15)$$

and by careful inspection we can see that we have three unknowns, which are the preload  $P$ , hoop thickness  $t_h$ , and the initial hoop inner radius  $R_{Hi}$ .

#### A.7. Solutions to the Given Equations

Since we have same number of equations and unknowns, theoretically these sets of equations can be solved. However, all three equations are nonlinear and it is very painful to solve these equations directly. Therefore, instead of solving the equations directly, I tried to get a conservative solution which will over satisfy the given criteria by an iterative process. The first step is to assume the hoop inner radius  $R_{Hi}$  and the hoop thickness  $t_h$ , and equation (13), we can get the preload  $P$ ,

$$P=\frac{R_{Mo}-R_{Hi}}{\left\{\frac{R_R}{E_R}(1-\nu_R)+\frac{R_{Mo}-R_R}{E_M}(1-\nu_M)\right\}+\frac{R_{Hi}^2}{t_H E_H}\left(1+\frac{t_H}{2R_{Hi}}\right)} \quad (16)$$

The next step is to check whether the magnet and the rotor is in contact. This can be checked by plugging in the assumed value hoop inner radius  $R_{Hi}$  and the hoop thickness  $t_h$  and the  $P$  from equation (16) into equation (14),

$$K_1 \delta_P \leq \delta_{\text{Expansion}} \leq K_2 \delta_P \leq \delta_P \quad (17)$$

$$\delta_{\text{Expansion}} = \frac{1-2\nu_R + \nu_R^2}{1-\nu_R} \left( \frac{\rho_R \omega^2 R_R^3}{4 E_R} \right) + \frac{(\rho_M t_M R_M \omega^2) R_{Hi}^2}{t_H E_H} \left( 1 + \frac{t_H}{2 R_{Hi}} \right) \quad (18)$$

$$\delta_P = P \left\{ \frac{R_R}{E_R} (1-\nu_R) + \frac{R_{Mo} - R_R}{E_M} (1-\nu_M) \right\} \quad (19)$$

where  $K_1$  and  $K_2$  are safety factors,  $K_1 < K_2 < 1$ ,

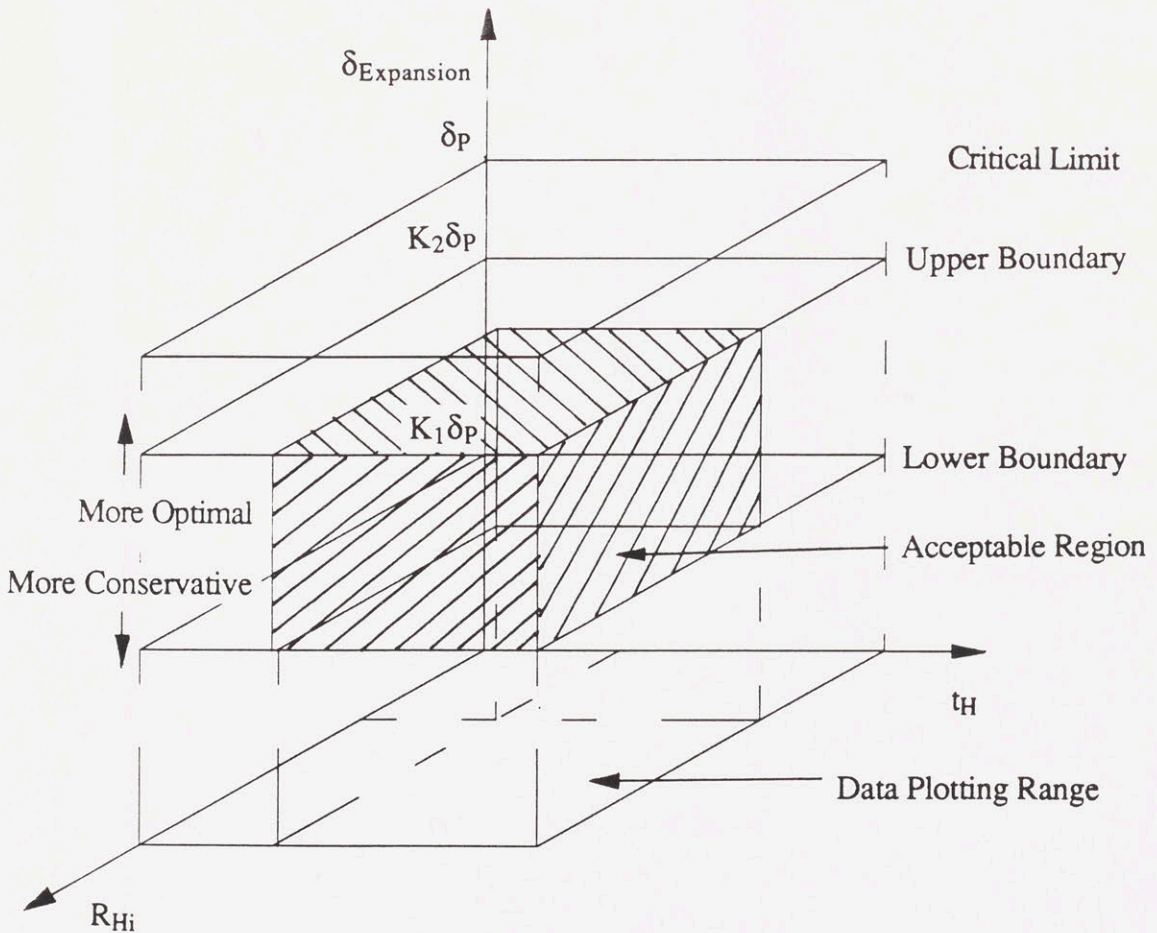


Figure A-2 Graphical Representation of the Hoop Contact Criterion

The final step is to check the hoop strain limit. This can be done by plugging the hoop inner radius  $R_{Hi}$ , the hoop thickness  $t_h$ , and the  $P$  into equation (15).

$$\epsilon_{H\theta} = \frac{1}{R_{Hi} + \frac{t_H}{2}} \left\{ \frac{1 - 2\nu_R + \nu_R^2}{1 - \nu_R} \left( \frac{\rho_R \omega^2 R_R^3}{4 E_R} \right) + \frac{(P + \rho_M t_M R_M \omega^2) R_{Hi}^2}{t_H E_H} \left( 1 + \frac{t_H}{2 R_{Hi}} \right) \right\} \quad (21)$$

and

$$K_3 \frac{\sigma_Y}{E_H} \leq \epsilon_{H\theta} \leq K_4 \frac{\sigma_Y}{E_H}$$

where  $K_3$  and  $K_4$  are safety factors,  $K_3 < K_4 < 1$ , say  $K_3 \approx 0.2$ ,  $K_4 \approx 0.9$

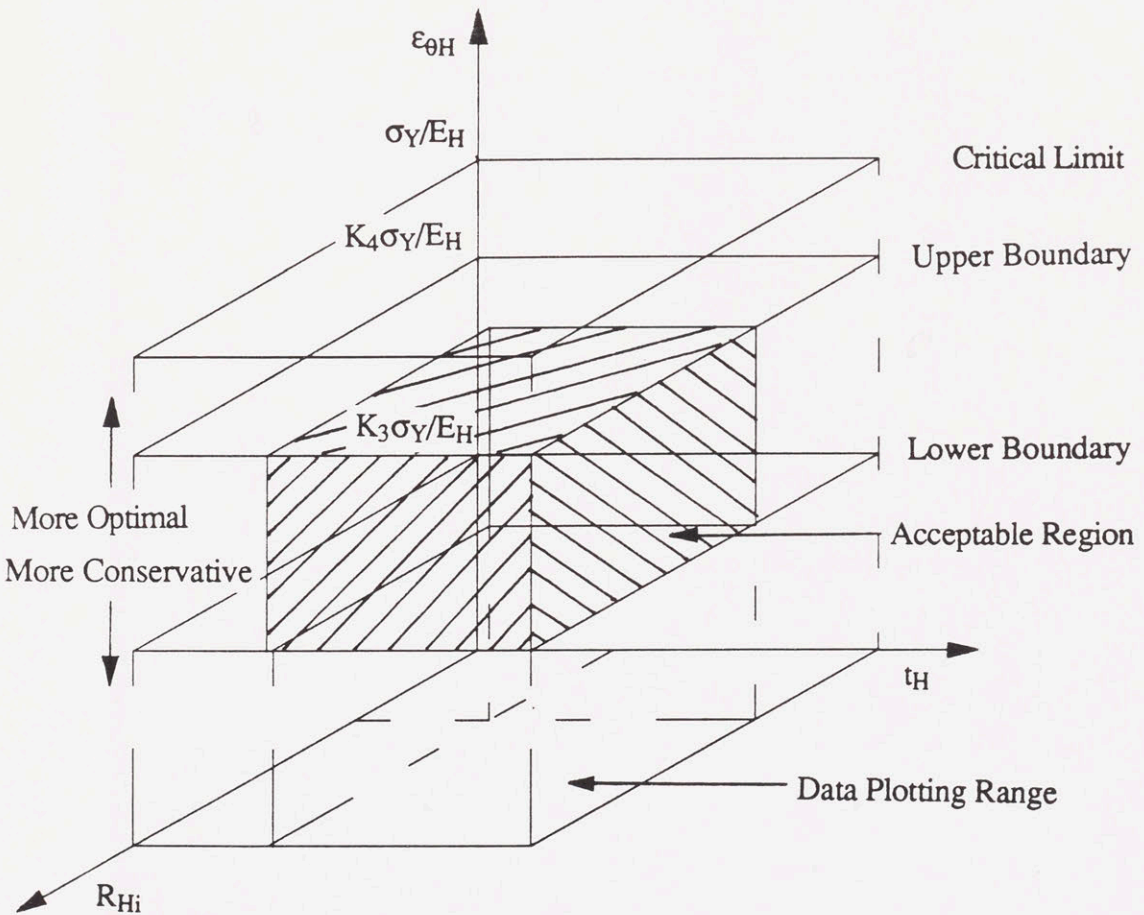


Figure A-3 Graphical Representation of the Hoop Strain Limit

## A.8. Summary of the Design Procedure

The following are the description of the variables used in the design procedure.

### - Known

- Rotor
  - $\rho_R$  : Density of the rotor
  - $E_R$  : Young's modulus of the rotor
- Magnet
  - $\rho_M$  : Density of the magnet
  - $E_M$  : Young's modulus of the magnet
- Hoop
  - $\rho_H$  : Density of the hoop
  - $E_H$  : Young's modulus of the hoop

Initial size before load is applied

- $R_R$  : Rotor outside radius
- $R_{M_o}$  : Magnet outside radius
- $R_M$  : Magnet middle radius
- $t_M$  : Magnet thickness

### - Unknown

- $P$  : Preload
- $t_H$  : Hoop thickness
- $R_{H_i}$  : Initial hoop inner radius
- $R_{H_o}$  : Initial hoop outer radius

$$R_{H_o} = R_H + t_H$$

- $R_H$  : Initial hoop middle radius

$$R_{H_o} = R_H + \frac{t_H}{2}$$

The design procedure has been summarized for the readers convenience. This design procedure starts with basic input data and two assumed variables  $R_{H_i}$  and  $t_h$ . By checking



the displacement condition and the hoop strain limit, the procedure decides to stop or continue the process. The following is the summarized design procedure.

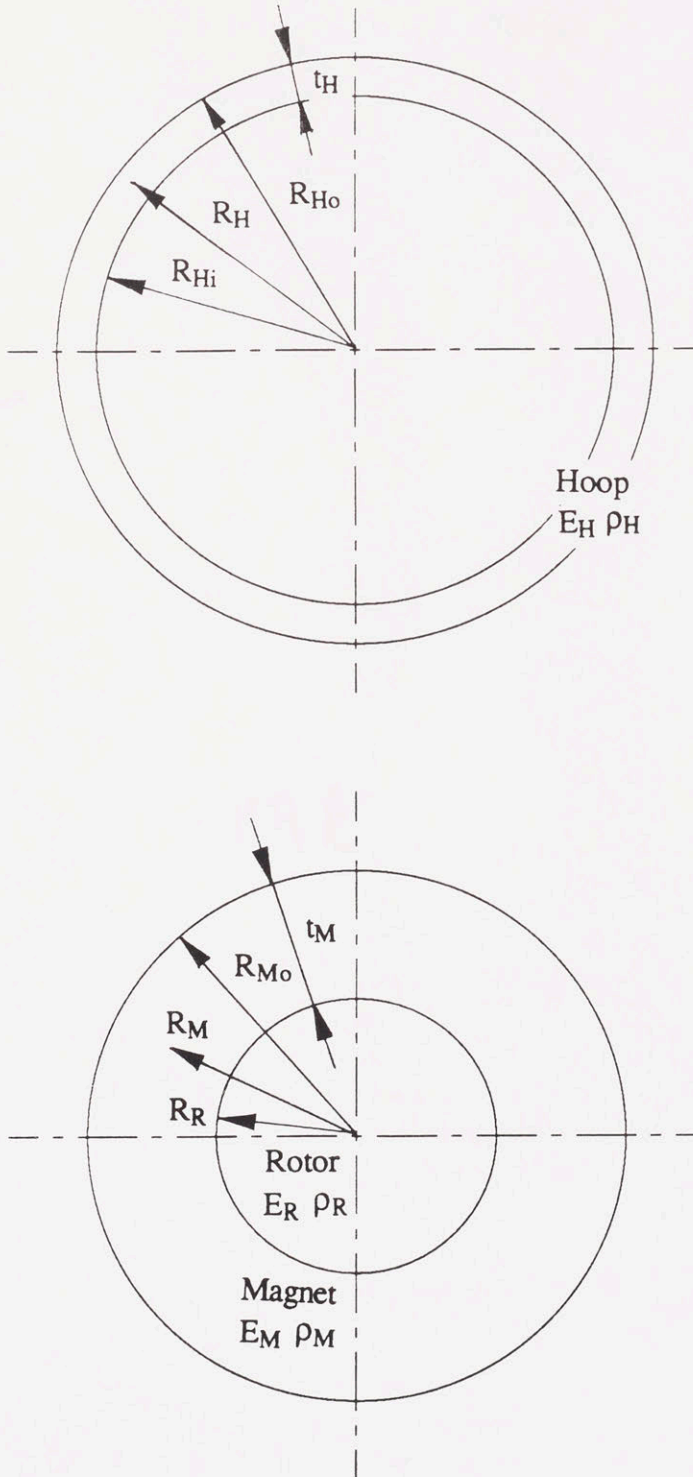


Figure A-4 Geometry of the Hoop and the Rotor

Step 1: Input information

Material data - Rotor :  $E_R, \nu_R, \rho_R$

- Magnet :  $E_M, \nu_M, \rho_M$

- Hoop :  $E_H, \nu_H, \rho_H$

Maximum rotating speed :  $\omega$

Initial size - Rotor radius :  $R_R$

- Magnet outside radius :  $R_{M_o}$

-  $t = R_{M_o} - R_R$

-  $R_M = 0.5 (R_{M_o} + R_R)$

Step 2 : Assume reasonable  $t_h$ . For this project  $t_h = 2\text{mm}$  will be fine.

Step 3: Assume  $R_{Hi} = R_{M_o}$ .

Step 4 : Calculate basic geometry of the hoop

$$R_{H_o} = R_{H_i} + t_h$$

$$R_H = R_{H_i} + \frac{t_h}{2}$$

Steps 5: Calculate P from assumed  $t_h$  and  $R_{Hi}$ .

$$P = \frac{R_{M_o} - R_{H_i}}{\left\{ \frac{R_R}{E_R} (1 - \nu_R) + \frac{R_{M_o} - R_R}{E_M} (1 - \nu_M) \right\} + \frac{R_{H_i}^2}{t_h E_H} \left( 1 + \frac{t_h}{2 R_{H_i}} \right)} \quad (22)$$

Step 6: Check the displacement condition.

$$\delta_{\text{Expansion}} = \frac{1 - 2\nu_R + \nu_R^2}{1 - \nu_R} \left( \frac{\rho_R \omega^2 R_R^3}{4 E_R} \right) + \frac{(\rho_M t_M R_M \omega^2) R_{H_i}^2}{t_h E_H} \left( 1 + \frac{t_h}{2 R_{H_i}} \right) \quad (23)$$

$$\delta_P = P \left\{ \frac{R_R}{E_R} (1 - \nu_R) + \frac{R_{M_o} - R_R}{E_M} (1 - \nu_M) \right\} \quad (24)$$

If  $K_1 \leq \delta_{Expansion} / \delta_p \leq K_2$  then goto the step 7, otherwise assume a new value of  $R_{Hi}$  such as  $R_{Hi}^{New} = R_{Hi} - \Delta$  and go back to the step 4 ( $\Delta$  is a small incremental value).

Step 7 : Check the hoop material strain limit.

$$\epsilon_{H\theta} = \frac{1}{R_{Hi} + \frac{t_H}{2}} \left\{ \frac{1 - 2\nu_R + \nu_R^2}{1 - \nu_R} \left( \frac{\rho_R \omega^2 R_R^3}{4 E_R} \right) + \frac{(P + \rho_M t_M R_M \omega^2) R_{Hi}^2}{t_H E_H} \left( 1 + \frac{t_H}{2 R_{Hi}} \right) \right\} \quad (25)$$

If  $K_3 \leq \epsilon_{H\theta} / (\sigma_Y / E_H) \leq K_4$  then accept  $t_H$ ,  $R_{Hi}$  and  $P$  as the final value. If this is not satisfied then increase the hoop thickness like  $t_H^{New} = t_H + \Delta$  and go to step 3.

## A.9. Miscellaneous Derivations.

### A.9.1. Derivation of Equation (2) [Reference 16]

From the stress-strain relationship in polar coordinates [Reference 16] we can get the radial component of the strain tensor as

$$\epsilon_r = \frac{1}{E} (\sigma_r - \nu_\theta \sigma_\theta) = \frac{\partial u}{\partial r} \quad (26)$$

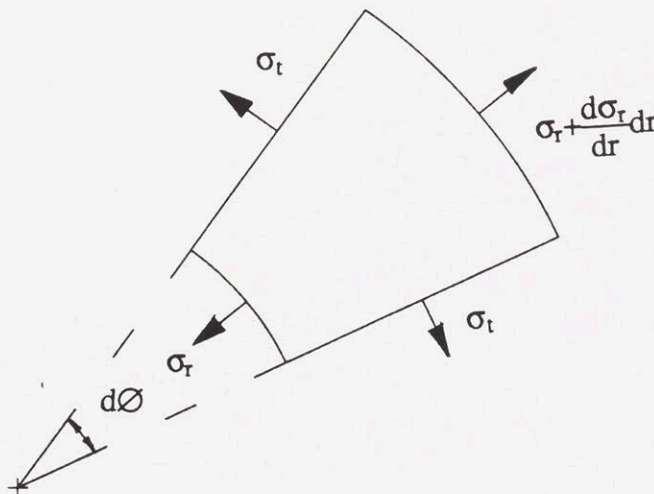


Figure A-5 Stresses in Polar Coordinates

where  $u$  is the deformation. Hence the strain at rotor ( $E=E_0$ ,  $\sigma_r=\sigma_\theta=-P$ ) becomes

$$\epsilon_r = \frac{1}{E_0}(-P + \nu_0 P) = \frac{-P}{E_0}(1 - \nu_0) = \frac{\partial u}{\partial r} \quad (27)$$

$$u = \frac{1}{E_0} \int_0^r du = \frac{-P}{E_0}(1 - \nu_0) \int_0^r dr = \frac{-P}{E_0}(1 - \nu_0)r \quad (\text{for } 0 < r < R_M)$$

and the strain at magnet ( $E=E_1$ ,  $\sigma_r=\sigma_\theta=-P$ ) becomes

$$\epsilon_r = \frac{1}{E_1}(-P + \nu_1 P) = \frac{-P}{E_1}(1 - \nu_1) = \frac{\partial u}{\partial r} \quad (28)$$

$u = (\text{Deformation of the rotor}) + (\text{Deformation of the magnet})$

$$= \frac{-P}{E_0}(1 - \nu_0) \int_0^{R_M} dr + \frac{-P}{E_1}(1 - \nu_1) \int_{R_M}^r dr \quad (29)$$

$$= \frac{-P}{E_0}(1 - \nu_0)R_M + \frac{-P}{E_1}(1 - \nu_1)(r - R_M) \quad (\text{for } R_M < r < r_o)$$

### A.9.2. Derivation of Equation (3) [Reference 13]

As far as the hoop satisfies

$$t_i = r_{2i} - R_{Hi} \ll R_i = \frac{r_{2i} + R_{Hi}}{2} \quad (30)$$

we can use a thin hoop model [Reference 13]. As we can see from figure A1-2, the force balance requires

$$\sum F = P - 2R_{Hi}(\text{breadth}) = 2\sigma_B(\text{breadth})t_i \quad (31)$$

therefore we get

$$\sigma_B = \frac{PR_{Hi}}{t_i} \quad (32)$$

and the deformation in tangential direction becomes

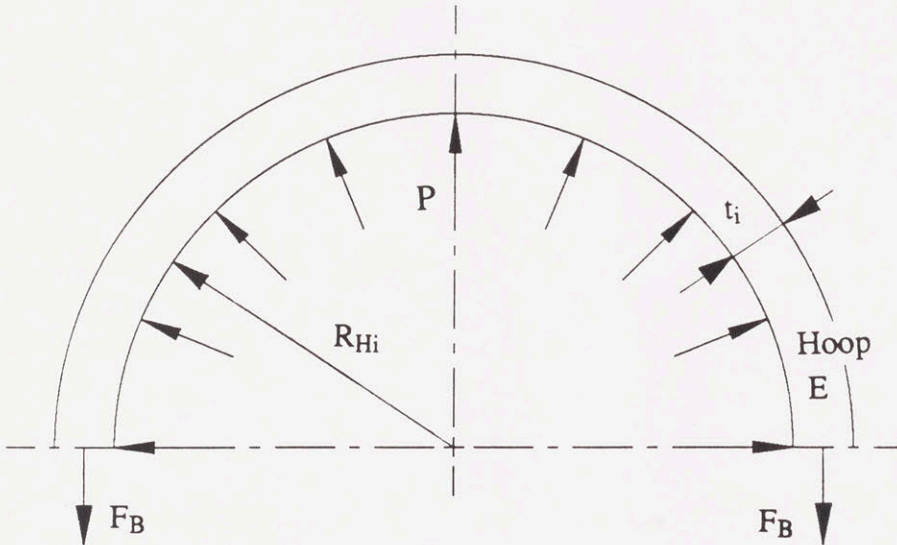


Figure A-6 Thin Hoop under Internal Pressure

$$\delta_T = \frac{F_B [2\pi(R_{Hi} + \frac{t_i}{2})]}{(\text{breadth})t_i E} = \frac{2\pi PR_{Hi}^2 (1 + \frac{t_i}{2R_{Hi}})}{t_i E} \quad (33)$$

$$\delta_R = \frac{\delta_T}{2\pi} = \frac{PR_{Hi}^2 (1 + \frac{t_i}{2R_{Hi}})}{t_i E} \quad (34)$$

### A.9.3. Derivation of Equation (7) [Reference 16]

For a long shaft with  $\epsilon_{zz}=0$ , the governing equation becomes

$$\frac{\partial \sigma_r}{\partial r} + \frac{1}{r} \frac{\partial \tau_{r\theta}}{\partial \theta} + \frac{\sigma_r - \sigma_\theta}{r} + R = 0 \quad (35)$$

for our case, by symmetry the shear stress  $\frac{\partial \tau_{r\theta}}{\partial \theta} = 0$ , and the body force R equals centrifugal force, hence the equation becomes

$$\sigma_\theta - \sigma_r - r \frac{\partial \sigma_r}{\partial r} - \rho r^2 \omega^2 = 0 \quad (36)$$

solving this equation yields

$$u = C_1 r + \frac{C_2}{r} - \frac{(1+\nu)(1-2\nu)\rho\omega^2 r^3}{8(1-\nu)E} \quad (37)$$

for solid shaft, the boundary conditions are

$$u(r=0) = 0 \quad \& \quad \sigma_r(r_2) = 0 \quad (38)$$

$$\int_0^{r_2} \sigma_z 2\pi r \, dr = 0 \Rightarrow \epsilon_z = \frac{\rho r^2 \omega^2}{2mE} \quad (39)$$

and from these boundary conditions we get

$$C_1 = \frac{(3m-5)\rho r_2^2 \omega^2}{8(m-1)E}, \quad m = \frac{1}{\nu} \quad (40)$$

$$C_2 = 0$$

and we get our final result as

$$u = \left\{ \frac{3m-5}{m-1} r_2^2 - \frac{(m+1)(m-2)}{m(m-1)} r^2 \right\} r \frac{\rho \omega^2}{8E} = \left\{ \frac{3-5\nu}{1-\nu} r_2^2 - \frac{(\nu+1)(1-2\nu)}{(1-\nu)} r^2 \right\} r \frac{\rho \omega^2}{8E} \quad (41)$$

$$= \frac{\rho \omega^2 r_2^3 2(1-\nu)^2}{8E(1-\nu)} = \frac{\rho \omega^2 r_2^3 2(1-\nu)}{4E} \quad (42)$$

## Appendix B. FINITE ELEMENT COMPUTER INPUT FILE

```

* ADINA - IN PR1
FILEUNITS LIST=8 LOG=7 ECHO=7
WORKSTATION 12 COLORS=RGB BACKGROUND=WHITE
COLORS ORI=INVERSE NODES=INVERSE EL=INVERSE,
        BC=INVERSE XYA=INVERSE XYL=INVERSE
FCONTROL HEADING=UPPER ORIGIN=UPPERLEFT
CONTROL PLOTUNIT=PERCENT HEIGHT=1.25
*
DATABASE CREATE
*
HEAD 'PR1 - PLANE STRAIN CYLINDER'
*
MASTER IDOF=100111
ANALYSIS STATIC MASS=CONSISTENT
PRINTOUT VOLUME=MAXIMUM IPRIC=0 IPRIT=0 IPDATA=0 CARDIMAGE=NO
PORTHOLE FORMATTED=YES FILE=60
*
SYSTEM 1 CYLINDRICAL
COORDINATES
ENTRIES NODE R THETA
1 0 0
2 20E-3 0
3 20E-3 45
4 20E-3 90
5 25E-3 45
6 35E-3 45
7 40E-3 0
8 40E-3 45
9 20E-3 45
10 20E-3 90
11 25E-3 45
12 35E-3 45
13 40E-3 45
14 40E-3 90
15 39.999E-3 0
16 39.999E-3 45
17 39.999E-3 90
18 42.999E-3 0
19 42.999E-3 45
20 42.999E-3 90
21 20E-3 90
22 40E-3 50.625
23 39.999E-3 50.625
*
LINE S 1 2 EL=4 MIDNODE=1
LINE S 2 7 EL=4 MIDNODE=1
LINE S 1 3 EL=4 MIDNODE=1
LINE S 3 5 EL=1 MIDNODE=1
LINE S 5 6 EL=2 MIDNODE=1
LINE S 6 8 EL=1 MIDNODE=1
LINE S 1 4 EL=4 MIDNODE=1
LINE COMBINED 3 8 5 6
LINE ARC 2 3 EL=8 MIDNODE=1 NCENTER=1
LINE ARC 3 4 EL=8 MIDNODE=1 NCENTER=1
LINE ARC 7 8 EL=8 MIDNODE=1 NCENTER=1
LINE S 9 11 EL=1 MIDNODE=1
LINE S 11 12 EL=2 MIDNODE=1
LINE S 12 13 EL=1 MIDNODE=1
LINE S 10 14 EL=4 MIDNODE=1
LINE COMBINED 9 13 11 12
LINE ARC 9 10 EL=8 MIDNODE=1 NCENTER=1
LINE ARC 13 22 EL=1 MIDNODE=1 NCENTER=1
LINE ARC 22 14 EL=7 MIDNODE=1 NCENTER=1
LINE COMBINED 13 14 22
LINE S 15 18 EL=3 MIDNODE=1
LINE S 16 19 EL=3 MIDNODE=1

```

```

LINE S 17 20 EL=3 MIDNODE=1
LINE ARC 15 16 EL=8 MIDNODE=1 NCENTER=1
LINE ARC 16 23 EL=1 MIDNODE=1 NCENTER=1
LINE ARC 23 17 EL=7 MIDNODE=1 NCENTER=1
LINE COMBINED 16 17 23
LINE ARC 18 19 EL=8 MIDNODE=1 NCENTER=1
LINE ARC 19 20 EL=8 MIDNODE=1 NCENTER=1
*
MATERIAL 1 ELASTIC E=2.0E11 NU=0.2 DENSITY=7.85E3
MATERIAL 2 ELASTIC E=3.0E11 NU=0.25 DENSITY=7.85E3
MATERIAL 3 ELASTIC E=4.0E11 NU=0.3 DENSITY=7.85E3
*
EGROUP 1 SPRING
ENODES
1 21 3 10 3
EDATA
ENTRIES EL PROPERTYSET
1 1
PROPERTYSET 1 K=1.0
EGROUP 2 TWODSOLID STRAIN MAT=1 RESULT=TABLES
GSURFACE 1 2 3 1 EL1=4 EL2=8 NODES=8
GSURFACE 1 3 4 1 EL1=4 EL2=8 NODES=8
GSURFACE 2 7 8 3 EL1=4 EL2=8 NODES=8
STRESSTABLE 2 1 2 3 4 5 6 7 8 9
EGROUP 3 TWODSOLID STRAIN MAT=2 RESULT=TABLES
GSURFACE 9 13 14 10 EL1=4 EL2=8 NODES=8
STRESSTABLE 3 1 2 3 4 5 6 7 8 9
EGROUP 4 TWODSOLID STRAIN MAT=3 RESULT=TABLES
GSURFACE 15 18 19 16 EL1=3 EL2=8 NODES=8
GSURFACE 16 19 20 17 EL1=3 EL2=8 NODES=8
STRESSTABLE 4 1 2 3 4 5 6 7 8 9
*
FIXB 123456 TYPE=NODES
1
FIXB 123456 TYPE=NODES
21
FIXB 13456 TYPE=LINES
1 2
FIXB 13456 TYPE=LINES
2 7
FIXB 13456 TYPE=LINES
15 18
FIXB 12456 TYPE=LINES
1 4
FIXB 12456 TYPE=LINES
10 14
FIXB 12456 TYPE=LINES
17 20
FIXB 12456 TYPE=NODES
10
*
CGROUP 1 CONTACT2 STRAIN FORCES=YES TRACTIONS=YES
CONTACTSURFACE 1 TYPE=LINES
16 15
CONTACTSURFACE 2 TYPE=LINES
17 23
CONTACTSURFACE 3 TYPE=LINES
10 9
CONTACTSURFACE 4 TYPE=LINES
11 12
CONTACTSURFACE 5 TYPE=LINES
22 14
CONTACTSURFACE 6 TYPE=LINES
3 4
CONTACTSURFACE 7 TYPE=LINES
6 5

```



```
CONTACTSURFACE 8 TYPE=LINES
7 8
```

```
CONTACTPAIR 1 8 1
CONTACTPAIR 2 5 2
CONTACTPAIR 3 7 4
CONTACTPAIR 4 6 3
*
```

```
LOADS CENTRIFUGAL OMEGA=8500 AX=0 AY=0 AZ=0 BX=1 BY=0 BZ=0
*
```

```
FRAME
MESH NODE=00 ELEMENT=00
*
ADINA
*
END
```

```
* HW1 - PLOT FILE
*
```

```
FILEUNITS LIST=8 LOG=7 ECHO=7
WORKSTATION 12 COLORS=RGB BACKGROUND=WHITE
COLORS FR=INVERSE HE=INVERSE TEXT=INVERSE AXES=INVERSE,
      ORIG=INVERSE DEF=INVERSE NODES=INVERSE ELE=INVERSE,
      BCODE=INVERSE XYAXES=INVERSE XYLINE=INVERSE VE=INVERSE
CONTROL PLOTUNIT=PERCENT HEIGHT=1.25
FCONTROL HEADING=UPPER ORIGIN=LOWERLEFT SIZE=DIRECT,
        XSF=5 YSF=5 XFMAX=90 YFMAX=90
DATABASE CREATE FORMATTED=YES
*
```

```
FRAME
PLOTAREA 1 10 90 5 60
MESH ORI=2 DEF=1 EL=0 NODE=00 DMAX=5 PLOTAREA=1
END
```

## Appendix C. CRITICAL SPEED ESTIMATION PROGRAM

```
/*
*****
*/
/*
This program calculates the critical speed of the
integrated hermetic compressor-motor unit
*/
/*
Program written by
Hayong Yun
*/
*****
*/

#include <stdio.h>
#include <math.h>

#define N 1000

main()
{
    int i;

    double a, b, d, Wo, E; /* input parameter */
    double w1, w2, n1, n2; /* output parameter */
    double I, Ra;
    double C1, Ymax, x; /* first estimation */
    double Y, sum1, sum2; /* second estimation */

    /* Input parameter */
    a = 10; /* in */
    b = 7; /* in */
    d = 4; /* in */
    Wo = (7.35/10000)*(9.807)*(3.14159*d*d/4); /* lbf/in */
    E = 30000000; /* lb/in^2 */

    /* Calculate basic parameter */
```

```

I = 3.14159*(d*d*d*d)/64; /* in^4 */
Ra = 0.5*Wo*b; /* lbf */
C1 = Wo*(a+b)*(a+b)*(a+b)*(a+b)/(24*(2*a+b))
    -Wo*a*a*a*a/(24*(2*a+b)) - Ra*(2*a+b)*(2*a+b)/6;

/* Rough estimation for critical speed */
x = a+b/2;
Ymax = (Ra*x*x*x/6-Wo*(x-a)*(x-a)*(x-a)/(24+C1*x))/(E*I);
w1 = sqrt(0 - 9.807/Ymax);
n1 = w1*60/(2*3.14159);

/* critical speed for distributed mass*/
sum1 = 0;
for(i=0; i<N; i++){
    x = a + (b)*i/N + (b)/(2*N);
    Y = (Ra*x*x*x/6-Wo*(x-a)*(x-a)*(x-a)/(24+C1*x))/(E*I);
    sum1 = sum1 + Wo*(b)*Y/N;
}
sum2 = 0;
for(i=0; i<N; i++){
    x = a + (b)*i/N + (b)/(2*N);
    Y = (Ra*x*x*x/6-Wo*(x-a)*(x-a)*(x-a)/(24+C1*x))/(E*I);
    sum2 = sum2 + Wo*(b)*Y*Y/N;
}
w2 = sqrt(0 - 9.807*sum1/sum2);

n2 = w2*60/(2*3.14159);

/* data output */          /* for a=10; b=7; d=4; E=3x10^6 */
printf("Ymax = %lf\n",Ymax); /* w1      = 3831.574466 */
printf("w1 = %lf\n",w1);     /* w2(N=1) = 3831.574466 */
printf("n1 = %lf\n",n1);     /* w2(N=10) = 3887.925543 */
printf("w2 = %lf\n",w2);     /* w2(N=100) = 3888.425916 */
printf("n2 = %lf\n",n2);     /* w2(N=1000) = 3888.430914 */
}

```

## Appendix D. CENTRIFUGAL COMPRESSOR DESIGN PROGRAM

```

/*****
/*
/*      This program calculates the basic dimensions of the      */
/*      centrifugal compressor for the                          */
/*      integrated hermetic compressor-motor unit                */
/*
/*
/*      Program written by                                     */
/*      Hayong Yun                                           */
/*
*****/

#include "stdio.h"
#include "math.h"
#include "conio.h"
#include "graphics.h"

#define Max 10
#define Mmax 11
#define Hmax 400
#define Shift 450
#define PI 3.141592653589793238462643

void drawcompressor();

main()
{
    int i;
    char ch;

/*****
***** Define Variables *****/
*****/
/* Temperature */

```

```
double T01, T02, T03, T04, T05;  
double T06, T07, T08, T09, T00;  
double T1, T2, T3, T4, T5;  
double T6, T7, T8, T9, T0;
```

```
/* Pressure */
```

```
double P01, P02, P03, P04, P05;  
double P06, P07, P08, P09, P00;
```

```
/* Density */
```

```
double p01, p02, p03, p04, p05;  
double p06, p07, p08, p09, p00;  
double p1, p2, p3, p4, p5;  
double p6, p7, p8, p9, p0;
```

```
/* Enthalpy */
```

```
double h1, h2, h5;  
double h6, h7, h0;
```

```
/* Absolute Velocity */
```

```
double V1, V2, V3, V4, V5;  
double V6, V7, V8, V9, V0;  
double Vt1, Vt2, Vt3, Vt4;  
double Vt6, Vt7, Vt8, Vt9;  
double Vm1, Vm2, Vm3, Vm4, Vtmp;  
double Vm6, Vm7, Vm8, Vm9;
```

```
/* Rotational Velocity */
```

```
double u1s, u2;  
double u6s, u7;
```

```
/* Relative Velocity */
```

```
double W1s, W2;  
double W6s, W7;  
double Wt1, Wt2;  
double Wt6, Wt7;
```

```

/* Compressor size */
double r1h, r1s, r2, r3, r4; /* radius */
double r6h, r6s, r7, r8, r9;
double l1; /* chord length */
double l2;
double sigma1; /* solidity */
double sigma2;
double Ax20, Ax290, Ax2180, Ax2270, Ax2360;

/* Impeller size */
double t1, t2, th1, th2, th3; /* Impeller thickness */
double breadth1, breadth2, br4;

/* Angles */
double a1, a2, a3, a4, alpha4;
double a6, a7, a8, a9;
double b1, b2;
double b6, b7;

/* Mach number */
double Va1, Va2, Va3; /* Speed of sound */
double Va6, Va7, Va8;

double M1rs, M1, M2, M3, Mtmp; /* Mach number */
double M6rs, M6, M7, M8;

/* Assumption Variables */
double R1h2; /* r1h/r2 */
double Rw1s2; /* W2/W1s */
double Rv34; /* ratio of V4/V3 of the Diffuser */
double theta1, theta2; /* impeller angle */
double Rr2t3; /* ratio of R2/t3 */
double K;

```

```

/* Air Property */
double Cp1, R1, g1;
double Cp2, R2, g2;

/* Initial Condition */
double m1, m2, Nc, Ni;

/* Variable to find rpm */
double Ns1, Ns2; /* Specific speed */
double N; /* Angular velocity */

/* Blade information */
double Z; /* Number of compressor blades */
double Zd; /* Number of impeller blades */
double slip; /* slip factor */

/***** Input Routine *****/
clrscr();
/*m1=0.03966360902;
T01=278.15;
P01=33120;
p01=2.236;
h1=218900;
T05=325.75;
P05=100000;
p05=5.848;
h5=249809.0909;
m2=0.04711365961;
T06=300.53;
P06=100000;
p06=6.425;
h6=231800;
T00=332.85;
P00=205800;
p00=12.19;

```

```

h0=252606.4927;
Nc=0.55;
Ni=0.6;
*/
/***** stage 1 *****/
printf(" * Input Data for Stage 1.\n");

printf(" => Inlet Temperature(T01 - oC) : ");
scanf("%lf",&T01);
T01 = T01+273.15;

printf(" => Inlet Pressure(P01 - kPa) : ");
scanf("%lf",&P01);
P01 = 1000*P01;

printf(" => Inlet Density(p01 - kg/m^3) : ");
scanf("%lf",&p01);

printf(" => Inlet Enthalpy (H1 - kJ/kg) : ");
scanf("%lf",&h1);
h1 = 1000*h1;

printf(" => Outlet Temperature(T05 - oC) : ");
scanf("%lf",&T05);
T05 = T05+273.15;

printf(" => Outlet Pressure(P05 - kPa) : ");
scanf("%lf",&P05);
P05 = 1000*P05;

printf(" => Outlet Density(p05 - kg/m^3) : ");
scanf("%lf",&p05);

printf(" => Outlet Enthalpy (H5 - kJ/kg) : ");
scanf("%lf",&h5);
h5 = 1000*h5;

```



```
printf(" => First Stage mass flow rate(m1 - kg/sec) : ");
```

```
scanf("%lf",&m1);
```

```
/****** stage 2 *****/
```

```
printf(" * Input Data for Stage 2.\n");
```

```
printf(" => Inlet Temperature(T06 - oC) : ");
```

```
scanf("%lf",&T06);
```

```
T06 = T06+273.15;
```

```
printf(" => Inlet Pressure(P06 - kPa) : ");
```

```
scanf("%lf",&P06);
```

```
P06 = 1000*P06;
```

```
printf(" => Inlet Density(p06 - kg/m^3) : ");
```

```
scanf("%lf",&p06);
```

```
printf(" => Inlet Enthalpy (H6 - kJ/kg) : ");
```

```
scanf("%lf",&h6);
```

```
h6 = 1000*h6;
```

```
printf(" => Outlet Temperature(T00 - oC) : ");
```

```
scanf("%lf",&T00);
```

```
T00 = T00+273.15;
```

```
printf(" => Outlet Pressure(P00 - kPa) : ");
```

```
scanf("%lf",&P00);
```

```
P00 = 1000*P00;
```

```
printf(" => Outlet Density(p00 - kg/m^3) : ");
```

```
scanf("%lf",&p00);
```

```
printf(" => Outlet Enthalpy (H0 - kJ/kg) : ");
```

```
scanf("%lf",&h0);
```

```
h0 = 1000*h0;
```

```

printf(" => Second Stage mass flow rate(m2 - kg/sec) : ");
scanf("%lf",&m2);

printf(" => Compressor Efficiency(Nc) : ");
scanf("%lf",&Nc);

printf(" => Impeller Efficiency(Ni) : ");
scanf("%lf",&Ni);

clrscr();
/***** Initial Condition *****/
/* Set Assumption Variables */
R1h2 = 0.2; /* r1h = 0.2 x r2 */
Rw1s2 = 0.685; /* W2%W1s = 0.685 */
Rv34 = 3; /* V4 = V3 : Diffusion ratio */
theta1 = 60*PI/180; /* Impeller Angle : Radian */
theta2 = 50*PI/180; /* Impeller Angle : Radian */
Rr2t3 = 3; /* Impeller height to width ratio : t3=r2%3 */

for(;;){
/* Variable Initial condition */
printf(" => Desired RPM(N) : ");
scanf("%lf",&N); /* RPM */

Z = 20; /* Blade number */
Zd = 20; /* Diffuser blade number */

/***** Calculate gas property *****/
/* stage 1 */
Cp1 = (h5-h1)/(T05-T01);
R1 = 0.5*(P01/p01/T01 + P05/p05/T05);
g1 = 0.5*(Cp1/(Cp1-P01/p01/T01) + Cp1/(Cp1-P05/p05/T05));
/* stage 2 */
Cp2 = (h0-h6)/(T00-T06);
R2 = 0.5*(P06/p06/T06 + P00/p00/T00);
g2 = 0.5*(Cp2/(Cp2-P06/p06/T06) + Cp2/(Cp2-P00/p00/T00));

```

```

/***** Adiabatic Assumption *****/
/* stage 1 */
T02 = T03 = T04 = T05;
h2 = h5;
/* stage 2 */
T07 = T08 = T09 = T00;
h7 = h0;

/***** Find Specific Speed *****/
/* stage 1 */
p01 = P01/R1/T01;
Ns1 = N*sqrt(m1/p01)/60/pow((h2-h1),0.75);
/* stage 2 */
p06 = P06/R2/T06;
Ns2 = N*sqrt(m2/p06)/60/pow((h7-h6),0.75);

/***** Find Dimensions of Impeller *****/
slip = 1-2/Z; /* Calculate slip factor */
/* stage 1 */
u2 = sqrt((h2-h1)/slip);
Vt2 = slip*u2;
r2 = 30*u2/(PI*N);
r1h = R1h2*r2; /* Hub radius */
/* stage 2 */
u7 = sqrt((h7-h6)/slip);
Vt7 = slip*u7;
r7 = 30*u7/(PI*N);
r6h = R1h2*r7; /* Hub radius */

/***** Find r1s to minimize M1rs *****/
/* stage 1 */
a1 = 0;
Vtmp = 10; /* Assume V1 */
Vm1 = Vtmp*cos(a1);
Vt1 = Vtmp*sin(a1);
T1 = T01-Vtmp*Vtmp/(2*Cp1);

```

```

p1 = p01*pow(T1/T01,1/(g1-1));
r1s = sqrt(m1/(Vm1*PI*p1)+r1h*r1h);
u1s = PI*N*r1s/30;
W1s = sqrt((u1s-Vt1)*(u1s-Vt1)+Vm1*Vm1);
Va1 = sqrt(g1*R1*T1);
Mtmp = W1s/Va1;
M1 = Vtmp/Va1;
for(i=0; i<1000+1; i++){
    V1 = 10+(i*0.4);
    Vm1 = V1*cos(a1);
    Vt1 = V1*sin(a1);
    T1 = T01-V1*V1/(2*Cp1);
    p1 = p01*pow(T1/T01,1/(g1-1));
    r1s = sqrt(m1/(Vm1*PI*p1)+r1h*r1h);
    u1s = PI*N*r1s/30;
    W1s = sqrt((u1s-Vt1)*(u1s-Vt1)+Vm1*Vm1);
    Va1 = sqrt(g1*R1*T1);
    M1rs = W1s/Va1;
    M1 = V1/Va1;
    if(Mtmp>M1rs){
        Vtmp = V1;
        Mtmp = M1rs;
    }
}
V1 = Vtmp;
Vm1 = V1*cos(a1);
Vt1 = V1*sin(a1);
T1 = T01-V1*V1/(2*Cp1);
p1 = p01*pow(T1/T01,1/(g1-1));
r1s = sqrt(m1/(Vm1*PI*p1)+r1h*r1h);
u1s = PI*N*r1s/30;
W1s = sqrt((u1s-Vt1)*(u1s-Vt1)+Vm1*Vm1);
Wt1 = u1s-Vt1;
Va1 = sqrt(g1*R1*T1);
M1rs = W1s/Va1;
M1 = V1/Va1;

```

```

b1 = atan(Wt1/Vm1); /* Radian */
/* stage 2 */
a6 = 0;
Vtmp = 10; /* Assume V6 */
Vm6 = Vtmp*cos(a6);
Vt6 = Vtmp*sin(a6);
T6 = T06-Vtmp*Vtmp/(2*Cp2);
p6 = p06*pow(T6/T06,1/(g2-1));
r6s = sqrt(m1/(Vm6*PI*p6)+r6h*r6h);
u6s = PI*N*r6s/30;
W6s = sqrt((u6s-Vt6)*(u6s-Vt6)+Vm6*Vm6);
Va6 = sqrt(g2*R2*T6);
Mtmp = W6s/Va6;
M6 = Vtmp/Va6;
for(i=0; i<1000+1; i++){
    V6 = 10+(i*0.4);
    Vm6 = V6*cos(a6);
    Vt6 = V6*sin(a6);
    T6 = T06-V6*V6/(2*Cp2);
    p6 = p06*pow(T6/T06,1/(g2-1));
    r6s = sqrt(m2/(Vm6*PI*p6)+r6h*r6h);
    u6s = PI*N*r6s/30;
    W6s = sqrt((u6s-Vt6)*(u6s-Vt6)+Vm6*Vm6);
    Va6 = sqrt(g2*R2*T6);
    M6rs = W6s/Va6;
    M6 = V6/Va6;
    if(Mtmp>M6rs){
        Vtmp = V6;
        Mtmp = M6rs;
    }
}
V6 = Vtmp;
Vm6 = V6*cos(a6);
Vt6 = V6*sin(a6);
T6 = T06-V6*V6/(2*Cp2);
p6 = p06*pow(T6/T06,1/(g2-1));

```

```

r6s = sqrt(m2/(Vm6*PI*p6)+r6h*r6h);
u6s = PI*N*r6s/30;
W6s = sqrt((u6s-Vt6)*(u6s-Vt6)+Vm6*Vm6);
Wt6 = u6s-Vt6;
Va6 = sqrt(g2*R2*T6);
M6rs = W6s/Va6;
M6 = V6/Va6;
b6 = atan(Wt6/Vm6); /* Radian */

```

```

/***** Calculate Exit Vector Diagram *****/

```

```

/* stage 1*/

```

```

Wt2 = u2-Vt2;
W2 = Rw1s2*W1s;
b2 = asin(Wt2/W2); /* Radian */
Vm2 = W2*cos(b2);
a2 = atan(Vt2/Vm2); /* Radian */
V2 = sqrt(Vm2*Vm2+Vt2*Vt2);

```

```

/* stage 2 */

```

```

Wt7 = u7-Vt7;
W7 = Rw1s2*W6s;
b7 = asin(Wt7/W7); /* Radian */
Vm7 = W7*cos(b7);
a7 = atan(Vt7/Vm7); /* Radian */
V7 = sqrt(Vm7*Vm7+Vt7*Vt7);

```

```

/***** Find width b of Impeller blades *****/

```

```

/* stage 1 */

```

```

P02 = P01*pow(((Ni/Nc)*(pow(P05/P01,(g1-1)/g1)-1)+1),g1/(g1-1));
p02 = P02/(R1*T02);
p2 = p02*pow(1-V2*V2/(2*Cp1*T02),1/(g1-1));
breadth1 = m1/(p2*V2*cos(a2)*2*PI*r2);

```

```

/* stage 2 */

```

```

P07 = P06*pow(((Ni/Nc)*(pow(P00/P06,(g2-1)/g2)-1)+1),g2/(g2-1));
p07 = P07/(R2*T07);
p7 = p07*pow(1-V7*V7/(2*Cp2*T07),1/(g2-1));
breadth2 = m2/(p7*V7*cos(a7)*2*PI*r7);

```

```

/***** Design of Vaneless Space *****/
/* stage 1 */
T2 = T02-V2*V2/(2*Cp1);
Va2 = sqrt(g1*R1*T2);
M2 = V2/Va2;
M3=0.8;
if(0.9*M2<0.8){
    M3=0.9*M2;
}
P03 = P02-(P02-P05)/2;
P04 = P05;
p03 = P03/(R1*T03);
T3 = T03/(1+(g1-1)*M3*M3/2);
p3 = p03*pow(T3/T03,1/(g1-1));
a3 = atan(p3*tan(a2)/p2);
Va3 = sqrt(g1*R1*T3);
V3 = Va3*M3;
Vt3 = V3*sin(a3);
Vm3 = V3*cos(a3);
r3 = r2*V2*sin(a2)/(V3*sin(a3));
/* stage 2 */
T7 = T07-V7*V7/(2*Cp2);
Va7 = sqrt(g2*R2*T7);
M7 = V7/Va7;
M8=0.8;
if(0.9*M7<0.8){
    M8=0.9*M7;
}
P08 = P07-(P07-P00)/3;
P09 = P00+(P07-P00)/3;
p08 = P08/(R2*T08);
T8 = T08/(1+(g2-1)*M8*M8/2);
p8 = p08*pow(T8/T08,1/(g2-1));
a8 = atan(p8*tan(a7)/p7);
Va8 = sqrt(g2*R2*T8);

```

```

V8 = Va8*M8;
Vt8 = V8*sin(a8);
Vm8 = V8*cos(a8);
r8 = r7*V7*sin(a7)/(V8*sin(a8));

```

```

/***** Design of the Vaned Diffuser *****/

```

```

/* stage 1 */

```

```

V4 = Vm6; /* Assume straight balde, br3=br4 */
p04 = P04/R1/T04;
p4 = p04*pow((1-V4*V4/2/Cp1/T04),1/(g1-1));
T4 = T04-V4*V4/2/Cp1;
a4 = atan(p4*V4*tan(a3)/p3/V3);
r4 = r3*sin(a3)/sin(a4);
br4 = r3*breath1*p3*V3*cos(a3)/r4/p4/V4; /* match br4 for continuity */
Vm4 = Vm6;

```

```

Vt4 = 0;

```

```

V4 = sqrt(Vm4*Vm4 + Vt4*Vt4);

```

```

alpha4 = atan(Vt4/Vm4);

```

```

l1 = r4*sin(a3-a4)/sin(a3);

```

```

sigma1 = Z*l1/2/PI/r3;

```

```

/* stage 2 */

```

```

V9 = V8/Rv34;

```

```

p09 = P09/(R2*T09);

```

```

T9 = T09-V9*V9/(2*Cp2);

```

```

p9 = p09*pow(1-V9*V9/(2*Cp2*T09),1/(g2-1));

```

```

a9 = atan(p9*V9*tan(a8)/(p8*V8));

```

```

r9 = r8*sin(a8)/sin(a9);

```

```

l2 = sin(a8-a9)*r9/sin(a8);

```

```

sigma2 = Zd*l2/(2*PI*r9);

```

```

Vt9 = V4*sin(a9);

```

```

Vm9 = V4*cos(a9);

```

```

/***** Design of the Volute *****/

```

```

/* stage 2 */

```

```

V0=Vt9;

```

```

p00 = P00/(R2*T00);

```



```
p0 = p05*pow(1-V0*V0/(2*Cp2*T00),1/(g2-1));
T0 = T00-V0*V0/(2*Cp2);
```

```
/****** Impeller Thickness *****/
```

```
/* stage 1 */
```

```
th1 = (r2-r1h)/tan(theta1);
```

```
th2 = (r2-r1s)/tan(theta2);
```

```
th3 = r2/Rr2t3;
```

```
/* find maximum t1 */
```

```
t1=th1;
```

```
if(th2>t1){
```

```
    t1=th2;
```

```
}
```

```
if(th3>t1){
```

```
    t1=th3;
```

```
}
```

```
/* stage 2 */
```

```
th1 = (r7-r6h)/tan(theta1);
```

```
th2 = (r7-r6s)/tan(theta2);
```

```
th3 = r7/Rr2t3;
```

```
/* find maximum t2 */
```

```
t2=th1;
```

```
if(th2>t2){
```

```
    t2=th2;
```

```
}
```

```
if(th3>t2){
```

```
    t2=th3;
```

```
}
```

```
/****** Cross-sectional Area of Volute *****/
```

```
/* stage 2 */
```

```
Ax20 = 0;
```

```
Ax290 = m2/(4*p0*V0);
```

```
Ax2180 = 2*m2/(4*p0*V0);
```

```
Ax2270 = 3*m2/(4*p0*V0);
```

```
Ax2360 = m2/(p0*V0);
```

```

/*****
/*          Printout Result          */
*****/

getchar();
clrscr();
printf("* Summary of Important Data.\n");
printf("  RPM = %lf (m)\n",N);
printf(" 1] Stage 1 :\n");
printf("  T01 = %lf (K)\n",T01);
printf("  T05 = %lf (K)\n",T05);
printf("  r1h = %lf (m)\n",r1h);
printf("  r1s = %lf (m)\n",r1s);
printf("  r2  = %lf (m)\n",r2);
printf("  r3  = %lf (m)\n",r3);
printf("  r4  = %lf (m)\n",r4);
printf("  b  = %lf (m)\n",breadth1);
printf("  t  = %lf (m)\n",t1);
printf("  Ns1 = %lf (m)\n",Ns1);
printf("  m1  = %lf (kg/s)\n",m1);

printf(" 2] Stage 2 :\n");
printf("  T06 = %lf (K)\n",T06);
printf("  T00 = %lf (K)\n",T00);
printf("  r6h = %lf (m)\n",r6h);
printf("  r6s = %lf (m)\n",r6s);
printf("  r7  = %lf (m)\n",r7);
printf("  r8  = %lf (m)\n",r8);
printf("  r9  = %lf (m)\n",r9);
printf("  b  = %lf (m)\n",breadth2);
printf("  t  = %lf (m)\n",t2);
printf("  Ns2 = %lf (m)\n",Ns2);
printf("  m2  = %lf (kg/s)\n",m2);

```

```

/***** Stage 1 *****/
getchar();
clrscr();
printf("* Impeller Inlet Data\n");
printf(" 1] Temperature :\n");
printf("  T01  = %lf (K)\n",T01);
printf("  T1   = %lf (K)\n",T1);
printf(" 2] Pressure :\n");
printf("  P01  = %lf (Pa)\n",P01);
printf(" 3] Density :\n");
printf("  p01  = %lf (kg/m^3)\n",p01);
printf("  p1   = %lf (kg/m^3)\n",p1);
printf(" 4] Velocity :\n");
printf("  V1   = %lf (m/sec)\n",V1);
printf("  Vt1  = %lf (m/sec)\n",Vt1);
printf("  Vm1  = %lf (m/sec)\n",Vm1);
printf("  u1s  = %lf (m/sec)\n",u1s);
printf("  W1s  = %lf (m/sec)\n",W1s);
printf("  Wt1  = %lf (m/sec)\n",Wt1);
printf("  alpha1 = %lf (degree)\n",a1*180/PI);
printf("  betha1 = %lf (degree)\n",b1*180/PI);
printf(" 5] Speed of Sound & Mach Number\n");
printf("  Va1  = %lf (m/sec)\n",Va1);
printf("  M1rs = %lf\n",M1rs);
printf("  M1   = %lf\n",M1);
printf(" 6] Radius :\n");
printf("  r1h  = %lf (m)\n",r1h);
printf("  r1s  = %lf (m)\n",r1s);
getchar();

/***** Stage 2 *****/
clrscr();
printf("* Impeller Outlet Data\n");
printf(" 1] Temperature :\n");
printf("  T02  = %lf (K)\n",T02);

```

```

printf("  T2  = %lf (K)\n",T2);
printf(" 2] Pressure :\n");
printf("  P02  = %lf (Pa)\n",P02);
printf(" 3] Density :\n");
printf("  p02  = %lf (kg/m^3)\n",p02);
printf("  p2   = %lf (kg/m^3)\n",p2);
printf(" 4] Velocity :\n");
printf("  V2   = %lf (m/sec)\n",V2);
printf("  Vt2  = %lf (m/sec)\n",Vt2);
printf("  Vm2  = %lf (m/sec)\n",Vm2);
printf("  u2   = %lf (m/sec)\n",u2);
printf("  W2   = %lf (m/sec)\n",W2);
printf("  Wt2  = %lf (m/sec)\n",Wt2);
printf("  alpha2 = %lf (degree)\n",a2*180/PI);
printf("  betha2 = %lf (degree)\n",b2*180/PI);
printf(" 5] Speed of Sound & Mach Number\n");
printf("  Va2  = %lf (m/sec)\n",Va2);
printf("  M2   = %lf\n",M2);
printf(" 6] Radius :\n");
printf("  r2   = %lf (m)\n",r2);
getchar();

```

```

/***** Stage 3 *****/

```

```

clrscr();
printf("* Vaneless Space Data\n");
printf(" 1] Temperature :\n");
printf("  T03  = %lf (K)\n",T03);
printf("  T3   = %lf (K)\n",T3);
printf(" 2] Pressure :\n");
printf("  P03  = %lf (Pa)\n",P03);
printf(" 3] Density :\n");
printf("  p03  = %lf (kg/m^3)\n",p03);
printf("  p3   = %lf (kg/m^3)\n",p3);
printf(" 4] Velocity :\n");
printf("  V3   = %lf (m)\n",V3);

```

```

printf("  Vt3  = %lf (m)\n",Vt3);
printf("  Vm3  = %lf (m)\n",Vm3);
printf("  alpha3 = %lf (degree)\n",a3*180/PI);
printf(" 5] Speed of Sound & Mach Number\n");
printf("  Va3  = %lf (m/sec)\n",Va3);
printf("  M3   = %lf\n",M3);
printf(" 6] Radius :\n");
printf("  r3   = %lf (m)\n",r3);
getchar();

```

```

/***** Stage 4 *****/

```

```

clrscr();
printf("* Vaned Diffuser Data\n");
printf(" 1] Temperature :\n");
printf("  T04  = %lf (K)\n",T04);
printf("  T4   = %lf (K)\n",T4);
printf(" 2] Pressure :\n");
printf("  P04  = %lf (Pa)\n",P04);
printf(" 3] Density :\n");
printf("  p04  = %lf (kg/m^3)\n",p04);
printf("  p4   = %lf (kg/m^3)\n",p4);
printf(" 4] Velocity :\n");
printf("  V4   = %lf (m/sec)\n",V4);
printf("  Vt4  = %lf (m/sec)\n",Vt4);
printf("  Vm4  = %lf (m/sec)\n",Vm4);
printf("  alpha4 = %lf (real:degree)\n",alpha4*180/PI);
printf("  alpha4 = %lf (straight:degree)\n",a4*180/PI);
printf(" 5] Radius :\n");
printf("  r4   = %lf (m)\n",r4);
printf("  br4  = %lf (m)\n",br4);
getchar();
clrscr();

```

```

printf("* Miscellaneous Data\n");
printf(" 1] Chord length(l) = %lf (m)\n",l1);
printf(" 2] Solidity      = %lf\n",sigma1);

```

```

printf(" 3] Thichkness(t) = %lf (m)\n",t1);
printf(" 4] Breadth(b) = %lf (m)\n",breadth1);
printf(" 5] RPM(N) = %lf (rpm)\n",N);
printf(" 7] Specific Speed = %lf (Ns)\n",Ns1);
printf(" 8] # of Blades(Z) = %lf\n",Z);

/*****
/***** Second Stage Compressor *****/
/*****/

getchar();
clrscr();
printf("* Impeller Inlet Data\n");
printf(" 1] Temperature :\n");
printf("  T06 = %lf (K)\n",T06);
printf("  T6 = %lf (K)\n",T6);
printf(" 2] Pressure :\n");
printf("  P06 = %lf (Pa)\n",P06);
printf(" 3] Density :\n");
printf("  p06 = %lf (kg/m^3)\n",p06);
printf("  p6 = %lf (kg/m^3)\n",p6);
printf(" 4] Velocity :\n");
printf("  V6 = %lf (m/sec)\n",V6);
printf("  Vt6 = %lf (m/sec)\n",Vt6);
printf("  Vm6 = %lf (m/sec)\n",Vm6);
printf("  u6s = %lf (m/sec)\n",u6s);
printf("  W6s = %lf (m/sec)\n",W6s);
printf("  Wt6 = %lf (m/sec)\n",Wt6);
printf("  alpha6 = %lf (degree)\n",a6*180/PI);
printf("  betha6 = %lf (degree)\n",b6*180/PI);
printf(" 5] Speed of Sound & Mach Number\n");
printf("  Va6 = %lf (m/sec)\n",Va6);
printf("  M6rs = %lf\n",M6rs);
printf("  M6 = %lf\n",M6);
printf(" 6] Radius :\n");
printf("  r6h = %lf (m)\n",r6h);
printf("  r6s = %lf (m)\n",r6s);

```

```

getchar();

/***** Stage 2 *****/
clrscr();
printf("* Impeller Outlet Data\n");
printf(" 1] Temperature :\n");
printf("   T07  = %lf (K)\n",T07);
printf("   T7   = %lf (K)\n",T7);
printf(" 2] Pressure :\n");
printf("   P07  = %lf (Pa)\n",P07);
printf(" 3] Density :\n");
printf("   p07  = %lf (kg/m^3)\n",p07);
printf("   p7   = %lf (kg/m^3)\n",p7);
printf(" 4] Velocity :\n");
printf("   V7   = %lf (m/sec)\n",V7);
printf("   Vt7  = %lf (m/sec)\n",Vt7);
printf("   Vm7  = %lf (m/sec)\n",Vm7);
printf("   u7   = %lf (m/sec)\n",u7);
printf("   W7   = %lf (m/sec)\n",W7);
printf("   Wt7  = %lf (m/sec)\n",Wt7);
printf("   alpha7 = %lf (degree)\n",a7*180/PI);
printf("   betha7 = %lf (degree)\n",b7*180/PI);
printf(" 5] Speed of Sound & Mach Number\n");
printf("   Va7  = %lf (m/sec)\n",Va7);
printf("   M7   = %lf\n",M7);
printf(" 6] Radius :\n");
printf("   r7   = %lf (m)\n",r7);
getchar();

```

```

/***** Stage 3 *****/
clrscr();
printf("* Vaneless Space Data\n");
printf(" 1] Temperature :\n");
printf("   T08  = %lf (K)\n",T08);
printf("   T8   = %lf (K)\n",T8);
printf(" 2] Pressure :\n");

```

```

printf(" P08 = %lf (Pa)\n",P08);
printf(" 3] Density :\n");
printf(" p08 = %lf (kg/m^3)\n",p08);
printf(" p8 = %lf (kg/m^3)\n",p8);
printf(" 4] Velocity :\n");
printf(" V8 = %lf (m)\n",V8);
printf(" Vt8 = %lf (m)\n",Vt8);
printf(" Vm8 = %lf (m)\n",Vm8);
printf(" alpha8 = %lf (degree)\n",a8*180/PI);
printf(" 5] Speed of Sound & Mach Number\n");
printf(" Va8 = %lf (m/sec)\n",Va8);
printf(" M8 = %lf\n",M8);
printf(" 6] Radius :\n");
printf(" r8 = %lf (m)\n",r8);
getchar();

```

/\*\*\*\*\*\* Stage 4 \*\*\*\*\*/

```

clrscr();
printf("* Vaned Diffuser Data\n");
printf(" 1] Temperature :\n");
printf(" T09 = %lf (K)\n",T09);
printf(" T9 = %lf (K)\n",T9);
printf(" 2] Pressure :\n");
printf(" P09 = %lf (Pa)\n",P09);
printf(" 3] Density :\n");
printf(" p09 = %lf (kg/m^3)\n",p09);
printf(" p9 = %lf (kg/m^3)\n",p9);
printf(" 4] Velocity :\n");
printf(" V9 = %lf (m/sec)\n",V9);
printf(" Vt9 = %lf (m/sec)\n",Vt9);
printf(" Vm9 = %lf (m/sec)\n",Vm9);
printf(" alpha9 = %lf (degree)\n",a9*180/PI);
printf(" 5] Radius :\n");
printf(" r9 = %lf (m)\n",r9);
getchar();

```



```

/***** Stage 5 *****/
clrscr();
printf("* Exit Data\n");
printf(" 1] Temperature :\n");
printf("   T00  = %lf (K)\n",T00);
printf("   T0   = %lf (K)\n",T0);
printf(" 2] Pressure :\n");
printf("   P00  = %lf (Pa)\n",P00);
printf(" 3] Density :\n");
printf("   p00  = %lf (kg/m^3)\n",p00);
printf("   p0   = %lf (kg/m^3)\n",p0);
printf(" 4] Velocity :\n");
printf("   V0   = %lf (m/sec)\n",V0);
printf("* Miscellaneous Data\n");
printf(" 1] Chord length(l) = %lf (m)\n",l2);
printf(" 2] Solidity      = %lf \n",sigma2);
printf(" 3] Thickness(t)  = %lf (m)\n",t2);
printf(" 4] Breadth(b)   = %lf (m)\n",breadth2);
printf(" 5] RPM(N)       = %lf (rpm)\n",N);
printf(" 7] Specific Speed = %lf (Ns)\n",Ns2);
printf(" 8] # of Blades(Z) = %lf \n",Z);
printf(" 9] Volute Area :\n");
printf("   Ax(0 degree)  = %lf (m^2)\n",Ax20);
printf("   Ax(90 degree) = %lf (m^2)\n",Ax290);
printf("   Ax(180 degree) = %lf (m^2)\n",Ax2180);
printf("   Ax(270 degree) = %lf (m^2)\n",Ax2270);
printf("   Ax(360 degree) = %lf (m^2)\n",Ax2360);
printf("Draw the compressor ? : ");
scanf("%c",&ch);
clrscr();
if((ch=='Y')||(ch=='y')){
drawcompressor(r1h,r1s,r2,r3,r4,t1,breadth1,Ns1,r6h,r6s,r7,r8,r9,t2,breadth2,Ns2,N);
} /* end of if */
} /* end of for loop */
}

```

```

void drawcompressor(r1h,r1s,r2,r3,r4,t1,br1,Ns1,r6h,r6s,r7,r8,r9,t2,br2,Ns2,N)
double r1h,r1s,r2,r3,r4,t1,br1,Ns1,r6h,r6s,r7,r8,r9,t2,br2,Ns2,N;
{
int i;
char ch;

double Lm1, Lm2; /* Length of the blades */
double sp, rmax; /* spacing between two stages */

/* Graphic Variables */
double x[Mmax], y[Mmax];
int Gr1s,Gr2,Gr3,Gr4,Gt1,Gb1, Gx1,Gx2,Gy1,Gy2, xo1,yo1;
int Gr6s,Gr7,Gr8,Gr9,Gt2,Gb2, Gx3,Gx4,Gy3,Gy4, xo2,yo2;
int Gsp;

/* Variables for graphic mode */
int g_driver, g_mode, g_error;

Lm1 = 1.2*sqrt((t1-br1/2)*(t1-br1/2)+(r2-(r1s+r1h)/2)*(r1s-(r1s+r1h)/2));
Lm2 = 1.2*sqrt((t2-br2/2)*(t2-br2/2)+(r2-(r1s+r1h)/2)*(r1s-(r1s+r1h)/2));

sp = 0.5*(t1+t2);

/***** Start Graphics *****/
/* scale data */
if(r4>=r9){
rmax = r4;
Gr4 = Hmax;
Gr9 = (int)(Hmax*r9/r4);
}
if(r9>r4){
rmax = r9;
Gr9 = Hmax;
}

```

```

    Gr4 = (int)(Hmax*r4/r9);
}
/* stage 1 */
Gr3 = (int)(Hmax*r3/rmax);
Gr2 = (int)(Hmax*r2/rmax);
Gr1s = (int)(Hmax*r1s/rmax);
Gb1 = (int)(Hmax*br1/rmax);
Gt1 = (int)(Hmax*t1/rmax);
/* stage 2 */
Gr8 = (int)(Hmax*r8/rmax);
Gr7 = (int)(Hmax*r7/rmax);
Gr6s = (int)(Hmax*r6s/rmax);
Gb2 = (int)(Hmax*br2/rmax);
Gt2 = (int)(Hmax*t2/rmax);
Gsp = (int)(Hmax*sp/rmax);

/*****
/***** Data plotting subroutine *****/
/*****/

detectgraph(&g_driver, &g_mode);
if(g_driver < 0){
    printf("No graphics hardware detected !\n");
    exit(1);
}
if(g_mode==EGAHI){ /* override mode if EGA detected */
    g_mode = EGALO;
}
initgraph(&g_driver, &g_mode, "");
g_error = graphresult();
if(g_error < 0) {
    printf("initgraph error: %s.\n",
           grapherrormsg(g_error));
    exit(1);
}

```

```

/***** Let's start to draw something : putpixelx,y,color) *****/
setbkcolor(1); /* See pp201, pp282, pp318 : Blue is <1> */

/* x increases from left to the right : Horizontal */
/* y increases from top to bottom : Vertical */

/***** text coordinate : x-horizontal, y-vertical *****/
/* The font size is x*y = 8*14 : gotoxy(x,y) positions */
/* top left of the font box to given position */

/***** Stage 1 *****/
/* Draw Impeller */
xo1 = 30;
yo1 = 20;
line(xo1,Shift-yo1,xo1,Shift-(Gr1s+yo1));
line(xo1+Gt1,Shift-yo1,xo1+Gt1,Shift-(Gr4+yo1));
line(xo1,Shift-yo1,xo1+Gt1,Shift-yo1);
line(xo1+Gt1-Gb1,Shift-(Gr2+yo1),xo1+Gt1,Shift-(Gr2+yo1));
line(xo1+Gt1-Gb1,Shift-(Gr3+yo1),xo1+Gt1,Shift-(Gr3+yo1));
line(xo1+Gt1-Gb1,Shift-(Gr4+yo1),xo1+Gt1,Shift-(Gr4+yo1));
line(xo1+Gt1-Gb1,Shift-(Gr2+yo1),xo1+Gt1-Gb1,Shift-(Gr4+yo1));

for(i=0; i<Mmax; i++){
  x[i] = (t1-br1)*i/Max;
  y[i] = r1s+x[i]*(r2-r1s)/(t1-br1)-(Lm1/7)*sin(PI*x[i]/(t1-br1));
}
for(i=1; i<Mmax ;i++){
  Gx1 = (int)(Hmax*x[i-1]/rmax);
  Gy1 = (int)(Hmax*y[i-1]/rmax);
  Gx2 = (int)(Hmax*x[i]/rmax);
  Gy2 = (int)(Hmax*y[i]/rmax);
  line(Gx1+xo1,Shift-(Gy1+yo1),Gx2+xo1,Shift-(Gy2+yo1));
}

for(i=0; i<Mmax; i++){
  x[i] = (t1-br1/2)*i/Max;

```

```

    y[i] = (r1h+r1s)/2+x[i]*(r2-(r1s+r1h)/2)/(t1-br1/2)-(Lm1/7)*sin(PI*x[i]/(t1-br1/2));
}
for(i=1; i<Mmax ;i++){
    Gx1 = (int)(Hmax*x[i-1]/rmax);
    Gy1 = (int)(Hmax*y[i-1]/rmax);
    Gx2 = (int)(Hmax*x[i]/rmax);
    Gy2 = (int)(Hmax*y[i]/rmax);
    line(Gx1+xo1,Shift-(Gy1+yo1),Gx2+xo1,Shift-(Gy2+yo1));
}

for(i=0; i<Mmax; i++){
    x[i] = (t1)*i/Max;
    y[i] = r1h+x[i]*(r2-r1h)/(t1)-(Lm1/7)*sin(PI*x[i]/t1);
}
for(i=1; i<Mmax ;i++){
    Gx1 = (int)(Hmax*x[i-1]/rmax);
    Gy1 = (int)(Hmax*y[i-1]/rmax);
    Gx2 = (int)(Hmax*x[i]/rmax);
    Gy2 = (int)(Hmax*y[i]/rmax);
    line(Gx1+xo1,Shift-(Gy1+yo1),Gx2+xo1,Shift-(Gy2+yo1));
}

/***** Stage 2 *****/
/* Draw Impeller */
xo2 = xo1+Gt1+Gsp;
yo2 = yo1;

line(xo1+Gt1,Shift-yo1,xo2,Shift-yo2);

line(xo2,Shift-yo2,xo2,Shift-(Gr6s+yo2));
line(xo2+Gt2,Shift-yo2,xo2+Gt2,Shift-(Gr9+yo2));
line(xo2,Shift-yo2,xo2+Gt2,Shift-yo2);
line(xo2+Gt2-Gb2,Shift-(Gr7+yo2),xo2+Gt2,Shift-(Gr7+yo2));
line(xo2+Gt2-Gb2,Shift-(Gr8+yo2),xo2+Gt2,Shift-(Gr8+yo2));
line(xo2+Gt2-Gb2,Shift-(Gr9+yo2),xo2+Gt2,Shift-(Gr9+yo2));
line(xo2+Gt2-Gb2,Shift-(Gr7+yo2),xo2+Gt2-Gb2,Shift-(Gr9+yo2));

```

```

for(i=0; i<Mmax; i++){
  x[i] = (t2-br2)*i/Max;
  y[i] = r6s+x[i]*(r7-r6s)/(t2-br2)-(Lm2/7)*sin(PI*x[i]/(t2-br2));
}
for(i=1; i<Mmax ;i++){
  Gx3 = (int)(Hmax*x[i-1]/rmax);
  Gy3 = (int)(Hmax*y[i-1]/rmax);
  Gx4 = (int)(Hmax*x[i]/rmax);
  Gy4 = (int)(Hmax*y[i]/rmax);
  line(Gx3+xo2,Shift-(Gy3+yo2),Gx4+xo2,Shift-(Gy4+yo2));
}

for(i=0; i<Mmax; i++){
  x[i] = (t2-br2/2)*i/Max;
  y[i] = (r6h+r6s)/2+x[i]*(r7-(r6s+r6h)/2)/(t2-br2/2)-(Lm2/7)*sin(PI*x[i]/(t2-br2/2));
}
for(i=1; i<Mmax ;i++){
  Gx3 = (int)(Hmax*x[i-1]/rmax);
  Gy3 = (int)(Hmax*y[i-1]/rmax);
  Gx4 = (int)(Hmax*x[i]/rmax);
  Gy4 = (int)(Hmax*y[i]/rmax);
  line(Gx3+xo2,Shift-(Gy3+yo2),Gx4+xo2,Shift-(Gy4+yo2));
}

for(i=0; i<Mmax; i++){
  x[i] = (t2)*i/Max;
  y[i] = r6h+x[i]*(r7-r6h)/(t2)-(Lm2/7)*sin(PI*x[i]/t2);
}
for(i=1; i<Mmax ;i++){
  Gx3 = (int)(Hmax*x[i-1]/rmax);
  Gy3 = (int)(Hmax*y[i-1]/rmax);
  Gx4 = (int)(Hmax*x[i]/rmax);
  Gy4 = (int)(Hmax*y[i]/rmax);
  line(Gx3+xo2,Shift-(Gy3+yo2),Gx4+xo2,Shift-(Gy4+yo2));
}

```

```
/* Print important geometric data */
```

```
gotoxy(55,4);  
printf("* Geometric Data\n\n");  
gotoxy(56,5);  
printf("RPM   = %lf\n",N);  
gotoxy(55,6);  
printf("<Stage 1>\n");  
gotoxy(56,7);  
printf("1] r1h = %lf\n",r1h);  
gotoxy(56,8);  
printf("2] r1s = %lf\n",r1s);  
gotoxy(56,9);  
printf("3] r2 = %lf\n",r2);  
gotoxy(56,10);  
printf("4] r3 = %lf\n",r3);  
gotoxy(56,11);  
printf("5] r4 = %lf\n",r4);  
gotoxy(56,12);  
printf("6] b1 = %lf\n",br1);  
gotoxy(56,13);  
printf("7] t1 = %lf\n",t1);  
gotoxy(56,14);  
printf("8] Ns1 = %lf\n",Ns1);
```

```
gotoxy(55,15);  
printf("<Stage 2>\n");  
gotoxy(56,16);  
printf("1] r6h = %lf\n",r6h);  
gotoxy(56,17);  
printf("2] r6s = %lf\n",r6s);  
gotoxy(56,18);  
printf("3] r7 = %lf\n",r7);  
gotoxy(56,19);  
printf("4] r8 = %lf\n",r8);  
gotoxy(56,20);
```

```
printf("5] r9 = %lf\n",r9);
gotoxy(56,21);
printf("6] b2 = %lf\n",br2);
gotoxy(56,22);
printf("7] t2 = %lf\n",t2);
gotoxy(56,23);
printf("7] Ns2 = %lf\n",Ns2);
getchar();
getchar();
clrscr();
textmode(3);
}
```



## Appendix E. Compressor Design Data Using "COMPAL"

COMPAL 6.21 f3502a.geo ( 6.13)  
 First stage - pr=1.775

15-JAN-93 16:12:16

**Rotor:**

T00 = 548.42	P00 = 16.81	M = .10	N = 90000.0
R1T = 1.0000	R1H = .4500	BTA1TB=-54.43	BTA1HB= .00 BETA1B= .00
LEN1 = .0000	PHI1 =90.0000	AK = 1.0300	RCR1 = .0000 ALPHA1= .00
BLCK1= .0500	LC1 = .0500	TLET = .0150	ZI = 7.0000 PHIA = .00
PHIB = .0000	BLCKPA= .0500	TPR = 1.0000	ALPGVB= .00 PHIL = .00
R2 = .0000	B2 = .0000	ZR =14.0000	TN = .0300 BETA2B= .00
CLRR = .0040	PHI2 =90.0000	DELTAp= .00	DELTAAs= .00
Rexp = .0000	Bexp = .0000		
R = 10.11	K = 1.1161	Msec/M= .300	

**Stator(s) Excluding Diffusers:**

D7 = 2.0000	D8 = 3.0000	RCR5 = .0000	TCOLL = .00
R6 = .0000	R7 = .0000	R8 = .0000	ALPH6B= .00
B6 = .0000	B7 = .0000	B8 = .0000	PRDES = 1.7753 LAMBDA= 4.00

**Control:**

TOLR1 = .10E-04	TOLR2 = .10E-04	TOLR3 = .10E-02	
NU = 3 NM =30	N1 = 3	N2 = 2	NS = 2 ND = 4 N8 = 4
KLO = 3 NBF = 1	NPRTYP = 1	ISWIRL = 1	NUT = 1 NOCW = 1 NP = 5
NUF = 1 NUP = 1	NA = 1	NDATA = 1	NMR2 = 1 QQSEALf= 0 QQSEALr= 0
SEALPT= 1	GVFLAG = 4	CKFLAG = 2	NMR5 = 1 NIT = 1
NL = 1	NAS4 = 0	NSTAG = 0	NDRB = 0 NGAS = 0 NWIRL =-1

Real gas option is "R12392"

-----  
 Diffusers: (in-inlet, ex-exit, thrt-throat,4-throat or traverse)  
 1 of 2 (vaneless)

QQNAS= 1			
Rpin = .0000	Rex = .0000	Bpin = .0000	Bex = .0000
	Pex = .00	POex = .00	ALPHAex= .00
R4 = .0000	P4 = .00	P04 = .00	ALPHA4= .00
BR2ex= .7500	RR2ex= 1.1500		

2 of 2 (vaneless)

QQNAS= 1			
Rpin = .0000	Rex = .0000	Bpin = .0000	Bex = .0000
	Pex = .00	POex = .00	ALPHAex= .00
R4 = .0000	P4 = .00	P04 = .00	ALPHA4= .00
BRinex= 1.0000	RRinex= 1.3910		

\*\*\*\*\*

**INLET CONDITIONS:**

CM1T= 159.16	CT1T= .00	C1T = 159.16	Inducer Tip (Sta. 1T)	W1T = 287.86	BTA1TB=-54.43
P1T = 15.61	P01T= 16.76	T1T = 544.37		I1T = 2.00	BETA1T=-56.43
MREL1T= .65	U1T = 239.85				ALPH1T= .00
CM1 = 154.53	CT1 = .00	C1 = 154.53	Inducer RMS (Sta. 1M)	W1 = 241.80	BETA1B=-47.32
P1 = 15.67	P01 = 16.76	T1 = 544.60		I1 = 2.96	BETA1 =-50.28
MREL1 = .54	U1 = 185.98				ALPHA1= .00
CM1H= 150.03	CT1H= .00	C1H = 150.03	Inducer Hub (Sta. 1H)	W1H = 184.82	BTA1HB=-32.18
P1H = 15.73	P01H= 16.76	T1H = 544.82		I1H = 3.55	BETA1H=-35.73
MREL1H= .42	U1H = 107.93				ALPH1H= .00
R1H = .1374	R1T = .3054	LEN1= .0000	Inducer General Output	PHI1= 90.00	AR01= 1.0520

HLCK1= .0500 RCR1= .0000 AK = 1.03 LC1 = .0500 ALPGVB= .00

THE RATIO BETWEEN THE ACTUAL MASS FLOW RATE AND THE IDEALIZED 1-D CHOKE FLOW RATE IS .652

Rotor TIP CONDITIONS (TWO ZONE MODEL) :

CM2P= 310.19	CT2P= 343.12	C2P = 462.55	Isentropic Core Conditions (2P)
P2P = 21.50	P02P= 37.91	T2P = 562.81	W2P = 325.83 BETA2P=-17.82
M2P = 1.02	MR2 = .90	MR2I= 3.39	T02P= 597.03 DELTAP=-17.83
			MR2-SOA= 1.61 ALPH2P= 47.89
			dMR2= .55 AR12 =2.895
CM2S= 45.91	CT2S= 442.86	C2S = 445.23	Secondary Zone Conditions (2S)
P2S = 21.50	P02S= 35.86	T2S = 579.85	W2S = 45.91 BETA2S= .00
M2S = .97	E = .747	Msec/M= .30	T02S= 611.55 DELTAS= .00
			ALPH2S= 84.08
CM2M= 93.27	CT2M= 373.04	C2M = 384.53	Mixed-Out State Conditions (2M)
P2M = 23.19	P02M= 34.09	T2M = 578.16	W2M = 116.50 BETA2M=-36.81
M2 = .84	LAM2= 4.000	SIG2= .842	T02M= 601.80 DELTAM=-36.81
R2 = .5639	B2 = .0733	CLRR = .0040	dH/U**2= .851 ALPH2M= 75.96
Rexp= .5639	Bexp= .0733		U2 = 442.85
PRD = .0076	PBF = .0000	BF-%EP= .0000	Parasitic Power Losses
			PFC = .0000 PRC = .0000

VANELESS DIFFUSER CALCULATION:

R	B	CM	CT	M	T	P	P0	ALPHA	CP	LC	%Tr-1	%FR-1
.56	.073	93.3	373.0	.84	578.2	23.19	34.09	76.0	.00	.00	.00	.00
.58	.071	92.9	363.1	.82	579.3	23.57	33.98	75.6	.03	.01	.00	-.45
.59	.068	93.4	353.5	.80	580.4	23.92	33.86	75.2	.07	.02	.00	-.32
.60	.065	94.1	344.3	.78	581.4	24.24	33.75	74.7	.10	.03	.00	-.19
.61	.063	95.2	335.4	.76	582.4	24.53	33.64	74.2	.12	.04	.00	-.08
.62	.060	96.5	327.0	.74	583.2	24.81	33.54	73.6	.15	.05	.00	.02
.64	.058	98.2	318.8	.72	584.0	25.06	33.44	72.9	.17	.06	.00	.12
.65	.055	100.2	310.9	.71	584.7	25.28	33.34	72.1	.19	.07	.00	.20

R5 = .648 B5 = .0550 P5 = 25.28 P05 = 33.34  
 RE = 374074.60 CF = .0086 CPinex = .1921 LCinex= .0690

VANELESS DIFFUSER CALCULATION:

R	B	CM	CT	M	T	P	P0	ALPHA	CP	LC	%Tr-1	%FR-1
.65	.055	100.2	310.9	.71	584.7	25.28	33.34	72.1	.00	.00	.00	.20
.67	.055	94.7	295.0	.67	586.4	25.85	33.14	72.2	.07	.02	.00	.41
.70	.055	89.9	280.4	.64	587.9	26.35	32.96	72.2	.13	.05	.00	.60
.72	.055	85.6	266.8	.61	589.2	26.78	32.80	72.2	.19	.07	.00	.76
.75	.055	81.8	254.2	.58	590.4	27.17	32.66	72.2	.23	.09	.00	.90
.78	.055	78.3	242.4	.55	591.4	27.51	32.52	72.1	.28	.10	.00	1.02
.80	.055	75.2	231.5	.52	592.3	27.82	32.40	72.0	.31	.12	.00	1.13
.83	.055	72.3	221.3	.50	593.1	28.09	32.29	71.9	.35	.13	.00	1.23
.85	.055	69.7	211.8	.48	593.9	28.33	32.19	71.8	.38	.14	.00	1.32
.88	.055	67.2	202.8	.46	594.5	28.55	32.10	71.7	.40	.15	.00	1.39
.90	.055	65.0	194.5	.44	595.1	28.74	32.02	71.5	.43	.16	.00	1.46

R5 = .902 B5 = .0550 P5 = 28.74 P05 = 32.02  
 RE = 254614.90 CF = .0093 CPinex = .4288 LCinex= .1642  
 CP2ex = .509 LC2ex = .190

VOLUTE COMPUTATIONS:

P7 = 28.74    P07 = 31.69    P8 = 29.83    P08 = 31.14    D7 = .3643  
 CPex7= .0000    LCex7= .1005    CP78= .3695    LC78= .1861    D8 = .5464  
 LAM5\*AR= 1.00    AR = .33    BLCK7= .1200    COEF57= 1.000    MULT= 1.000

FINAL STAGE OUTPUT:

Stage Efficiency Decrements:	Pressure Rise:	K.E. Levels:
INLET DUCT LOSS = .004	P1T/P00= .928	KE1-W= .248
INTERNAL IMPELLER LOSS = .101	P2/P1T = 1.377	
IMPELLER EXIT MIXING LOSS = .104	P2M/P2 = 1.079	KE2-C= .443
IMPELLER RECIRC. LOSS = .000		
IMPELLER DISK FRICTION = .008		
IMPELLER LEAK POWER:FRONT = .000		
REAR = .000		
DIFFUSER INLET LOSS = .000	P4/P2M = 1.000	KE4-C= .000
vaneless 1 of 2		
EXIT LOSS = .026	PSRATIO= 1.090	KE-C= .320
vaneless 2 of 2		
EXIT LOSS = .046	PSRATIO= 1.137	KE-C= .126
DIFFUSER LOSS = .072	P5/P4 = 1.239	KE5-C= .126
VOLUTE LOSS :		
Station 5 to 7 Loss = .012	P7/P5 = 1.000	KE7-C= .000
Station 7 to 8 Loss = .020	P8/P7 = 1.038	KE8-C= .000
Total 5 to 8 Loss = .032	P8/P5 = 1.038	KE8-C= .000
EXIT LEAVING KE = .049		

ROTOR EFF. (T-T, w/o LEAK) = .788    TORatio = 1.097  
 ROTOR EFF. (T-T, w/ LEAK) = .788

STAGE EFFICIENCY, T-S = .631\*    .631    .631    .642    .634\*  
 STAGE EFFICIENCY, T-T = .680\*    .680    .680    .690    .697\*  
 (VAR-P    K-AVG-T    CONST-K    POLYSHEP    POLYASME)  
           K=1.116    K=1.116                    NK=1.221  
 (Note: '\*' indicates mapfile item.)

	Head (Length)	Head Coefficients
Isentropic T-S (REAL)	3274.53	.537
Polytropic T-S	3330.13	1.792
Polytropic T-T	3579.89	1.927
Isentropic T-S (k=1.116)	3274.53	.537
Volumetric Flow	.22	9999.000 PSIp04 (Ignore if 9999.)

STAGE PRESSURE RATIO,    TS = 1.774    TT    = 1.852    POWER    =    .97  
 SPECIFIC SPEED,        NS = .675    NS(US) = 98.283  
 FLOW COEFFICIENTS,    PHI0 = .179    PHIEX = .101    PHISTAT = .098  
                           PHI2 = .095    PHIROT = .137    PHI(A1T)= .834  
                           PHIin= .073

(Note: PHI0=Q/N/D2\*\*3    PSI=DEL(H, isen)/(D2\*N)\*\*2    NS=PHI0\*\*0.5/PSI\*\*0.75)

ENTHALPY:

INLET STAG.=        68.48    OUTLET STAG.=        75.14    OUTLET ISENTR.=        72.69

STALL CONDITIONS THROUGHOUT STAGE (0.0=NO STALL, 1.0=STALL MODE PRESENT)

INDUCER STALL: .0    ROTATING STALL IN DIFF.: .0    VANELESS SPACE STALL: .0  
 CHANNEL DIFFUSER STALL: .0    VOLUTE DISTORTION STALL: .0

Rotor:

T00 = 548.42 P00 = 16.81 M = .10 N = 90000.0  
 R1T = 1.0000 R1H = .4500 BTA1TB=-53.83 BTA1HB= .00 BETA1B= .00  
 LEN1 = .0000 PHI1 =90.0000 AK = 1.0300 RCR1 = .0000 ALPHA1= .00  
 BLCK1= .0500 LC1 = .0500 TLET = .0150 ZI = 7.0000 PHIA = .00  
 PHIB = .0000 BLCKPA= .0500 TPR = 1.0000 ALPGVB= .00 PHIL = .00  
 R2 = .0000 B2 = .0000 ZR =14.0000 TN = .0300 BETA2B= .00  
 CLRR = .0070 PHI2 =90.0000 DELTAp= .00 DELTAs= .00  
 Rexp = .0000 Bexp = .0000  
 R = 10.11 K = 1.1161 Msec/M= .300

Stator(s) Excluding Diffusers:

D7 = 2.0000 D8 = 3.0000 RCR5 = .0000 TCOLL = .00  
 R6 = .0000 R7 = .0000 R8 = .0000 ALPH6B= .00  
 B6 = .0000 B7 = .0000 B8 = .0000 PRDES = 1.7753 LAMBDA= 4.00

Control:

TOLR1 = .10E-04 TOLR2 = .10E-04 TOLR3 = .10E-02  
 NU = 3 NM =30 N1 = 3 N2 = 2 NS = 2 ND = 4 N8 = 4  
 KLO = 3 NBF = 1 NPRTYP = 1 ISWIRL = 1 NUT = 1 NOCW = 1 NP = 5  
 NUF = 1 NUP = 1 NA = 1 NDATA = 1 NMR2 = 1 QQSEALf= 0 QQSEALr= 0  
 SEALPT= 1 GVFLAG = 4 CKFLAG = 2 NMR5 = 1 NIT = 1  
 NL = 1 NAS4 = 0 NSTAG = 0 NDRB = 0 NGAS = 0 NWIRL = -1  
 Real gas option is "R12392"

Diffusers: (in-inlet, ex-exit, thrt-throat,4-throat or traverse)  
 1 of 2 (vaneless)

-----  
 QQNAS= 1  
 Rpin = .0000 Rex = .0000 Bpin = .0000 Bex = .0000  
 Pex = .00 P0ex = .00 ALPHAex= .00  
 R4 = .0000 P4 = .00 P04 = .00 ALPHA4= .00  
 BR2ex= .7500 RR2ex= 1.1500  
 2 of 2 (vaneless)

-----  
 QQNAS= 1  
 Rpin = .0000 Rex = .0000 Bpin = .0000 Bex = .0000  
 Pex = .00 P0ex = .00 ALPHAex= .00  
 R4 = .0000 P4 = .00 P04 = .00 ALPHA4= .00  
 BRinex= 1.0000 RRinex= 1.3910

\*\*\*\*\*

INLET CONDITIONS:

CM1T= 159.16	CT1T= .00	C1T = 159.16	Inducer Tip (Sta. 1T)	W1T = 287.86	BTA1TB=-54.43
P1T = 15.61	P01T= 16.76	T1T = 544.37	I1T = 2.00	BETA1T=-56.43	ALPH1T= .00
MREL1T= .65	U1T = 239.85				
CM1 = 154.53	CT1 = .00	C1 = 154.53	Inducer RMS (Sta. 1M)	W1 = 241.80	BETA1B=-47.32
P1 = 15.67	P01 = 16.76	T1 = 544.60	I1 = 2.96	BETA1=-50.28	ALPHA1= .00
MREL1 = .54	U1 = 185.98				
CM1H= 150.03	CT1H= .00	C1H = 150.03	Inducer Hub (Sta. 1H)	W1H = 184.82	BTA1HB=-32.18
P1H = 15.73	P01H= 16.76	T1H = 544.82	I1H = 3.55	BETA1H=-35.73	ALPH1H= .00
MREL1H= .42	U1H = 107.93				
R1H = .1374	R1T = .3054	LEN1= .0000	Inducer General Output	PHI1= 90.00	AR01= 1.0520

BLCK1= .0500 RCR1= .0000 AK = 1.03 LC1 = .0500 ALPGVB= .00

THE RATIO BETWEEN THE ACTUAL MASS FLOW RATE AND THE IDEALIZED 1-D CHOKE FLOW RATE IS .652

Rotor TIP CONDITIONS (TWO ZONE MODEL) :

<hr/>			Isentropic Core Conditions (2P)		
CM2P= 361.38	CT2P= 360.74	C2P = 510.61	W2P = 376.28	BETA2P=-16.18	
P2P = 20.64	P02P= 41.16	T2P = 560.45	T02P= 602.15	DELTAP=-16.18	
M2P = 1.13	MR2 = .78	MR2I= 3.50	MR2-SOA= 1.64	ALPH2P= 44.95	
			dMR2= .55	AR12 =2.774	
<hr/>			Secondary Zone Conditions (2S)		
CM2S= 47.59	CT2S= 465.59	C2S = 468.02	W2S = 47.59	BETA2S= .00	
P2S = 20.64	P02S= 36.17	T2S = 583.21	T02S= 618.24	DELTAS= .00	
M2S = 1.02	E = .770	Msec/M= .30		ALPH2S= 84.16	
<hr/>			Mixed-Out State Conditions (2M)		
CM2M= 97.98	CT2M= 392.19	C2M = 404.25	W2M = 122.42	BETA2M=-36.84	
P2M = 22.78	P02M= 34.77	T2M = 581.36	T02M= 607.49	DELTAM=-36.84	
M2 = .88	LAM2= 4.003	SIG2= .842	dH/U**2= .852	ALPH2M= 75.97	
R2 = .5928	B2 = .0679	CLRR = .0070	U2 = 465.59		
Rexp= .5928	Bexp= .0679				
<hr/>			Parasitic Power Losses		
PRD = .0094	PBF = .0000	BF-%EP= .0000	PFC = .0000	PRC = .0000	

VANELESS DIFFUSER CALCULATION:

R	B	CM	CT	M	T	P	P0	ALPHA	CP	LC	%Tr-1	%FR-1
.59	.068	98.0	392.2	.88	581.4	22.78	34.77	76.0	.00	.00	.00	.00
.61	.065	97.5	381.4	.86	582.7	23.20	34.62	75.6	.03	.01	.00	-.43
.62	.063	97.9	371.0	.83	584.0	23.57	34.46	75.2	.07	.03	.00	-.28
.63	.061	98.6	361.0	.81	585.1	23.92	34.32	74.7	.09	.04	.00	-.14
.64	.058	99.6	351.4	.79	586.2	24.24	34.18	74.2	.12	.05	.00	-.02
.66	.056	100.9	342.2	.77	587.1	24.53	34.04	73.6	.15	.06	.00	.10
.67	.053	102.6	333.3	.75	588.0	24.80	33.91	72.9	.17	.07	.00	.21
.68	.051	104.6	324.8	.74	588.9	25.05	33.79	72.1	.19	.08	.00	.30

R5 = .682 B5 = .0509 P5 = 25.05 P05 = 33.79  
 RE = 353961.70 CF = .0087 CPinex = .1886 LCinex= .0823

VANELESS DIFFUSER CALCULATION:

R	B	CM	CT	M	T	P	P0	ALPHA	CP	LC	%Tr-1	%FR-1
.68	.051	104.6	324.8	.74	588.9	25.05	33.79	72.1	.00	.00	.00	.30
.71	.051	98.8	307.6	.70	590.8	25.65	33.53	72.2	.07	.03	.00	.54
.74	.051	93.7	291.7	.66	592.5	26.18	33.30	72.2	.13	.06	.00	.74
.76	.051	89.1	277.0	.63	594.0	26.65	33.10	72.2	.18	.08	.00	.92
.79	.051	85.1	263.3	.60	595.2	27.06	32.91	72.1	.23	.10	.00	1.07
.82	.051	81.4	250.7	.57	596.4	27.42	32.74	72.0	.27	.12	.00	1.21
.84	.051	78.1	238.9	.54	597.4	27.74	32.59	71.9	.31	.14	.00	1.33
.87	.051	75.1	227.9	.51	598.3	28.02	32.46	71.8	.34	.15	.00	1.44
.89	.051	72.4	217.7	.49	599.1	28.28	32.34	71.6	.37	.17	.00	1.53
.92	.051	69.8	208.1	.47	599.8	28.50	32.22	71.4	.40	.18	.00	1.61
.95	.051	67.5	199.1	.45	600.4	28.70	32.12	71.3	.42	.19	.00	1.69

R5 = .948 B5 = .0509 P5 = 28.70 P05 = 32.12  
 RE = 240698.00 CF = .0094 CPinex = .4185 LCinex= .1902  
 CP2ex = .494 LC2ex = .221

VOLUTE COMPUTATIONS:

P7 = 28.70 P07 = 31.77 P8 = 29.84 P08 = 31.20 D7 = .3618  
 CPex7= .0000 LCex7= .1030 CP78= .3695 LC78= .1861 D8 = .5426  
 LAM5\*AR= 1.00 AR = .34 BLCK7= .1200 COEF57= 1.000 MULT= 1.000

FINAL STAGE OUTPUT:

Stage Efficiency Decrements:	Pressure Rise:	K.E. Levels:
INLET DUCT LOSS = .003	P1T/P00= .928	KE1-W= .224
INTERNAL IMPELLER LOSS = .121	P2/P1T = 1.323	
IMPELLER EXIT MIXING LOSS = .138	P2M/P2 = 1.104	KE2-C= .442
IMPELLER RECIRC. LOSS = .000		
IMPELLER DISK FRICTION = .009		
IMPELLER LEAK POWER:FRONT = .000		
REAR = .000		
DIFFUSER INLET LOSS = .000	P4/P2M = 1.000	KE4-C= .000
vaneless 1 of 2		
EXIT LOSS = .030	PSRATIO= 1.099	KE-C= .315
vaneless 2 of 2		
EXIT LOSS = .052	PSRATIO= 1.146	KE-C= .120
DIFFUSER LOSS = .082	P5/P4 = 1.260	KE5-C= .120
VOLUTE LOSS :		
Station 5 to 7 Loss = .011	P7/P5 = 1.000	KE7-C= .000
Station 7 to 8 Loss = .019	P8/P7 = 1.039	KE8-C= .000
Total 5 to 8 Loss = .030	P8/P5 = 1.039	KE8-C= .000
EXIT LEAVING KE = .046		

ROTOR EFF. (T-T, w/o LEAK) = .732 TORatio = 1.108  
 ROTOR EFF. (T-T, w/ LEAK) = .732

STAGE EFFICIENCY, T-S = .571\* .571 .571 .583 .575\*  
 STAGE EFFICIENCY, T-T = .617\* .617 .617 .629 .634\*  
 (VAR-P K-AVG-T CONST-K POLYSHEP POLYASME)  
 K=1.116 K=1.116 NK=1.241  
 (Note: '\*' indicates mapfile item.)

	Head (Length)	Head Coefficients
Isentropic T-S (REAL)	3276.14	.486
Polytropic T-S	3347.68	1.630
Polytropic T-T	3608.45	1.757
Isentropic T-S (k=1.116)	3276.14	.486
Volumetric Flow	.22	9999.000 PSIp04 (Ignore if 9999.)

STAGE PRESSURE RATIO, TS = 1.775 TT = 1.856 POWER = 1.07  
 SPECIFIC SPEED, NS = .675 NS(US) = 98.247  
 FLOW COEFFICIENTS, PHI0 = .154 PHIEX = .087 PHISTAT = .084  
 PHI2 = .080 PHIROT = .117 PHI(A1T)= .793  
 PHIin= .063

(Note: PHI0=Q/N/D2\*\*3 PSI=DEL(H,isen)/(D2\*N)\*\*2 NS=PHI0\*\*0.5/PSI\*\*0.75)

ENTHALPY:

INLET STAG.= 68.48 OUTLET STAG.= 75.85 OUTLET ISENTR.= 72.69

STALL CONDITIONS THROUGHOUT STAGE (0.0=NO STALL, 1.0=STALL MODE PRESENT)

INDUCER STALL: .0 ROTATING STALL IN DIFF.: .0 VANELESS SPACE STALL: .0  
 CHANNEL DIFFUSER STALL: .0 VOLUTE DISTORTION STALL: .0

## REFERENCES

1. A.E.Fitzgerald, C. Kingsley,Jr., S.D.Umans, "Electric Machinery",1990, McGraw-Hill, N.Y.
2. Ralph J.Smith, A.E.Fitzgerald, "Introduction to Electrical and Electronic Engineering", 1980, John Wiley & sons, N.Y.
3. 2.151 Class Note for Brushless DC Motors
4. J.P.Den Hartog, "Mechanical Vibrations", 1934, McGraw-Hill, N.Y., Chapter 6.
5. Leonard Meirovitch, "Elements of Vibration Analysis", 1986, McGraw Hill, N.Y.
6. R.F.Steidel,Jr, "An Introduction to Mechanical Vibrations", 1979, John Wiley & Sons, N.Y.
7. F.S.Tse, I.E.Morse, R.T.Hinkle, "Mechanical Vibrations", 1978, Allyn Bacon, Newton,MA
8. S.H.Crandall, D.C.Karnopp, E.F.Kurtz,Jr, D.C.Pridmore-Brown, "Dynamics of Mechanical and Electromechanical Systems", 1968, McGraw Hill, N.Y.
9. S.M.Lord, "Analysis of Lateral vibration Modes of a Superconducting Generator", 1979, M.S. Thesis
10. J.W.Simpson, "Vibration Analysis of a Superconducting Generator Rotor on Flexible Supports", 1982, M.S. Thesis
11. K.A.Tepper, "Mechanical Design of the Rotor of a Fault-Worthy 10 MVA Superconducting Generator", 1980, Ph.D Thesis
12. G.Niemann, "Machinen Elemente", 1981, Springer-Verlag, Berlin

13. S.H.Crandall, N.C.Dahl, T.J.Lardner, "An Introduction to the Mechanics of Solids", 1978, McGraw Hill, N.Y., pp.92-94.
14. J.M.Gere, S.P.Timoshenko, "Mechanics of Materials", 1984, Wadsworth , Belmont,CA
15. R.G.Budynas, "Advanced Strength and Applied Stress Analysis", 1977, McGraw Hill, N.Y.
16. S.P.Timoshenko, J.N.Goodier, "Theory of Elasticity", 1934, McGraw Hill, N.Y., Chapter 4.
17. Warren C.Young, "Roark's Formulas for Stress and Strain",6th edition, 1989, McGraw Hill, N.Y.
18. Klaus-Jurgen Bathe, "Finite Element Procedures in Engineering Analysis", 1982, Prentice-Hall, Englewood Cliffs,NJ
19. R.D.Cook, D.S.Malkus, M.E.Plesha, "Concepts and Applications of Finite Element Analysis",3rd edition, 1989, John Wiley and Sons, N.Y.
20. "ADINA Manual"
21. E.G.Cravalho, J.L.Smith,Jr, "Engineering Thermodynamics", 1981, MIT, Chapter 12.
22. G.J.Van Wylen, R.E.Sonntag, "Fundamentals of Classical Thermodynamics ", 1985, John Wiley & Sons, N.Y.
23. E.P.Gyftopoulos, G.P.Beretta, "Thermodynamics: Foundations and Applications", 1991, Macmillan Publishing Company, N.Y.
24. T.Baumeister, "Mark's Standard Handbook for Mechanical Engineers", pp.11-19, 1978, McGraw Hill, N.Y.



25. George Clifford, "Modern Heating, Ventilating and Air Conditioning", 1984, Prentice-Hall, Englewood Cliffs, NJ
26. Rudolf Plank, "Handbuch der Kältetechnik", TP492.P712
27. Arthur P.Fraas, "Heat Exchanger Design", 2nd edition, 1989, John Wiley & Sons, N.Y.
28. Sadik Kakac, "Boilers Evaporators and Condensers", 1991, John Wiley & Sons, N.Y.
29. Frank P.Incropera, David P.Dewitt, "Introduction to Heat Transfer", 1985, John Wiley & Sons, N.Y.
30. J.P.Holman, "Heat Transfer", 1986, McGraw Hill, N.Y.
31. W.M.Kays, A.L.London, "Compact Heat Exchangers", 1964, McGraw Hill, N.Y.
32. "HVAC Handbook", 1987, ASHRAE
33. M.N.Oziscic, "Heat Transfer", 1985, McGraw Hill, N.Y.
34. W.M.Rohsenow, H.Y.Choi, "Heat Mass and Momentum Transfer", 1961, Prentice-Hall, Englewood Cliffs, NJ
35. "Thermodynamic Properties of Refrigerants", 1969, ASHRAE
36. "Advertisement material and data from DuPont"
37. James F.Ely, "Application of the Extended Corresponding States Model to Hydrocarbon Mixtures(Computer Program EXCST)", 1984, Proceedings, 63rd Gas Processors Association Annual Convention
38. M.O.McLinden et. al., "Measurement and Formulation of the Thermodynamic Properties of Refrigerants 134a and 123", 1989, ASHRAE Transactions V95

39. R.D.McCarty, "Interactive Fortran IV Computer Programs for the Thermodynamic and Transport Properties of Selected Cryogens", 1980, NBS TN 1025
40. R.T.Jacobsen, R.B.Steward, "Thermodynamic properties of Nitrogen Including Liquid and Vapor Phases from 63K to 2000K with Pressures to 10000 Bar", 1973, Journal of Physical Chemistry, Vol.2, No.4
41. R.T.Jacobsen, R.B.Steward, "Thermophysical Properties of Nitrogen from the Fusion Line to 3500R for Pressures to 150000 psia", 1973, NBS TN 648
42. H.J.M.Hanley, R.D.McCarty, W.M.Haynes, "The Viscosity and Thermal conductivity Coefficients for Dense Gaseous and Liquid Argon, Krypton, Xenon, Nitrogen, and Oxygen", 1974, Journal of Physical Chemistry, Vol.3 No.4
43. "Advertisement material from NATRON"
44. John Dieckmann, David Mallory, "Variable Speed Compressor, HFC-134a Based Airconditioning System for Electric Vehicles", SAE Technical Paper 920444, Appendix E.
45. John Dieckmann, David Mallory, "Climate Control for Electric Vehicles", SAE Technical Paper 910250
46. David Gordon Wilson, "The Design of High-Efficiency Turbomachinery and Gas Turbines", 1984 MIT Press, Cambridge,MA
47. Jack L. Kerrebrock, "Aircraft Engines and Gas Turbines", 1977, MIT Press, Cambridge,MA
48. S.L.Dixon, "Fluid Mechanics, Thermodynamics of Turbomachinery", 1978, Pergamon Press, Oxford
49. Philip Hill, Carl Peterson, "Mechanics and Thermodynamics of Propulsion", 1965, Addison-Wesley, MA
50. E.T.Vincent, "The Theory and Design of Gas Turbines and Jet Engines", 1950, McGraw Hill, N.Y.

51. John W. Sawyer, "Sawyer's Gas Turbine Engineering Handbook", Vol.I, 1972, Gas Turbine Publications, Stamford
52. Asher H. Shapiro, "The Dynamics and Thermodynamics of Compressible Fluid Flow", 1953, Ronald Press Company, N.Y.
53. A. Stodola, Louis C. Loewenstein, "Steam and Gas Turbines", 1945, Peter Smith, N.Y.
54. John D. Stanitz, Vasily D. Prian, "A Rapid Approximate Method for Determining Velocity Distribution on Impeller Blades of Centrifugal Compressor", 1951, NACA TN 2421
55. John D. Stanitz, "Approximate Design Method for High-Solidity Blade Elements in Compressors and Turbines", 1951, NACA TN 2408
56. Chung-Hua Wu, "A General Theory of Three-Dimensional Flow in Subsonic and Supersonic Turbomachines of Axial-, Radial-, and Mixed-Flow Types", 1952, NACA TN 2604
57. Chung-Hua Wu, Curtis A. Brown, "Method of Analysis for Compressible Flow Past Arbitrary Turbomachine Blades on a General Surface of Revolution", 1951, NACA TN 2407
58. H.E. Sheets, "Nondimensional Compressor Performance for a Range of Mach Numbers and Molecular Weight", 1952, ASME
59. John M. Schultz, "The Polytropic Analysis of Centrifugal Compressors", 1962, Journal of Engineering for Power(Transactions of ASME)
60. ASHRAE Handbook, 1987, 1986, 1985, 1984, 1983, 1982
61. H. Davis, H. Kottas, A.M.G. Moody, "The Influence of Reynolds Number on the Performance of Turbomachinery", 1951, ASME Transactions

62. H.E.Caswell, F.J.Wiesner,Jr., "How Refrigerant Properties affect Impeller Dimensions", 1959, ASHRAE Journal
  
63. Joseph T. Hamrick, Ambrose Ginsburg, "Methods of Analysis for Compressible Flow through Mixed-Flow Centrifugal Impellers of Arbitrary Design", 1950, NACA TN 2165
  
64. Kenneth S.Smith, Joseph T.Hamrick, "A Rapid Approximate Method for the Design of Hub Shroud Profiles of Centrifugal Impellers of Given Blade Shape", 1955, NACA TN 3395
  
65. Robert J.Anderson, William K.Ritter, Dean M.Dildine, "An Investigation of the Effect of Blade Curvature on Centrifugal-Impeller Performance", 1947, NACA TN 1313
  
66. Gaylord O.Ellis, John D.Stanitz, "Two-Dimensional Compressible Flow in Centrifugal Compressors with Logarithmic-Spiral Blades", 1951, NACA TN 2255
  
67. "2.601J Design of Thermal Power System : Class Note"
  
68. J.H.Horlock, "Axial Flow Compressor", 1958, Butterworth, London
  
69. W.A.Gross, "Gas Film Lubrication", 1962, John Wiley & Sons, N.Y.
  
70. B.Sternlicht, O.Pinkus, "Theory of Hydrodynamic Lubrication", 1961, McGraw Hill, N.Y.
  
71. M.Wildmann, "Foil Bearings", 1969 Jan., Journal of Lubrication Technology
  
72. M.Wildmann, "Foil Bearings - Their General Behaviour with Particular Emphasis on the Externally Pressurized Bearing"
  
73. A. Eshel, "The Propagation of Disturbances in the Infinitely Wide Foil Bearing", 1969 Jan., Journal of Lubrication Technology, Transaction of ASME
  
74. L.Licht, "Effect of Rotation of the Clearance Topography of a Pressurized Foil Bearing", 1971 March, Gas Bearing Symposium

75. R.C.Elwel, J.A.Findlay, "Design of Pivoted-Pad Journal Bearings", 1969 Jan.,  
Journal of Lubrication Technology